STUDY OF RADIOACTIVITY IN CHEMICAL AND ORGANIC FERTILISERS USED IN CHATTOGRAM AREA, BANGLADESH.

By

Kanchan Sarkar

ID: 17MPHY006P

A thesis submitted in partial fulfilment of the requirement for the degree of Master of Philosophy

Department of Physics

Chittagong University of Engineering and Technology

February

2024

Declaration

I hereby declare that the work contained in this thesis has not been previously submitted to meet requirements for an award at this or any other higher education institution. To the best of my knowledge and belief, the thesis contains no material previously published or written by another person accept where due reference is cited. Furthermore, the thesis complies with PLAGIARISM and ACADEMIC INTEGRITY regulation of CUET.

Kanchan Sarkar

17MPHY006P

Department of Physics

Chittagong University of Engineering and Technology (CUET)

Dedicated to my parents

and

all the people who supported my research work

List of Publication

Journal Article

- Publication 1: Kanchan Sarkar, Animesh Kumer Chakraborthy, Mahiudddin Ahmed, Shahadat Hossain, "Assessment of naturally occurred radiation hazards in Chattogram area, Bangladesh. International Journal Environmental Analytical Chemistry. https://doi.org/10.1080/03067319.2022.2135998

Declaration by the Supervisor

This is certified that Kanchan Sarkar has carried out his research work under my/our supervision, and that he has fulfilled the relevant Academic ordinance of the Chittagong University of Engineering and Technology. So that he is qualified to submit the following thesis in the application for the degree of MASTER of PHYLOSOPHY. Furthermore, the Thesis complies with the PLAGIARISM and ACADEMIC INTEGRITY regulation of CUET.

Dr. Animesh Kumer Chakraborty

Principal Supervisor

and

Professor,

Department of Physics,

Chittagong University of Engineering & Technology

Dr. Shahadat Hossain

Co-Supervisor

and

Chief Scientific Officer,

Atomic Energy Centre, Chattogram

Acknowledgment

I owe my deep indebtedness to my respected supervisor Dr. Animesh Kumer Chakraborty, Professor, Department of Physics, Chittagong University of Engineering & Technology (CUET) for his indispensable guidance full of innovative ideas, keen interest, constructive criticism and suggestions, constant inspiration and hearty assistance throughout this research work for fruitful finishing and in preparing this manuscript with necessary correction. His invaluable expertise by the way of continual motivation and provocative remarks helped me to generate the conceptual grid of this thesis.

I express my deepest sense of gratitude and sincere appreciation to my honourable co-supervisor Dr. Shahadat Hossain, Chief Scientific Officer, Atomic Energy Centre, Chattogram (AECC) for his valuable guidance, suggestions and functional supports regarding experimental works and data analysis. I, also, convey my sincere gratitude and regards to Mr. Mohiuddin Ahmed, Scientific Officer, Health Physics and Radioactive Waste Management Unit (HPRWMU), Institute of Nuclear Science and Technology, Bangladesh Atomic Energy Commission (BAEC), Dhaka for his cordial involvement and overall supports.

I would like to take the privilege to confer my honour and sense of profound gratitude to Dr. AKM Saiful lslam Bhuian, Principle Scientific Officer & Mr. Manish Debnath, Scientific Officer, Atomic Energy Centre, Chittagong for their time-to-time supports and helpful attitudes throughout my experiments over there.

I gratefully acknowledge the authority of CUET, all teachers and staffs of the Department of Physics, CUET and all the lab assistances of AECC for their utmost cooperation. Special gratitude to honourable Head of the department of Physics, CUET for his overall supports.

Finally, my heartfelt indebtedness to my family members and friends for their regular encouragement. Special appreciation is expressed to my wife Adv. Shoily Chowdhury, who supported, inspired and assisted me all the way of this research.

Kanchan Sarkar

Abstract

The present work deals with identifying and determining the activity levels of naturally occurring radionuclides ^{226}Ra and ^{232}Th series, their decay products and ^{40}K in chemical and organic fertilisers used in Chattogram area, Bangladesh. A total of 39 samples collected from retail markets were investigated, out of which 28 are chemical fertilisers and the others are organic fertilisers. Gamma-ray spectrometry was applied as the measurement technique using a High Purity Germanium (HPGe) gamma-ray detector at the Atomic Energy Centre, Chattogram, Bangladesh. The average activity concentration of ^{226}Ra and ^{232}Th found in TSP fertiliser are 304.57 ± 36.0 $Bqkg^{-1}$ and 19.1 ± 6.8 $Bqkg^{-1}$ respectively and the average activity concentration of ^{40}K in MOP fertiliser is found as 10,311.11 ± 1168 $Bqkg^{-1}$. In the organic fertiliser samples, the mean concentration of ^{226}Ra, ^{232}Th and ^{40}K are 17.35 ± 3.11 Bq kg^{-1}, 7.20 ± 1.74 $Bqkg^{-1}$ and 437.14 ± 42.58 $Bqkg^{-1}$, respectively. The mean absorbed dose rates were measured after the end of our experiment and the value was found to be 91.39 $nGyh^{-1}$. The combined (indoor + outdoor) annual effective dose equivalent was also estimated as 0.322 $mSvyr^{-1}$. The mean radium equivalent activity found to be 190.15 ± 26.74 $Bqkg^{-1}$ is well below the recommended level of 370 $Bqkg^{-1}$. The internal hazard index, external hazard index and radioactivity level index of the investigated fertiliser samples were found as 0.56 ± 0.034, 0.54 ± 0.08 and 0.69 ± 0.10, respectively. From the calculated hazard parameters, the excess lifetime cancer risk (ELCR) was found to be higher than the world average in most of the chemical fertilisers except in DAP and BOR, while the organic fertilisers show lower than the world average. The obtained results reveal that there are no significant radiation hazards due to natural radionuclides of the fertiliser samples in the studied area, but the higher concentration of ^{40}K in MOP suggests strengthening the regulatory work. Overall, this study highly recommends the use of organic fertilisers, as these kinds have hazard parameters lower than the recommended levels.

বিমূর্ত

বর্তমান কাজটি বাংলাদেশের চট্টগ্রাম অঞ্চলে ব্যবহৃত রাসায়নিক ও জৈব সারের নমুনাগুলিতে তেজস্ক্রিয় উপাদান ^{226}Ra এবং ^{232}Th ও এদের সিরিজ, এবং ^{40}K ও এদের সিরিজের মধ্যে অন্যান্য প্রাকৃতিক রেডিও-নিউক্লাইডগুলোর কার্যকলাপের মাত্রা সনাক্তকরণ এবং নির্ধারণের সাথে সম্পর্কিত। খুচরা বাজার থেকে সংগ্রহ করা মোট ৩৯টি নমুনা পরীক্ষা করা হয়েছে, যার মধ্যে ২৮টি রাসায়নিক সার এবং বাকিগুলি জৈব সার। টি এস পি সারে ^{226}Ra, ^{232}Th এর গড় পরিমাণ 304.57 ± 36.0 $Bqkg^{-1}$ ও 19.1 ± 6.8 $Bqkg^{-1}$ এবং এমওপি সারে ^{40}K এর গড় পরিমাণ 10,311.11 ± 1168 Bq kg^{-1}। জৈব সারের নমুনাগুলিতে তেজস্ক্রিয় উপাদান ^{226}Ra এবং ^{232}Th সিরিজ, এবং ^{40}K এর গড় উপস্থিতি যথাক্রমে 17.35 ± 3.11 Bq kg^{-1} , 7.20 ± 1.74 $Bqkg^{-1}$ and 437.14 ± 42.58 Bq kg^{-1} পাওয়া গেছে। সকল নমুনা পরীক্ষা শেষে গড় শোষিত ডোজ পরিমাপ করা হয়েছে 91.39 nGy h^{-1}। সম্মিলিত (indoor + outdoor) বাষিক তুল্য ডোজ পরিমাপ করা হয়েছে 0.322 $mSvy^{-1}$। গড় রেডিয়াম তুল্য কার্যকারিতা পাওয়া গেছে 190.15 ± 26.74 $Bqkg^{-1}$ যেটি বিশ্ব স্বীকৃত মান 370 $Bqkg^{-1}$ এর চেয়ে কম। পরীক্ষাকৃত নমুনাগুলির সারগুলিতে ইন্টারনাল হ্যাজার্ড ইনডেক্স (internal hazard index), এক্সটারনাল হ্যাজার্ড ইনডেক্স (external hazard index) এবং তেজস্ক্রিয়তার মাত্রা সুচক (radioactivity level index) যথাক্রমে 0.56 ± 0.034, 0.54 ± 0.08 এবং 0.69 ± 0.10 পাওয়া গেছে। ডায়ামোনিয়াম ফসফেট (ডিএপি) ও বোরন সার ছাড়া নির্ণয়কৃত হ্যাজার্ড প্যারামিটারে একসেস লাইফ টাইম রিস্ক [Excess lifetime cancer risk (ELCR)] পাওয়া গিয়েছে যেটি বিশ্ব স্বীকৃত মানের চেয়ে বেশি, যেখানে জৈব সারে এর মান আদর্শ মানের চেয়ে কম। প্রাপ্ত ফলাফলগুলি থেকে এটা পরিষ্কার যে, পরীক্ষাকৃত সারের নমুনাগুলিতে প্রাকৃতিক রেডিও-নিউক্লাইডগুলোর কারণে কোনো উল্লেখযোগ্য বিকিরণ বিপত্তি নেই, তবে মিওরেট অব পটাশ-তে ^{40}K এর পরিমাণ বেশি পাওয়ার কারণে , ভবিষ্যতে এটা নিয়ে আরও উচ্চতব পরীক্ষার প্রয়োজন আছে। সামগ্রিকভাবে, এই গবেষণায় ব্যবহৃত নয়টি জৈব সারে নির্ণয়কৃত হ্যাজার্ড প্যারামিটার আদর্শ মানের চেয়ে কম হওয়ার কারণে তা ব্যবহারে ঝুঁকি অনেক কম থাকবে।

Table of Contents

Declaration of Candidate i

List of Publications iii

Declaration by the Supervisor x

Acknowledgements xiii

Abstract v

বিমূর্ত vii

Table of Contents viii

List of Figures

List of Tables

Table of Contents

Chapter	Title/Sub Title	Page
Chapter1:	**INTRODUCTION**	01
1.1	Background	01
1.2	Context	10
1.2.1	Biological Effects of Radiation	10
1.2.2	Role of Free Radicals on Radiation Damage	16
1.2.3	DNA Damage Caused by Ionizing Radiation	17
1.2.4	Effects of Ionizing Radiation on the Human Body	19
1.2.5	Effects of Ionizing Radiation on Embryos	21
1.2.6	Health Effects of Low-Level Radiation on Health	22
1.3	Aims and Objectives	23
1.4	Significance, Scope and Definitions	26
1.4.1	Radium equivalent activity (Ra_{eq})	28
1.4.2	Air absorbed gamma dose rate	28
1.4.3	Annual effective dose equivalent (AEDE)	29
1.4.4	External (H_{ex}) and internal (H_{in}) hazard index	29
1.4.5	γ-Radiation hazard index	29
1.4.6	Excess lifetime cancer risk (ELCR)	30
1.5	Thesis Outline	30
Chapter 2:	**LITERATURE REVIEW** [x]	**31**

2.1. General 31

2.2 Review of Previous Works 32

Chapter 3: MATERIALS AND METHODOLOGY 44

3.1 Basic Research Materials 44

3.2 Experimental Investigation 46

3.2.1 High Purity Germanium (HPGe) Detectors 46

3.2.2 Processing of Detector and Associated Electronics 50

3.2.3 Setup of HPGe Detector in Lab 51

3.2.4 P-type HPGe Detector GCD-40 190 51

3.2.5 Instrumental Set up of Gamma-ray Detection Unit Based on P-type 53

HPGe Detector GCD-40 190 in the present work

3.2.6 Multi-Channel Analyser, MCA527 56

3.2.7 Spectra Line GP Process 57

3.3 Research Design 58

3.1 Sample Collection and Preparation 58

3.3.2 Specific Radioactivity measurement in lab by using HPGe detector 61

3.3.3 Pre-sets 68

3.3.4 Pulse height analyser and counting technique 69

3.3.5 Background effect 70

3.3.6 Shielding arrangement of the detector 70

3.3.7 Peak area determination 72

3.3.8 Peak uncertainty 74

3.3.9 Peak centroid 75

3.4 Prior Tasks to be Accomplished 75

3.4.1 Energy Calibration 76

3.4.2 Energy resolution 76

3.4.3 Efficiency Calibration 78

3.4.4 Absolute efficiency 78

3.4.5 Intrinsic Efficiency 79

3.4.6 Full energy photo-peak efficiency 79

3.4.7 The minimum detectable activity 80

3.5 Radiological Parameters 81

3.5.1 Measurement of Activity Concentration 81

Chapter 4 : RESULTS AND DISCUSSION 82

4.1 General 82

4.2. Specific Activity 82

4.3 Radium Equivalent Activity 88

4.4 Hazard Indices 90

4.5 Exposures, Dose Rates And Cancer Risk 94

Chapter 5 : CONCLUSION 103

5.1. General 103

5.2. Key Findings 104

5.3. Limitation of the Study 105

5.4. Recommendation for Further Study 108

References:

Appendix:

List of Figures

Fig. No	Figure Caption	Page No
Fig. 1.1	Decay series of Uranium-235.	04
Fig. 1.2	Decay series of Thorium-232	06
Fig. 1.3	Decay series of Actinium-227	07
Fig. 3.1	A detector block schematic for HPGe γ-rays.	50
Fig. 3.2	Gamma-ray spectrometry system	52
Fig. 3.3	Typical electric configurations diagram for spectroscopy system of HPGE detector use in lab	54
Fig. 3.4	The site where the study was conducted	59
Fig. 3.5	Sample collection from study area.	60
Fig. 3.6	Sample packaging, levelling and coding.	60
Fig. 3.7	Sample weighing by digital balance machine.	61
Fig. 3.8	Analysing the gamma-ray spectrum with Spectra-line GP software.	63
Fig. 3.9	Schematic diagram of HPGe detector unit used in this study	64
Fig. 3.10	Schematic diagram of HPGe detector crystal used in this study	64
Fig. 3.11	Gamma spectrum processing report of background	65
Fig. 3.12	Digital MCA 527	66
Fig. 3.13	Certificate of calibration of slandered calibration.	67
Fig. 3.14	Block diagram of electronic system for Gamma spectrometry	68

Fig. 3.15	Spectrum of TSP sample-05	69
Fig. 3.16	Multi-channel analyser components.	71
Fig. 3.17	Typical spectral peak with parameters used in peak area determination.	74
Fig. 3.18	Energy calibration curve of HPGe γ - ray detector.	77
Fig. 4.1	Average specific activity in studied samples compared to the worldwide average activity in soil reported by UNSCEAR 2000	84
Fig. 4.2	Average radium equivalent activity (Ra_{eq}) in different fertiliser samples.	90
Fig.4.3	Average absorbed dose rate (D_{out}) and annual effective dose equivalent ($AEDE_{outdoor}$) with compared to the worldwide average value reported in UNSCEAR 2000.	96
Fig. 4.4	Indoor dose rate in Fertiliser samples	100
Fig. 4.5	Outdoor dose rate in fertiliser samples.	100
Fig. 4.6	AEDE (indoor) in fertiliser samples.	100
Fig. 4.7	AEDE (outdoor) in fertiliser samples.	101
Fig. 4.8	AEDE in fertiliser samples.	101
Fig. 4.9	ELCR in fertiliser samples	101
Fig. 4.10	Radioactivity level index in Fertiliser samples.	102
Fig. 4.11	Internal hazard index in Fertiliser samples.	102
Fig. 4.12	External hazard index in Fertiliser samples.	102

List of Tables

Table No	Table caption	Page No
Table 3.1	Key feature of MCA527	57
Table: 3.2	Data for energy calibration of the HPGe γ-ray detector	76
Table 4.1	Specific Activity concentrations of ^{226}Ra, ^{232}Th, and ^{40}K in all Fertiliser samples in $Bqkg^{-1}$ nm in all fertiliser samples.	83
Table 4.2	Average specific Activity concentrations of ^{226} Ra, ^{232}Th, and ^{40}K in TSP, MOP, Q-Potash, DAP, GYP, SSP, Organic and BORON fertiliser samples in $Bqkg^{-1}$.	84
Table 4.3	Activity concentrations of ^{226}Ra, ^{232}Th, and ^{40}K in TSP fertiliser samples in $Bqkg^{-1}$.	85
Table 4.4	Activity concentrations of ^{226}Ra, ^{232}Th, and ^{40}K in DAP fertiliser samples in $Bqkg^{-1}$.	86
Table 4.5	Activity concentrations of ^{226} Ra, ^{232}Th, and ^{40}K in MOP fertiliser samples $Bqkg^{-1}$.	86
Table 4.6	Table 4.6. Activity concentrations of ^{226} Ra, ^{232}Th, and ^{40}K in BORON fertiliser samples in $Bqkg^{-1}$.	87
Table 4.7	Specific activity concentrations of ^{226}Ra, ^{232}Th, and ^{40}K in organic fertiliser samples in $Bqkg^{-1}$.	88
Table 4.8	Specific activity concentrations of ^{226} Ra, ^{232}Th, and ^{40}K	88

in Gypsum and SSP fertiliser samples in $Bqkg^{-1}$.

Table 4.9. The average Radium equivalent activity (Ra_{eq}), external hazard index (H_{ex}), Internal hazard. Index, H_{in}, Gamma radiation hazard and index, I_γ in different fertiliser. 89

Table 4.10 The average radium equivalent activity (Ra_{eq}), external hazard index (Hex), Internal hazard index (H_{in}), Radioactivity level index, I_γ in TSP fertiliser. 91

Table 4.11 The radium equivalent activity (Ra_{eq}), external hazard index (H_{ex}), Radioactivity level index, I_γ in DAP fertiliser. 92

Table 4.12 The radium equivalent activity (Ra_{eq}), external hazard index (H_{ex}), Radioactivity level index, I_γ in MOP fertiliser. 93

Table 4.13 The average radium equivalent activity (Ra_{eq}), external hazard index (H_{ex}), Internal Hazard Index $H_{in,}$ Radioactivity level index I_γ in organic Fertiliser. 93

Table 4.14 Air absorbed dose rate and Annual effective dose equivalent at indoor and outdoor, and excess lifetime 95

cancer risk at outdoor in different Fertiliser.

Table 4.15 Air absorbed dose rate and Annual effective dose equivalent at indoor and outdoor, and excess lifetime cancer risk at outdoor in TSP Fertiliser. 97

Table 4.16 Air absorbed dose rate and Annual effective dose equivalent at indoor and outdoor, and excess lifetime cancer risk at outdoor in DAP Fertiliser. 97

Table 4.17 Air absorbed dose rate and Annual effective dose equivalent at indoor and outdoor, and excess lifetime cancer risk at outdoor in Muriate of Potash fertiliser. 98

Table 4.18 Air absorbed dose rate and Annual effective dose equivalent at indoor and outdoor, and excess lifetime cancer risk at outdoor in Boron fertiliser. 98

Table 4.19 Air absorbed dose rate and Annual effective dose equivalent at indoor and outdoor, and excess lifetime cancer risk at outdoor in Gypsum, Simple Super Phosphate and Organic Phosphate Fertiliser. 99

Chapter 1: INTRODUCTION

1.1 BACKGROUND

Earth is continuously surrounded by background and artificial radiation, exposing all living beings to varying levels of radiation. Cosmic radiation and terrestrial radiation is the main source of the natural radiation, where terrestrial radiation emit from earth crust for having radioactive substances. Earth soil and rock act as a source of radioactive substances like uranium, thorium, radium and their daughter products. Our environment receives radon gas from the background radiation. Radioactive materials can pass through living organism as well as it can be absorbed by water. Radon gasses are ingested to most of the organism by inhalation process. Concentration of dose depends on the presence of the radionuclides and their decay products [1].

Outer space acts as a source of natural radiation and it can create ionizing radiation. Earth can get huge amount of cosmic radiation like a uniform storm. Amount of dose depends on the elevation, atmospheric density and magnetic fields of earth. Space can donate high energetic proton, particles and heavy nuclei that compose primary radiation. When cosmic ray interacts with atmosphere, a heavy storm called 'air showers' is created. From this interaction various particles like mesons, proton, electron are created [2].

Entire terrestrial radiation is mainly produced by four decay series: uranium, thorium, actinium and neptunium series. Earth rocks, soil and water are the main sources of terrestrial radiation. It is a major component of background radiation experienced by all living beings on Earth. Uranium (^{238}U) and thorium ^{232}Th can produce alpha radiation **(**α**),** potassium(^{10}K) Beta radiation (β) Gamma radiation (γ) highly penetrating and emitted by isotopes such as uranium and thorium series radionuclides. ^{232}Th, ^{238}U and ^{10}K can produce above 50 nuclide and they can produce α, β and γ radiation. The Thorium (^{232}Th)**,** Uranium (^{238}U)**,** and Actinium (^{235}U) decay series are natural radioactive series with long-

lived parent isotopes. These series undergo sequential radioactive decay, producing a chain of daughter isotopes. For example, ^{232}Th has a half-life of 13.9 billion years, and its decay products form the Thorium series. Similarly, ^{238}U and ^{235}U serve as parents in the Uranium and Actinium series, respectively. Some natural isotopes, such as Rubidium-87 (^{87}Rb), Potassium-40 (^{40}K), Carbon-14 (^{14}C), and Tritium (^{3}H), are not part of any decay series and take part in natural radiation where two radionuclides; ^{14}C and ^{3}H are produced by cosmic ray interactions in the atmosphere. Sources of natural radiation are radiation are cosmic radiation, terrestrial radiation and internal body radiation. Cosmic Radiation is high-energy particles from outer space that interact with the Earth's atmosphere and terrestrial Radiation is emitted by natural radionuclides in soils, rocks, air and water. Internal Body Radiation are naturally occurring isotope in the human body, like Potassium-40, which contributes to internal exposure. These emit alpha (α), beta (β), gamma (γ), and sometimes neutron or X-ray radiation [3].

Various human activities like industrial advancements, nuclear technology, radioactive laboratories, seabed disposal, accidents in nuclear facilities and past nuclear weapons testing, have been creating large presence of radioactivity across the earth. Gradually our habitat earth is going to vulnerable for the living beings for the presence of radioactivity. The pervasive presence of man-made radioactivity reflects humanity's profound and lasting impact on the planet. While nuclear technology has brought benefits in energy and medicine, it’s environmental and health consequences highlight the need for responsible management and global cooperation to minimize further harm. In between 1945 and 1963 various countries extensive atmospheric nuclear weapons tests had been occurred and a vast amount of radionuclide was emitted in the environment like ^{137}Cs, ^{90}Sr, and ^{131}I. Radioactive spread from these tests globally through atmospheric transmission, contaminating soil, sea, and arctic ice. Catastrophic events like the Chernobyl disaster (1986) and Fukushima

Daiichi accident released significant quantities of radioactive materials into the environment. Radionuclides, including iodine-131, cesium-134, cesium-137, and plutonium isotopes, spread across continents via air and water currents. Routine operations of nuclear reactors and fuel reprocessing facilities emit small amounts of radioactive materials into the atmosphere and water systems. While these releases are within regulated limits, their cumulative effects contribute to the global spread of man-made radioactivity. Radioactive isotopes are used in medicine (e.g., cancer treatment), industry (e.g., radiography, smoke detectors), and agriculture (e.g., food irradiation). Improper disposal of radioactive waste from these applications can result in environmental contamination [4].

Prolonged radiation exposure can damage human cells, increasing the risk of cancer and other health issues. Even small doses may harm sensitive organs like the thyroid, lungs, and breasts. Moreover, radiation effects can extend to future generations, as defective genes caused by radiation can be passed down [5].

Uranium is a heavy, naturally occurring metallic element with the atomic number 92. It is a critical component in nuclear science and is notable for its radioactivity, contributing significantly to terrestrial radiation. Uranium exists in various isotopic forms, with three primary naturally occurring isotopes: i) ^{238}U; the most abundant isotope with a half-life of 4.5 billion years ii) Uranium-235 is fissile, meaning it can sustain a nuclear chain reaction. iii) Uranium-234; a trace isotope formed as part of uranium-238's decay series. Uranium is inherently radioactive, emitting alpha particles as it decays. Its isotopes undergo radioactive decay through alpha and beta decay processes, producing a series of intermediate daughter isotopes before stabilizing. This process is a significant source of natural background radiation on Earth. Uranium plays a pivotal role in radioactive decay, particularly through the uranium decay series.

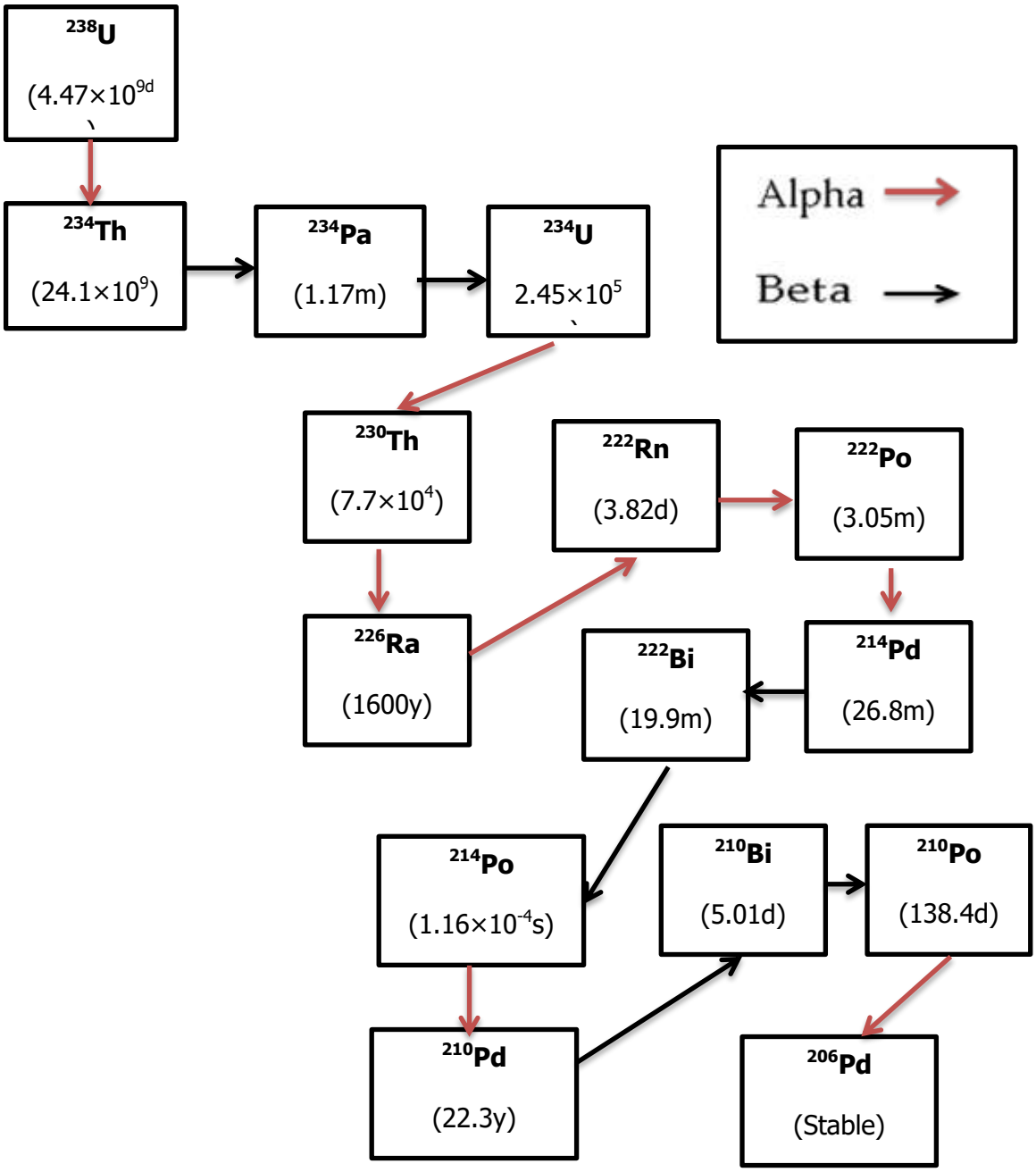

Fig. 1.1 Natural decay series of Uranium-235

This series, also known as the uranium-radium series, starts with uranium-238 and ends with a stable isotope of lead. The decay process involves multiple steps and emits energy in the form of alpha, beta, and gamma radiation is shown in fig 1.1.[6]

The thorium-232 decay series is a sequence of radioactive decay events that begins with thorium-232 and ultimately ends with a stable isotope of lead. This series is a naturally occurring radioactive decay chain and involves multiple intermediate isotopes and the emission of alpha and beta particles is shown in fig.1.2. In earth crust amount of thorium if highest level than any other radionuclide and its half-life is so long. It decays by alpha emission into radium-226**,** which is part of the thorium decay series**.** This series produces other radioactive elements, including radon gas [7].

Actinium emits alpha and beta particles and is highly radioactive, used in research and medicine, such as in targeted alpha therapy for cancer. The actinium decay series is a radioactive decay chain that starts with uranium-235 and ends with the stable isotope of ^{207}Pb, lead is shown in fig.1.3. Actinium's alpha radiation cannot penetrate the skin, but if actinium particles enter the body (through inhalation, ingestion, or wounds), the alpha particles can cause severe damage to cells and tissues. It targets soft tissues, particularly bone tissue, because actinium chemically behaves similarly to calcium and accumulates in bones. Radiation from actinium radioactive materials poses significant risks to health and the environment due to its strong alpha and beta emissions. While its controlled use in medicine holds promise, mishandling or accidental exposure can have severe consequences [8].

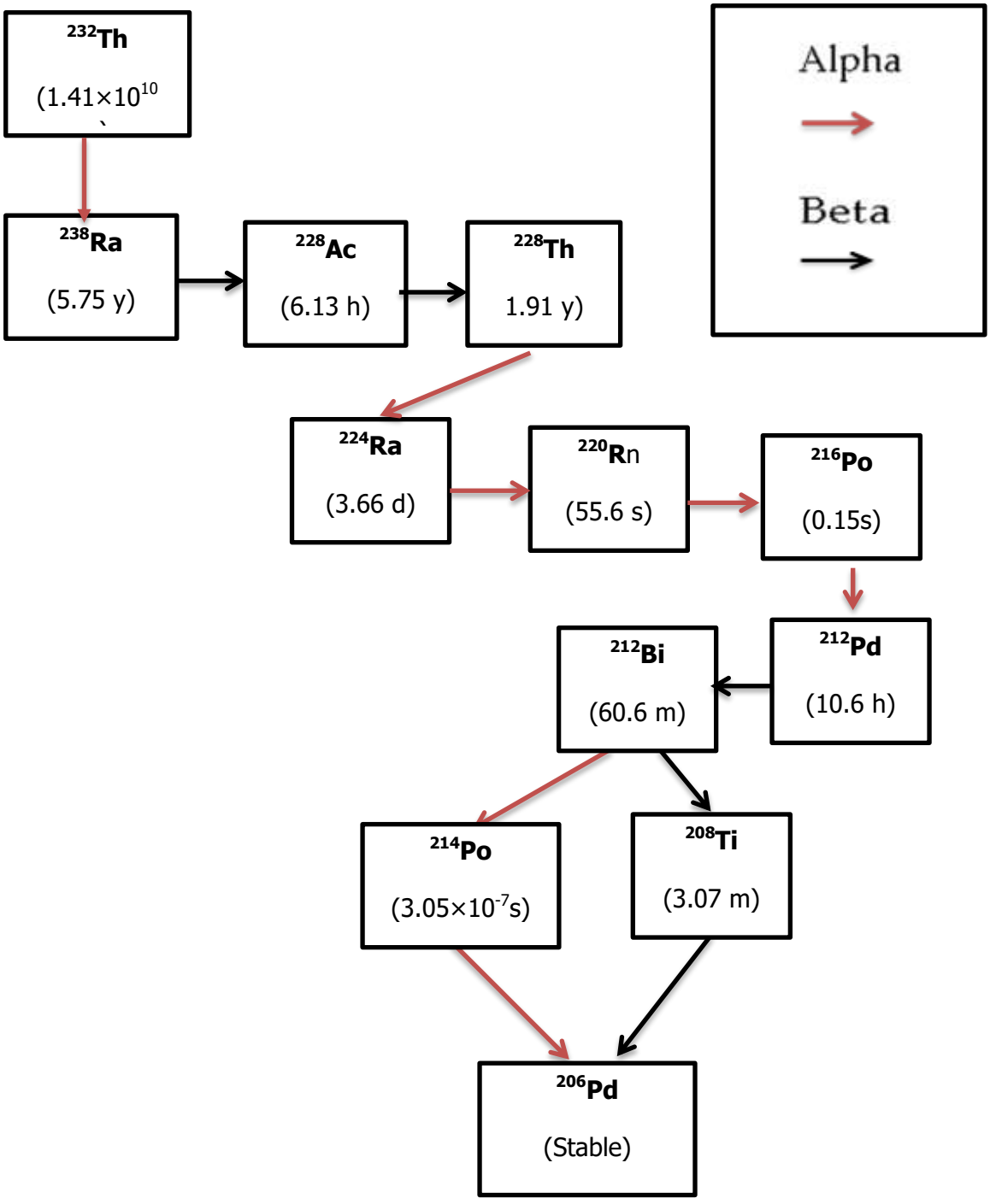

Fig. 1.2 Natural decay series of Thorium-232

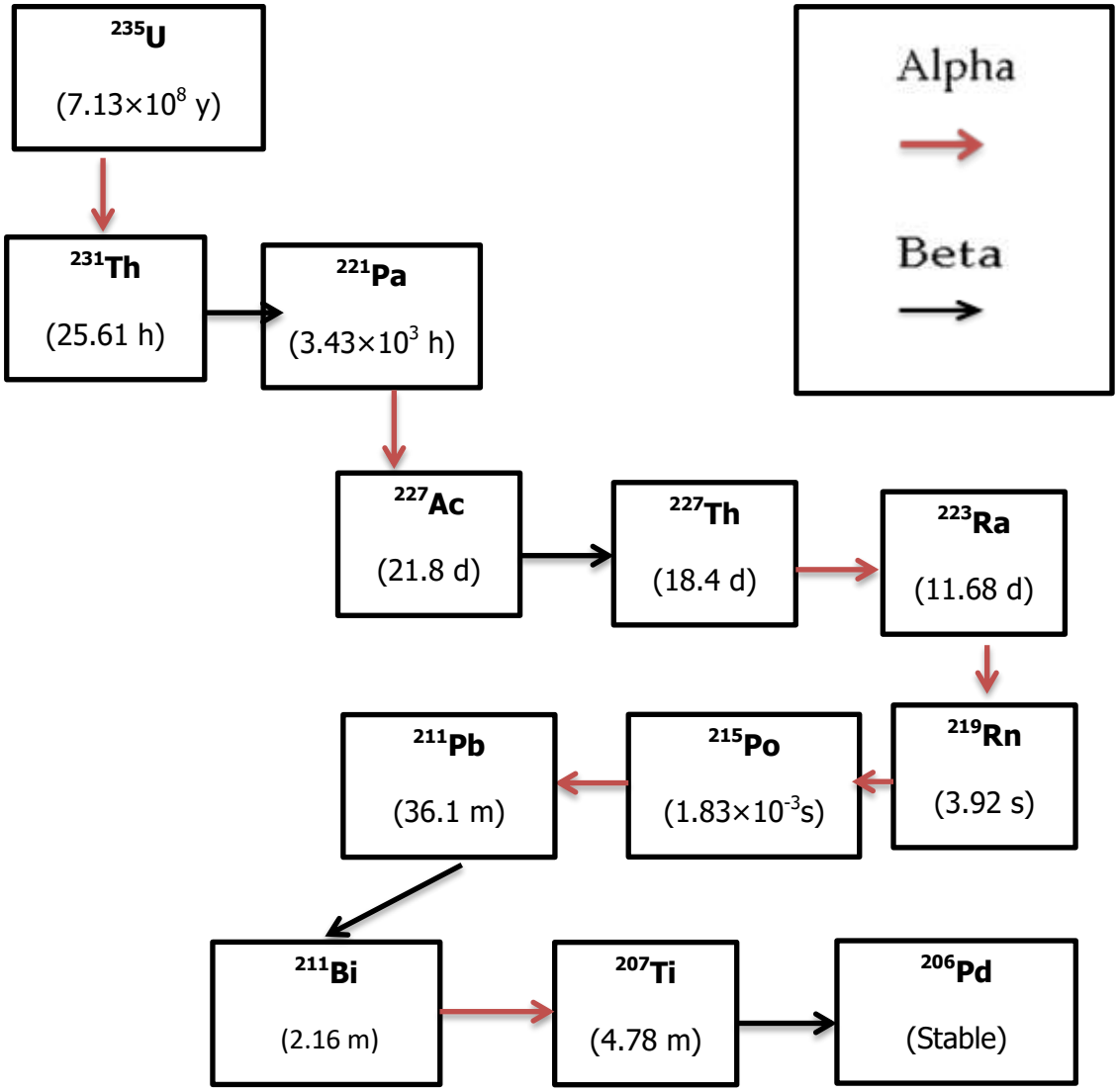

Fig. 1.3 Natural decay series of Actinium-227

In the last decade, Bangladesh has drawn enormous global attention for its remarkable advances in agricultural products, attaining food self-sufficiency and ensuring sustainable food security. To achieve high-yielding varieties of crops for her 168 million population, it is needed to use the same cultivable land at least three times a year. Recurrent use of the land severely depletes the essential nutrients for the plants and consequently lessens the production. To cover up this challenge, it is recommended to use fertilisers for dispensing the

required nutrients in the soil. In 2019, around 5.58 million metric tons of fertilisers were used for growing 41.5 million metric tons of food grain and other harvests. Among the two general categories of fertilisers, inorganic and organic, the former kind mixes with soil at a faster rate. On the other hand, organic or bio or natural fertilisers, which are mostly made from animal manure and plant compost, mixes with the soil at a slower rate. This particular type is good at raising the physical and chemical properties of soil, holding intermediate nitrogen, and controlling over-fertilisation. Then again, chemical fertilisers from potassium ores, nitrogenous compounds, gypsum, alluvial and incendiary rock mostly contain potassium, fluorapatite, goethite, quartz mineral, anatase, magnetite, thorium and uranium. Among these elements, potassium (^{40}K), thorium (^{232}Th) and uranium (^{238}U) are radioactive and capable of producing radioactive progenies like radium (^{226}Ra). Thus, the use of these fertilisers in agricultural activities leads to an increase in radioactivity in soil and the environment. Eventually, these radionuclides will be absorbed by the plant and transferred to the human body through the food chain. Workers in fertiliser production factories and agricultural fields are mostly exposed to gamma radiation externally and the consumers of the final products are expected to have internal exposure by inhalation and ingestion of the radionuclides thrown up from fertilisers. Besides this, human activities of utilising nuclear materials and radiation sources in technology, industry, medicine, and the military are increasing day by day, which is contributing to elevating the terrestrial background radiation level. But it is unpleasant that exposure to ionisation radiation is also one of the reasons for malignant diseases. So, from the perspective of radiation protection, i.e. keeping the exposure level as low as possible, monitoring the radioactivity in one of the widely used commodities like fertiliser is highly regarded. Researchers all around the world, most noticeably from neighbouring countries, have done studies on radionuclide concentrations in fertilisers and related hazards. In this

era of extensive transboundary trading, the quality of crops is one of the priorities. To maintain so, monitoring the constituents in fertilisers and related effects is like solving an issue from the root level. Therefore, it is obligatory to identify and assess the concentration of gamma radiation emitting Naturally Occurring Radioactive Materials (NORM) and artificially produced radioisotopes in numerous fertilisers, which are commercially available in Chattogram, the largest geographical division of Bangladesh. In this study, High Purity Germanium (HPGe) spectroscopy set-up of 40% relative efficiency at Atomic Energy Centre, Chattogram has been used for acquiring data. Afterwards, radiation-induced hazard indices like Radium equivalent activity (R_{aeq}), external hazard index (H_{ext}), internal hazard index (H_{int}), external (γ-radioactivity) level index (I_{γ}), annual effective dose equivalent (AEDE) and excess lifetime cancer risk (ELCR) were estimated. The obtained results were compared with other research of a kind from different parts of the world and were justified with safety standards suggested by the United Nations Scientific Committee on the Effects of Atomic Radiation (UNSCEAR). Thus, the output of this research could contribute to making the baseline data of health risks due to radiation from fertiliser, establishing a justified regulatory framework, and further awareness of using those fertilisers.

1.2 CONTEXT

1.2.1 Biological Effects of Radiation

We are surrounded by an environment that contains low levels of ionizing radiation, which has been a part of Earth's composition since its formation. Both living and non-living entities are continuously exposed to this type of radiation. Ionizing radiation can originate from nuclear or extra-nuclear sources and is classified into directly ionizing radiation, such as α, β, $^{1}H(P)$, and $^{2}H(D)$, and indirectly ionizing radiation, such as X-rays, γ-rays, and neutrons. Although α-particles have a very short range, their biological impact is approximately twenty times greater than that of β- or γ-rays. β-particles have a longer range than α-particles but a significantly shorter range than γ-rays. Since γ-photons lack an electric charge, they are generally unaffected by electric and magnetic fields. Additionally, γ-rays encounter minimal obstruction due to their lack of rest mass, giving them a longer range and the ability to cause ionization at any point within the human body. This study primarily focuses on assessing the radiation dose to the population of Bangladesh caused by γ-emitting radionuclides present in the environment [9].

Ionizing radiation can easily interact with various material and can change the molecular pattern. This type of radiation damages molecular patterns by transferring energy to molecules, which results in the emission of electrons. In biological systems, ionization causes electrons to be released from water molecules, leading to oxidation processes that can modify molecular structures. Consequently, ionizing radiation poses significant risks to living organisms, potentially causing genetic and somatic effects in the human body. Due to the presence of environmental radiation, both human and animal bodies are continuously exposed to its effects.

Ionizing radiation primarily interacts with atoms through ionization, which serves as the basis for all biological damage. These effects can be classified as direct or indirect. Direct effects occur when radiation interacts with critical

components such as DNA, potentially disrupting cellular reproduction and survival. Indirect effects arise when radiation interacts with water, leading to the production of toxic substances like hydrogen peroxide, which can harm cells.

Cells exhibit varying sensitivity to radiation, largely determined by their rate of reproduction. Rapidly dividing cells, such as lymphocytes and blood-producing cells, are most sensitive, while slower-reproducing cells, like nerve and muscle cells, are less affected. Although cells have a remarkable ability to repair damage, severe exposure can lead to cell death or mutations. Mutated cells may reproduce, perpetuating the mutation and potentially initiating malignant tumours.

Ionizing radiation can have profound and potentially harmful effects on biological tissues. These effects are primarily due to the ionization process, in which radiation ejects electrons from atoms or molecules. A common target for this interaction within biological systems is water, as it constitutes the majority of cellular content. When ionizing radiation interacts with water molecules, it can lead to the formation of highly reactive species such as free radicals, including hydroxyl radicals (OH) and hydrogen atoms (H). These reactive species can initiate a cascade of chemical reactions that significantly alter the molecular structure and function of cellular components [10].

The oxidative damage caused by these reactive species can disrupt cellular processes by damaging proteins, lipids, and, most critically, DNA. This damage to DNA can result in mutations or interfere with the cell's ability to replicate accurately. Depending on the extent and location of the damage, cells may repair the injury, lose their ability to function, or undergo apoptosis (programmed cell death). If the repair mechanisms fail, the mutations may accumulate, potentially leading to somatic effects such as the development of cancer or genetic effects that could affect future generations.

The somatic effects of ionizing radiation are often severe, as they can impact the overall health and functionality of the exposed organism. Acute exposure to high doses can cause immediate health problems, such as radiation sickness, while chronic exposure to lower doses over time can increase the risk of developing long-term conditions like cancers. Genetic effects, on the other hand, involve changes in the hereditary material that can be passed on to offspring. These effects may result in congenital disabilities or predispose future generations to certain diseases [11].

Ionizing radiation's impact on biological tissue underscores its dual role as both a powerful scientific tool and a significant health risk. Its ability to cause severe somatic and genetic effects necessitates careful management and protective measures to minimize exposure, particularly in environments where radiation is frequently encountered, such as medical imaging, nuclear energy production, or space exploration [12].

The interaction of ionizing radiation with matter can be understood through three primary mechanisms: the photoelectric effect, the Compton Effect, and pair production. Each of these processes describes a distinct way in which radiation interacts with atoms, leading to ionization or energy transfer. Let us delve into each process for a comprehensive understanding.

The photoelectric effect occurs when a photon interacts with an atom and transfers all its energy to an electron, ejecting the electron from the atom. This process primarily involves photons of low to moderate energy, such as X-rays or gamma rays. The ejected electron, known as a photoelectron, carries away the energy imparted by the photon, minus the energy required to overcome the binding energy of the electron within the atom [13].

This process is highly dependent on the atomic number of the material, with higher atomic number elements being more likely to undergo the photoelectric effect. For example, in biological tissues, elements such as calcium in bones have a higher probability of interacting via the photoelectric effect compared to

softer tissues. This property is widely utilized in medical imaging, such as X-ray radiography, to create contrast between different tissue types.

The Compton Effect, also known as Compton scattering, occurs when a photon interacts with a loosely bound or free electron in an atom. In this interaction, the photon transfers only a portion of its energy to the electron, ejecting it from the atom. The photon itself is scattered in a different direction with reduced energy. The Compton Effect is more common at intermediate photon energies and is largely independent of the atomic number of the material. This makes it the dominant interaction mechanism for gamma rays and X-rays in soft tissues. The scattered photons can contribute to background radiation, reducing image quality in medical imaging and posing challenges in radiation protection [14].

Pair production is a process that occurs when a high-energy photon interacts with the strong electric field near the nucleus of an atom. In this interaction, the photon is annihilated, and its energy is converted into a pair of particles: an electron and a positron. This process requires the photon to have energy greater than 1.02 MeV, which is equivalent to the combined rest mass energy of the electron and positron. The electron and positron produced in pair production can further interact with the surrounding matter, contributing to ionization and energy transfer. The positron, being an antimatter particle, will eventually annihilate with an electron, producing two gamma photons in the process. Pair production is significant in high-energy physics and in environments involving very high-energy radiation, such as particle accelerators or cosmic ray interactions[15].

Energy is transferred from the incident photon to the interacting medium and electron absorbed energy. Secondary photons and high energy electrons are being made from the product of each interaction. For the deposition of energy in matter all highly electron is responsible [16].

When ionizing radiation, such as X-rays or gamma rays, interacts with body tissue, it transfers a portion of its energy to the tissue. This energy transfer,

referred to as energy deposition, can lead to biological and potentially harmful effects. The extent of the energy absorbed by the tissue is expressed as the absorbed dose, which is scientifically defined as the amount of energy absorbed per unit mass of the material, typically measured in units of grays (Gy), where 1 Gy equals 1 joule per kilogram [17].

The relationship between the absorbed dose and the resulting biological damage is highly intricate. Several factors play a crucial role in determining the severity and nature of the effects. Different types of ionizing radiation, such as alpha particles, beta particles, gamma rays, or neutrons, interact with biological tissues in distinct ways. For instance, alpha particles deposit energy over short distances and cause dense ionization, leading to significant localized damage. In contrast, gamma rays and X-rays have greater penetration power but create less localized ionization. The energy level of the radiation impacts how deeply it penetrates and the amount of energy it deposits within the tissue. High-energy radiation may pass through tissues with less energy deposition, while lower-energy radiation may deposit more energy locally, increasing the risk of damage. Tissues and organs have varying sensitivities to radiation. Factors such as the rate of cell division, oxygen content, and the tissue's ability to repair damage influence vulnerability. For example, rapidly dividing cells, such as those in bone marrow or the gastrointestinal lining, are more susceptible to radiation-induced harm compared to non-dividing cells.

This complexity makes the prediction of biological effects from a specific absorbed dose challenging and necessitates the use of additional concepts like dose equivalent (measured in sieverts, Sv), which considers the biological effectiveness of different radiation types. Understanding the absorbed dose and its interaction with biological systems is fundamental to radiation protection, medical imaging, and radiotherapy [18].

Biological damage from radiation results from interactions at the cellular and molecular levels. Ionizing radiation interacts with atoms in the cells, primarily

those of low atomic number, such as carbon (C), hydrogen (H), oxygen (O), and nitrogen (N). These atoms are the fundamental building blocks of biological molecules, including DNA, proteins, and lipids, all of which are essential for cellular structure and function. When radiation interacts with these atoms, it can cause ionization and the formation of free radicals, initiating a chain reaction of chemical and biological changes.

The adult human body, composed of approximately 10^{14} cells, serves as a highly intricate system in which each cell plays a role in maintaining homeostasis. Radiation-induced damage to individual cells may disrupt these functions. For instance, DNA damage caused by radiation can result in mutations, cell death, or changes in cellular reproduction. These effects can accumulate over time, leading to significant health impacts such as tissue dysfunction, cancer, or hereditary effects in future generations [19].

The extent of biological damage depends not only on the absorbed dose but also on the sensitivity of the specific tissue or cell type to radiation. Actively dividing cells, such as those in the bone marrow, gastrointestinal tract, or reproductive system, are more vulnerable to radiation than non-dividing cells like nerve or muscle cells. This variability underscores the complexity of radiation's effects on biological tissues [20].

Biological tissue consists primarily of water, comprising approximately 70% of its composition, while the remaining 30% is made up of macromolecules such as proteins, lipids, carbohydrates, and nucleic acids, along with various other elements. A cell, the fundamental unit of life, has three main components: the nucleus, cytoplasm, and membrane. The cytoplasm is a fluid-filled region that surrounds the nucleus and is encased by a protective membrane. The nucleus contains chromosomes, which are composed of DNA (deoxyribonucleic acid). DNA is the molecular blueprint of life, storing genetic information in genes—segments of DNA that carry hereditary codes.

The primary role of chromosomes and their genes is to transmit genetic information from one generation to the next, ensuring continuity of life. Because DNA is central to the maintenance and propagation of life, it is especially vulnerable to the effects of ionizing radiation. The structure of biological tissues, including cells, is held together by covalent bonds. When ionizing radiation interacts with these cells, it disrupts these bonds, leading to ionization and the formation of free radicals and ions.

Water, being the most abundant molecule in biological tissues, is particularly affected by ionizing radiation. Radiation can split water molecules into free radicals, such as hydroxyl radicals (OH) and hydrogen atoms (H). These reactive species can damage surrounding molecules, including DNA, proteins, and lipids, initiating a cascade of chemical reactions. The damage to DNA is of particular concern, as it can result in mutations, cellular dysfunction, or death[21].

The biological changes induced by ionizing radiation at the molecular and cellular levels can manifest later as clinical symptoms. These symptoms may range from acute effects, such as inflammation and cell death, to long-term consequences like cancer or hereditary genetic disorders. The extent of damage depends on factors such as the dose of radiation, the type of radiation, and the sensitivity of the tissue or cell type [22].

1.2.2 Role of Free Radicals in Radiation Damage

Ionizing radiation generates free radicals, which are molecules with an unpaired electron. This unpaired electron makes free radicals highly reactive and chemically unstable. Due to their reactivity, these free radicals interact with a variety of inorganic and organic molecules, including proteins, lipids, and carbohydrates. Notably, they target essential biological components such as cellular membranes and nucleic acids, leading to significant molecular damage[23].

Free radicals can initiate autocatalytic reactions, turning the molecules, they interact with into new free radicals and amplifying the chain of damage. These reactive species primarily target cellular membranes, lipids, sulfhydryl groups in proteins, and nucleotides. In the presence of oxygen, they can trigger lipid peroxidation in cellular and organelle membranes, leading to structural and functional damage to components like the endoplasmic reticulum, mitochondria, and other microsomal structures. When radiation interacts with biological tissues, it generates free radicals, which then react with various organic compounds. As a result, organic molecules, including hydrocarbon chains, undergo significant damage [23].

1.2.3 DNA Damage by Ionizing Radiation

DNA is composed of polynucleotides, consisting of two long chains that are susceptible to damage by ionizing radiation. Each DNA molecule is made up of numerous units known as nucleotides, which comprise three main components: a nitrogenous base, a sugar molecule (deoxyribose), and a phosphate group. DNA contains four nitrogenous bases: adenine (A), guanine (G), thymine (T), and cytosine (C). These bases store genetic information in a precise sequence. Adenine and guanine belong to the purine group, whereas thymine and cytosine are categorized as pyrimidines.

The two DNA strands run in opposite directions and are connected by hydrogen bonds between complementary base pairs—adenine pairs with thymine, and guanine pairs with cytosine. The strands twist into a right-handed double helix, where ten nucleotide pairs form one complete turn. During cell division, the DNA strands separate, and each serve as a template for synthesizing a complementary strand through specific base pairing. This process ensures the accurate replication and transmission of genetic information to daughter cells.

The human genome demonstrates remarkable complexity, with each haploid set comprising approximately 3 billion (3×10^9) base pairs [24].

A specific segment of DNA within chromosomes serves as a blueprint, carrying the genetic instructions essential for determining heritable characteristics in cells. This "genetic blueprint" is encoded within the DNA molecule, which forms part of the chromosome structure. Each chromosome contains a portion of the DNA double helix, where the genetic message is encoded by the sequence of purine (adenine and guanine) and pyrimidine (thymine and cytosine) bases in the nucleotide chain.

The genetic code specifies the arrangement of amino acids in proteins synthesized by the cell. This information is conveyed to the cytoplasm, where protein synthesis occurs, via messenger RNA (mRNA). The proteins produced include enzymes, which regulate the cell's metabolism. A gene is defined as the smallest functional unit of DNA required to specify a single peptide molecule. However, the protein encoded by a gene may serve as a precursor to multiple physiologically active proteins. Genes also contain promoter regions, which are DNA sequences that initiate RNA synthesis. Mutations, which involve changes in the DNA base sequence, can be caused by ionizing radiation or other mutagenic factors. The human genome comprises approximately 3 billion base pairs and contains an estimated 50,000 to 100,000 genes [25].

Ionizing radiation can directly or indirectly cause changes in the nucleotide base sequences of DNA through the action of chemical radicals. These alterations, collectively referred to as mutations or DNA damage, disrupt the genetic code. If not adequately repaired, such damage can lead to cellular dysfunction and impaired DNA replication, potentially altering the genetic information transmitted to progeny cells.

While cells possess efficient DNA repair mechanisms, these processes are not entirely error-free. Although most DNA damage is successfully repaired, some damage may remain unrepaired or only partially resolved, leading to long-term consequences for the affected cell and its descendants. Severe cases may involve breaks in both strands of the DNA molecule, potentially resulting in

chromosomal fragmentation. If the damage is limited to a single strand, repair may occur through unscheduled DNA synthesis, a process outside the standard DNA replication cycle [26].

1.2.4 Effects of Ionizing Radiation on Human body

When ionizing radiation passes through the human body, it interacts with cells and can damage cellular structures and genetic material. If a damaged cell fails to undergo proper repair, it may result in a mutated cell with altered DNA. Such mutations can lead to harmful effects. Broadly, the biological effects of radiation are categorized into somatic and genetic effects. The health effects of ionizing radiation are typically classified as either stochastic or deterministic. The impact of radiation on biological tissues depends on several factors, including: (a) The type and energy of the radiation, (b)The dose rate,(c)The volume of tissue exposed, and (d)The sensitivity of the tissue to radiation. Deterministic effects arise when radiation exposure surpasses a defined threshold, with the severity of the effects increasing in proportion to the dose received. For instance, skin reddening (erythema) is a deterministic effect that typically occurs at a threshold dose of about 300 rad (3 Gy). Deterministic effects are often short-term health consequences. In contrast, stochastic effects, such as cancer, do not have a threshold and are probabilistic in nature. The damage caused by ionizing radiation can be classified into somatic effects, which impact the individual exposed, and genetic effects, which may be passed on to future generations [27].

The impact of ionizing radiation on the human body stems from damage inflicted on individual cells. These effects are broadly categorized into somatic effects, which impact the individual exposed, and genetic effects, which may affect future generations. Such effects can result from both acute and chronic radiation exposure [17].

The human body's organs and tissues exhibit a variety of responses to ionizing radiation, which can occur at different rates. Some reactions, such as the

immediate killing of cells in exposed tissues, may become evident within minutes after exposure. On the other hand, long-term effects, including tissue degeneration, scarring, and breakdown, may take months or even years to develop. Radiation exposure causes somatic effects, which directly impact the individual exposed. These effects may manifest after a latent period of years or decades, with cancer being a significant stochastic outcome. Acute or chronic radiation exposure can damage human body cells, leading to somatic effects that are influenced by factors such as oxygenation, temperature, and metabolic activity.

Genetic effects refer to changes in chromosome structure or variations in the germ cells (sperm or ova). These mutations may be passed on to subsequent generations, posing long-term risks. Ionizing radiation can directly interact with genetic material, causing mutations in a dose-dependent manner. The relationship between dose and effect is typically linear, with no threshold, meaning any level of exposure carries a risk of genetic mutation. Natural background radiation contributes to spontaneous mutations, with estimates ranging from 4% to 40% of all genetic changes. Acute genetic effects often appear within weeks of exposure, while stochastic effects, such as genetic mutations, may take longer to manifest [28]. These are bodily effects and inevitable. The immediate results manifest as: chromosome aberration, blood changes, nausea, vomiting, diarrhoea (NVD), loss of appetite, fatigue, epilation, skin erythema, sterility, etc. and death [17]. There is no clearly established threshold dose below which the risk of death from acute radiation exposure can be ruled out, nor is there a precise dose above which death is guaranteed. However, survival becomes highly unlikely when the dose reaches approximately 8 Gy [29].

The effects of radiation exposure can result from either acute or chronic exposure, often manifesting several years after the initial exposure. These effects include various cancers, leukaemia, cataracts, and genetic disorders.

While no threshold dose exists below which there is no risk of cancer or hereditary damage, the threshold dose for cataract development over a working lifetime is approximately 15 Sv. Radiation effects on the human body are categorized into two types: (a) Stochastic Effects (b) Non-Stochastic Effects. Stochastic Effects do not have a clearly defined threshold dose and can occur at any level of exposure. The likelihood of stochastic effects, such as cancer and genetic mutations, increases with the absorbed dose. For example, occupational radiation exposure and therapeutic radiation provide data supporting the linear increase in risk with dose. Non-Stochastic Effects also known as deterministic effects; these have a well-defined threshold dose. Such effects only occur when the exposure exceeds a certain level, and their severity increases with the dose. Examples include early effects like nausea, vomiting, diarrhoea, and cataract formation [30].

1.2.5 Effects lionizing Radiation on Embryo

The effects of ionizing radiation on the developing embryo are typically referred to as embryonic effects. Radiation exposure during this stage can significantly impact embryonic development due to the high sensitivity of fatal tissues. These tissues are composed of immature, undifferentiated cells that are rapidly dividing, making them highly vulnerable to radiation damage. Even the loss or mutation of a small number of these cells can result in irreversible harm. Such effects can manifest at any stage of embryonic development, from the zygote to the foetus, and may include malformations, lethality, intellectual disabilities, cancer, and other malignancies[31]. The most severe deterministic effects are often observed during critical periods of organogenesis, particularly between the second and twelfth weeks of gestation, when organ systems are forming. Congenital disabilities are typically observed in children who were exposed to radiation doses between 0.1 and 0.2 Gy throughout pregnancy [32].

1.2.6 Health Effects of Low-Level Radiation

There is no definitive threshold dose below which the induction of various adverse health effects, such as cancer, life-shortening conditions, leukaemia, or hereditary disorders, caused by ionizing radiation can be ruled out. This indicates that even exposure to low levels of radiation carries a certain probability of inducing these conditions, though the likelihood is extremely low. The absence of a safe threshold underscores the potential risk associated with minimal radiation exposure [33]. Radiobiological models and estimates for low-level radiation exposure, such as 1 mSv per year. Lifetime Probability is the probability of developing a health effect from low-level radiation exposure over a lifetime is estimated at 0.5%. This reflects the increased risk of cancer and other radiation-induced diseases over the span of an individual's life due to prolonged or continuous exposure [33].

Radiobiological models have been developed to estimate the potential health impacts of low-dose radiation exposure, with an annual dose of 1 mSv often used as a reference level for these calculations. The lifetime probability of developing radiation-induced health effects, including cancer, from such low-level exposure, is estimated at approximately 0.5%. This figure reflects the cumulative risk associated with long-term or continuous exposure to low doses of radiation over an individual's lifetime [34].

The risk of cancer and other radiation-induced diseases correlates with the dose absorbed by the body. While the probability of harm from low doses is small, it is not negligible. For this reason, regulatory bodies such as the International Commission on Radiological Protection (ICRP) and the United Nations Scientific Committee on the Effects of Atomic Radiation (UNSCEAR) emphasize the importance of the ALARA principle (As Low As Reasonably Achievable) to minimize exposure and reduce potential risks, even at low levels [35].

1.3 AIMS AND OBJECTIVES

Due to increasing crop yields all over the world, production of fertilisers is increasing gradually to fulfil the demand of farmers. But the most probable risk factor is that there are more impurities of radioactive isotopes in the fertiliser products. Raw materials are used in fertiliser industries like phosphate rock, phosphonium and potassium composition material. Generally, fertilisers are mainly composed of nitrogen, phosphorus and potassium exigent elements for plant yields. The phosphorus portion comes from phosphate rocks, which hold many radionuclides. For long time uses of fertilisers, it will be contaminated with radionuclides and their radiation which gradually increases than natural origin. The wide use of fertilisers is the leading cause of enhancing radionuclides in soil and underground water [36].

In last 20 years, Bangladesh has garnered significant global attention for its remarkable progress in agricultural production, achieving food self-sufficiency and ensuring sustainable food security for its population of around 170 million [37]. To achieve high crop yields for this population, cultivable land needs to be utilized at least three times a year. However, the repeated use of land severely depletes essential nutrients, leading to decreased production. To address this challenge, the use of fertilisers is recommended to supply the required nutrients to the soil.

In 2019, approximately 5.58 million metric tons of fertilisers were used in Bangladesh to cultivate 41.5 million metric tons of food grain and other crops [38]. Fertilisers can be categorized as inorganic and organic, with the former type mixing with the soil at a faster rate. Organic or natural fertilisers, mainly derived from animal manure and plant compost, are mixed with the soil at a slower rate. Organic fertilisers are beneficial for improving the physical and chemical properties of the soil, retaining intermediate nitrogen levels and preventing over-fertilisation. Chemical fertilisers, composed of potassium ores, nitrogenous compounds, gypsum, alluvial and igneous rock, typically contain

elements such as potassium (^{40}K), thorium (^{232}Th) and uranium (^{238}U). These elements are radioactive and capable of producing radioactive progenies like radium (^{226}Ra).

The application of chemical fertilizers in farming has been found to lead to heightened levels of radioactivity in the soil and its environment. These fertilizers, especially those with phosphate content, frequently contain trace quantities of naturally occurring radionuclides such as uranium, thorium, and their decay products like radium. When these fertilizers are spread across agricultural lands, the radionuclides become part of the soil structure, gradually increasing its natural radioactivity levels. As plants develop, they take up nutrients from the soil, including the radionuclides present. These radionuclides are then integrated into the plant's composition, encompassing roots, leaves, and fruits. Through the food web, radionuclides enter the human body when people consume contaminated plants directly or indirectly, for example, via livestock that have grazed on the tainted crops. This process of bioaccumulation poses potential health risks, as prolonged exposure to radionuclides can result in internal radiation exposure, raising the chances of harmful biological effects, including cellular damage and the possibility of cancer development. Effective monitoring of fertilizer composition and the adoption of sustainable agricultural practices are essential to minimize the accumulation of radionuclides in the environment and their subsequent transfer through the food chain [39]. Workers in fertiliser production factories and agricultural fields are primarily exposed to external gamma radiation, while consumers of the final products may experience internal exposure through inhalation and ingestion of radionuclides emitted from fertilisers. Human activities that involve nuclear materials and radiation sources, which occur in various fields including technology, industry, medicine, and the military, lead to an increase in background radiation levels. The link between exposure to ionizing radiation and the development of cancer and other malignant diseases

is well-documented. As a result, it is crucial to monitor radioactivity in commonly used products like fertilizers to ensure radiation safety and reduce exposure. Worldwide studies conducted by researchers have investigated radionuclide levels in fertilizers and the related risks [40]. These radionuclides enter the human body via soil and drinking water, becoming integrated into the food chain. A major concern is the accumulation of the highly radioactive ^{226}Ra isotope in bone marrow, which can lead to significant biological harm. Individuals working in agricultural production and distribution, such as factory employees and farmers, face heightened exposure risks to these radionuclides. Studies indicate that these workers are susceptible to radiation emissions due to radionuclide contaminants present in fertilizers. External exposure mainly occurs through gamma radiation, while internal exposure is a result of inhaling alpha particles emitted by radon and its decay products. Alpha particles represent a direct health hazard when taken up by specific tissues. In the context of fertilizers that contain radioactive elements, these particles may accumulate in sensitive tissues such as the bronchial epithelium in the lungs, resulting in cellular damage. Over an extended period, this concentrated exposure raises the risk of developing lung cancer due to radiation-induced mutations. Fertilizers, especially those based on phosphate, might include naturally occurring radioactive materials (NORMs) like uranium, thorium, and radium. When such fertilizers are applied, radioactive decay leads to the release of alpha particles, which can be inhaled as part of airborne dust or accumulate in the environment. Upon inhalation, alpha particles have a strong interaction with lung tissues, causing cellular damage and heightening the chance of cancer development, particularly lung cancer. Given the severe health risks posed by these radioactive substances, it is essential to continuously monitor natural radioactivity levels in fertilizers as part of a thorough radiation protection strategy. Establishing regulatory standards for safe radioactivity levels in agricultural products, along with regular testing of fertilizers, can assist in

minimizing these risks. Implementing such actions is crucial for safeguarding public health and reducing the likelihood of cancers resulting from agricultural practices [41].

Hence our aim is to assess the radioactivity level in organic and inorganic fertilisers those are frequently used in agricultural purposes in Chattogram area as well as to measure related hazard indices.

1.4 SIGNIFICANCE, SCOPE AND DEFINITIONS

The existence of radioactive isotopes, referred to as radionuclides, in fertilizers presents major concerns due to the potential dangers they pose to human health and the environment. Radionuclides release radiation as they decay, and if these substances contaminate fertilizers, they can transfer to soil, crops, and water sources, threatening ecosystems and human health. It is essential to detect radionuclides in fertilizers for several reasons. The radiation emitted by radionuclides can damage living cells, raising the risk of cancer and other health issues if consumed through contaminated crops. Moreover, radionuclide contamination can linger in soil for long periods, disrupting natural processes and putting wildlife and water sources at risk [42].

Regulatory authorities depend on the identification of radionuclides to implement safety standards for fertilizers before they are distributed for agricultural purposes. Various factors, such as the level of radioactivity in the fertilizer and the specific radionuclides involved, help in accurately evaluating potential dangers. Additionally, assessing radiation doses from exposure to radionuclides in fertilizers takes into account aspects like the type of radiation and exposure routes. The hazard index consolidates these elements to thoroughly assess the overall risk of radionuclide contamination in fertilizers, factoring in elements such as activity concentration and exposure pathways [43].

Through the assessment of these factors and the calculation of hazard indices, regulators and stakeholders can be informed about the safe use and disposal of

radionuclide-contaminated fertilizers, ultimately protecting human health and the environment from the threats linked to radioactive contamination. In our country, farmers rely on a variety of chemical and organic fertilizers for crop production. In 1997, Alam et al. conducted a study in Bangladesh on eight fertilizers and discovered elevated levels of ^{40}K radionuclide in MOP fertilizer, while the other seven fertilizers contained ^{226} Ra, ^{238}Th, and ^{40}K radionuclides at levels below the global recommended limits. Even after 27 years, it remains crucial to analyse the presence of radionuclides in various fertilizers [44].

In Bangladesh, the use of phosphate fertilizers has been instrumental in achieving a significant increase in agricultural output. This increase in productivity can be attributed to the widespread adoption of phosphate fertilizers, which are favoured for their cost efficiency and impressive yields. In recent years, the consumption of these fertilizers has skyrocketed, driven primarily by the economic advantage of low-cost fertilizers. This increase in phosphate fertilizer use, especially those that are imported and contain natural radionuclides, has resulted in a noticeable change in the radiological profile of Bangladeshi soil. The degree of this change depends on the application rates of these fertilizers.

Given these circumstances, it is essential to carry out a comprehensive evaluation of the radiological risks posed by fertilizers in Bangladeshi agricultural soils, particularly concerning health effects. Therefore, this study aims to assess the influence of fertilizers on radiation levels in the soil. It also seeks to examine the potential health risks associated with these modified soil conditions, particularly for those involved in agricultural work.

The rapid and considerable adoption of phosphate fertilizers, along with their varied radionuclide content, highlights the necessity for a detailed investigation of their radiological effects on soil and, in turn, on the health of those engaged in farming. By methodically exploring and measuring possible risks, this study aims to provide valuable insights into the complex relationship between

agricultural practices, fertilizer use, and radiological safety. The results seek to enable informed decision-making for sustainable and health-oriented agricultural practices in Bangladesh.

1.4.1 Radium equivalent activity (Ra_{eq})

The Radium Equivalent Concentration (Raeq) serves as a hazard index for comparing the activity levels of radium, thorium, and potassium in a sample. This index operates under the premise that 370 Bq/kg of ^{226}Ra, 259 Bq/kg of ^{232}Th, and 4810 Bq/kg of ^{40}K generate an equivalent dose of gamma radiation. In this research, Equation (1.1) was utilized to determine the Ra_{eq} value [42].

$$Ra_{\mathrm{eq}} = C_{\mathrm{Ra}} + 1.43C_{\mathrm{Th}} + 0.077 \quad (1.1)$$

In this equation, C_{Ra}, C_{Th}, and C_K represent the specific activities (measured in Bq/kg) of ^{226}Ra, ^{232}Th, and ^{40}K, respectively. The radium equivalent value is pertinent to both external exposure from gamma radiation and internal exposure from alpha radiation due to radon and its decay products. A threshold Ra_{eq} value of 370 Bq/kg has been set, which corresponds to an effective dose of 1.5 mSv y^{-1}.

1.4.2 Air absorbed gamma dose rate

The external gamma radiation doses for outdoor (D_{out}) and indoor (D_{in}) environments were estimated under the assumption that gamma-emitting radionuclides ^{226}Ra, ^{232}Th, and ^{40}K are uniformly distributed in the ground. Additionally, it was assumed that the decay products of ^{226}Ra and ^{232}Th were in secular equilibrium with their parent isotopes. The external dose rate outdoors (D_{out}), representing the gamma radiation exposure in the air at a height of 1 meter above the ground, was determined using the methodology outlined in Equation (1.2) [45].

$$D_{\mathrm{out}} = 0.462\ C_{\mathrm{Ra}} + 0.604CC_{\mathrm{Th}} + 0.041C_{\mathrm{k}} \quad (1.2)$$

Likewise, the γ-ray dose (D_{in}) present in the indoor is calculated using Equation

$$D_{\mathrm{in}} = 0.92\ C_{\mathrm{Ra}} + 1.1C_{\mathrm{Th}} + 0.081C_{\mathrm{k}} \quad (1.3$$

Where D_{out} and D_{in} are in $nGyh^{-1}$.

1.4.3 Annual effective dose equivalent (AEDE)

To estimate the annual effective dose equivalent (AEDE) from natural radioactivity, a conversion coefficient of 0.7 Sv/Gy was applied to assess the associated radiological health risks. It was presumed that an individual's annual occupancy factor, totalling 8760 hours, was distributed as 0.8 indoors and 0.2 outdoors. The AEDE values for outdoor and indoor exposure, expressed in mSv/y, were computed using the following equations [46] .

$$\text{AEDC(Outdoor)} = D_{out} \times 8760 \times 0.2 \times 0.7 \times 10^{-6} \quad (1.4)$$

$$\text{AEDC(indoor)} = D_{in} \times 8760 \times 0.2 \times 0.7 \times 10^{-6} \quad (1.5)$$

In these equations, D_{out} and D_{in} represent the absorbed dose rates in nGy/h, and the factor 10^{-10} is for unit conversion.

1.4.4 External (Hex) and internal (H_{in}) hazard index

The use of materials containing naturally occurring radioactive material (NORM) isotopes is regulated by two dimensionless radiological health hazard indices: the external hazard index (H_{ex}) and the internal hazard index (H_{in}). These indices are critical for ensuring safety against exposure to external gamma radiation and internal exposure from radon and its decay products. To comply with established safety standards, the values of H_{ex} and H_{in} must remain below one. The formulas for Hex and H_{in} are expressed as follows [47].

$$H_{ex} = \frac{C_{Ra}}{370} + \frac{C_{Th}}{259} + \frac{C_K}{4810} \quad (1.6)$$

$$H_{in} = \frac{C_{Ra}}{185} + \frac{C_{Th}}{259} + \frac{C_K}{4810} \quad (1.7)$$

Here, Where C_{Ra}, C_{Th} and C_K represent the specific activity concentrations of ^{226}Ra, ^{232}Th and ^{40}K, respectively. These indices provide a standardized approach to evaluating the radiological safety of materials containing NORM isotopes.

1.4.5 γ-Radiation hazard inde

To assess radiation safety levels, the European Commission introduced an index known as the activity concentration index (or representative level index). This index, denoted as I_γ , is calculated using the following formula [48].

$$I_\gamma = \frac{C_{Ra}}{300} + \frac{C_{Th}}{200} + \frac{C_K}{3000} \quad (1.8)$$

1.4.6 Excess lifetime cancer risk (ELCR)

Excess lifetime cancer risk (ELCR) quantifies the increased probability of developing cancer due to prolonged exposure to ionizing radiation at specific levels. The ELCR is computed using the following equation[49]

$$\mathrm{ELCR} = \mathrm{AEDC} \times \mathrm{DL} \times \mathrm{RF} \quad (1.9)$$

In this formula, AEDE The annual effective dose equivalent for outdoor exposure (measured in mSv/year). DL: Duration of life, assumed to be 70 years, RF: Risk factor, representing the probability of fatal cancer per unit dose of radiation (Sv)

The risk factor (RF) is set at 0.05 Sv^{-1} for the general public, based on the stochastic effects of radiation exposure as recommended by the International Commission on Radiological Protection (ICRP) in its publications [50].This calculation helps estimate the additional risk of cancer associated with long-term exposure to ionizing radiation.

1.5 THESIS OUTLINE

In chapter two a review on available reported and related works has been illustrated from a comparative point of view. Chapter three describes the methodology applied for this study in detail including all instruments and techniques used. Obtained results of this work are presented in Chapter four and discussed them clearly. Overall summary of the work has been composed in brief in Chapter five as the conclusion of this thesis.

Chapter 2: LITERATURE REVIEW

2.1 GENERAL

Since the formation of Earth, natural radioactivity has been an intrinsic feature of the planet. Among the naturally occurring radioactive elements, uranium plays a prominent role. This element is widely distributed in the Earth's crust and is present in soil, water, and various terrestrial materials. Geological and volcanic activities have significantly contributed to the deposition and accumulation of uranium in specific regions, enriching the soil with this radioactive element.

Uranium, along with its decay products (daughter isotopes), tends to concentrate in particular types of rocks and minerals, such as monazite sands and lignite deposits. The accumulation and concentration processes are influenced by diverse chemical conditions, including the pH and redox potential of the surrounding environment. Natural phenomena such as wind, rainfall, and ongoing geological processes further redistribute uranium across the land, rocks, and aquatic ecosystems. These mechanisms ensure that uranium remains a dynamic part of the Earth's geochemical cycles, influencing the composition of soils and sediments worldwide [51].

Uranium presents a significant environmental and health risk due to its potential to dissolve in water, leading to contamination that can enter and affect biological systems. This risk is further exacerbated by human activities, particularly in agriculture, where fertilisers are widely used to enhance crop production. Fertiliser industries have proliferated globally to meet the increasing demand for food production, making them a vital component of modern agriculture.

Fertilisers are primarily composed of nitrogen (N), phosphorus (P), and potassium (K), elements essential for plant growth. The phosphorus component, however, is derived from phosphate rocks, which often contain

elevated concentrations of naturally occurring radioactive isotopes, such as uranium-238 (^{238}U), thorium-232 (^{232}Th), and potassium-40 (^{40}K), along with their radioactive decay products. When these fertilisers are applied to agricultural soils, they contribute to the background levels of natural radioactivity in the environment.

The use of such phosphate-based fertilisers causes variations in soil radioactivity, as the extent of contamination depends on the type and quantity of fertiliser applied. This makes the soil in some areas more radioactive than others, introducing a source of radiation exposure beyond its natural origins. Consequently, monitoring and regulating the use of fertilisers containing radioactive materials is crucial to ensure environmental safety and public health [52].

2.2 REVIEW OF SOME PREVIOUS WORKS

In a study conducted in Egypt by Hassan et al., the concentrations of radionuclides uranium-238 (^{238}U), thorium-232 (^{232}Th), and potassium-40 (^{40}K) were assessed in ten phosphate ore samples and five fertiliser samples. The measurements were carried out using a high-purity germanium (HPGe) detector, a sensitive tool widely used for detecting and quantifying radionuclides. The results revealed that the concentrations of radionuclides in phosphate ore were significantly higher compared to the fertiliser samples, indicating that processing reduced the radionuclide content. For the phosphate ore samples, radium-226 (^{226}Ra), a decay product of ^{238}U, exhibited relatively high concentrations, with a mean value of 871.37 ± 91.90 Bq/kg, while thorium-232 and potassium-40 were present at much lower concentrations of 19.21 ± 2.42 Bq/kg and 176.06 ± 17.66 Bq/kg, respectively. On the other hand, the fertiliser samples showed much lower radionuclide concentrations, demonstrating a reduction in radioactive content during manufacturing. To assess potential radiological hazards, the researchers calculated several indices, including Radium Equivalent Activity (Ra_{eq}). External Hazard Index (H_{ex}), Internal

Hazard Index (H_{in}), Annual Effective Dose. Calculates the radiation dose received by individuals annually from the radionuclides present. Additionally, the study measured radon release from the samples using an Alpha Guard radon monitor, a precise instrument for detecting radon levels. The radon emanation coefficient, which quantifies the proportion of radon escaping from the sample, and the radon exhalation rate, indicating the release rate of radon gas per unit area or mass, were also determined. These measurements provide critical insights into the potential health risks associated with radon exposure from these materials [53].

Hassan et al. conducted a comparative study on the natural radioactivity levels in commonly used fertilisers in Egypt and Japan, focusing on the specific activities of radionuclides such as uranium-238 (^{238}U), thorium-232 (^{232}Th), and potassium-40 (^{40}K). Their research highlighted how agricultural use of fertilisers redistributes these radionuclides in the environment. Using a high-purity germanium detector, they measured the natural radioactivity of radium-226 (^{226}Ra), thorium-232 (^{232}Th), and potassium-40 (^{40}K) in different fertiliser samples.

In Egyptian fertilisers, the specific activities ranged as follows: ^{226}Ra (312 ± 14 to 782 ± 24 Bq/kg), ^{232}Th (not detected to 67 ± 13 Bq/kg), and ^{40}K (88 ± 22 to 251 ± 94 Bq/kg). For Japanese fertilisers, the specific activities ranged from ^{226}Ra (25 ± 1 to 1265 ± 5 Bq/kg), ^{232}Th (5 ± 2 to 15 ± 1 Bq/kg), and ^{40}K (31 ± 5 to 3909 ± 21 Bq/kg). The results indicated that Egyptian fertilisers generally had higher specific radio activities compared to their Japanese counterparts, though all values fell within the recommended limits set by UNSCEAR 2008. Further analysis revealed that the radiological hazard indices—including radium equivalent activities (Ra_{eq}), external hazard index (H_{ex}), internal hazard index (H_{in}), gamma index, absorbed dose rates, and annual effective doses—were significantly higher for Egyptian fertilisers than for Japanese fertilisers. In some cases, these values exceeded the safety thresholds of 370 Bq/kg for radium

equivalent activities, unity for hazard indices, 59 nGy/h for absorbed dose rates, and 480 μSv/year for annual effective doses. These findings underscore the need for monitoring and regulating fertiliser usage to ensure radiation safety [54].

A study by Garcêz et al. investigated the levels of environmental radioactivity in fertilisers from Rio de Janeiro, Brazil, focusing on radium-226 (^{226}Ra), thorium-232 (^{232}Th), and potassium-40 (^{40}K). To measure the specific activities of these radionuclides, the researchers utilized a high-purity germanium (HPGe) detector. Their findings revealed that the specific activity of ^{226}Ra ranged between 1.48 Bq/kg and 597 Bq/kg, while ^{232}Th exhibited a range of 2.66 Bq/kg to 832 Bq/kg. For ^{40}K, the observed specific activity spanned from 16 Bq/kg to 13,941 Bq/kg. Despite detecting these radionuclides in the fertilisers, the study concluded that their levels posed negligible health risks, suggesting minimal radiological hazards to humans and the environment [55].

Alam et al. conducted a study to evaluate the radioactivity concentrations of radionuclides ^{238}Th, ^{226}Ra, and ^{40}K in various fertilisers, including triple superphosphate (TSP), single superphosphate (SSP), muriate of potash, Phosphogypsum, urea, zinc sulphate, and zinc oxysulphide. The activity of ^{226}Ra in these fertilisers was found to range from 4.8 ± 0.8 Bq/kg to 323.8 ± 24.4 Bq/kg, with phosphate-based fertilisers such as TSP, SSP, Phosphogypsum, and DAP showing higher concentrations of ^{226}Ra.For ^{238}Th, the activity ranged between 3.4 ± 1.7 Bq/kg and 22.0 ± 2.8 Bq/kg, while ^{40}K exhibited a broader range from 7.9 ± 2.3 Bq/kg to 12,628.5 ± 169.0 Bq/kg. The radium-to-thorium ratio (^{226}Ra/^{238}Th) in the fertilisers was also calculated, ranging from 0.232 to 18.63 [44].

Taher et al. investigated natural radioactivity levels in chemical factories (ECF) and various fertilisers, including Simple Superphosphate (SSP), Triple Superphosphate (TSP), and Urea, in Egypt. The study revealed that in both organic and chemical fertilisers, the activity concentrations of ^{232}Th were

generally lower than those of ^{226}Ra. In chemical fertilisers, the activity of ^{226}Ra ranged from 21.5 ± 3.6 Bq/kg to 112.2 ± 8.7 Bq/kg, with TSP showing the highest concentration. The average ^{226}Ra activity was reported as 51.1 ± 4 Bq/kg in SSP, 79.2 ± 7.3 Bq/kg in TSP, and 35.2 ± 3.3 Bq/kg in Urea. For ^{232}Th, activity levels varied between 1.4 ± 1.2 Bq/kg and 9.9 ± 3.1 Bq/kg, with the highest concentration observed in SSP. The activity of ^{40}K was notably high in TSP, with a mean activity of 478.2 ± 21.3 Bq/kg. In organic fertilisers, the average activity concentrations of ^{226}Ra, ^{232}Th, and ^{40}K were 40 ± 1.4 Bq/kg, 3.2 ± 1.2 Bq/kg, and 427.1 ± 21 Bq/kg, respectively [56].

Mostafa et al. conducted a study in Upper Egypt to assess the radiological hazard indices and concentrations of natural radionuclides, including ^{232}Th, ^{226}Ra, and ^{40}K, in seven types of chemical fertilisers commonly used in the region. The concentration levels of these radionuclides were found to range from 3 ± 0.2 to 98 ± 4.8 Bq/kg for ^{232}Th, 12 ± 0.6 to 245 ± 12.5 Bq/kg for ^{226}Ra, and 107 ± 5.5 to 671 ± 33 Bq/kg for ^{40}K. Additionally, the radiological parameters calculated from the fertiliser samples showed ranges of 0.5 to 2.4 nGy/h for the dose rate, 33.1 to 392.3 Bq/kg for radium equivalent activity, 20.2 to 227.2 μSv/year for annual effective dose equivalent (AED), and 15.6 to 176.7 nGy/h for the gamma radiation hazard index (Iγr) in the air [46].

In 2006, Jebur et al. collected fertiliser samples from local markets in Basrah Governorate to study the activity concentrations of naturally occurring radionuclides, including ^{228}Ra, ^{226}Ra, ^{238}U, ^{232}Th, and ^{40}K. The samples were analysed using a high-purity germanium (HPGe) detector and sodium iodide NaI(Tl) γ-ray spectrometry. The findings revealed that the average specific activity values for ^{226}Ra, ^{232}Th, and ^{40}K in nitrogen, phosphorus, and potassium fertilisers were 107.4 ± 8.6 Bq/kg, 107.0 ± 7.6 Bq/kg, and 1206.0 ± 9.8 Bq/kg, respectively. The highest radium activity was observed in Crop Complex fertilisers compared to the organic fertilisers studied. Furthermore, some

samples exceeded the radium equivalent activity limit of 371 Bq/kg, which is the maximum allowable threshold for radiation exposure [57].

Manyama et al. investigated the radioactivity levels of the Minjingu phosphorite deposit in Arusha, Tanzania, using radiochemical and radiometric analytical methods. The study focused on the activity concentrations of radionuclides such as ^{238}U, ^{235}U, ^{232}Th, and their decay products in various materials, including rock phosphate, phosphate concentrate, phosphate fertilisers, and Phosphogypsum. The results indicated that ^{238}U and its decay products exhibited high activity concentrations, reaching up to 4000 Bq/kg across all sample types. Phosphogypsum showed elevated levels of ^{226}Ra, contrasting with lower levels in triple superphosphate fertilisers. The widespread use of rock phosphate from the mine and phosphate fertilisers was evaluated concerning their radiological impact on farmers. The activity concentrations of ^{238}U ranged from 85 to 97 Bq/kg, ^{235}U from 154 to 1999 Bq/kg, and ^{232}Th from 407 to 627 Bq/kg. Despite the presence of these radionuclides, the external radiation exposure from phosphate fertilisers in agricultural fields was found to contribute less than 2% to the normal background radiation level of 51 nGy/h [58].

Hesham A. Yousef et al. conducted a study to determine the radon concentration and surface exhalation rate in phosphate samples collected from El-Sebaeya and Abu-Tartur, Egypt. Solid-state nuclear track detectors of the CR-39 and LR-115 types were used for the measurements. The average radon concentrations in the El-Sebaeya region were found to be 12,711.01 Bq/m³ and 10,925.03 Bq/m³ when measured with CR-39 and LR-115 detectors, respectively. Similarly, in the Abu-Tartur area, the average radon concentrations were 15,824.12 Bq/m³ and 13,601.48 Bq/m³, as determined using CR-39 and LR-115 detectors, respectively [59].

Samad et al. investigated the activity concentrations of ^{226}Ra, ^{232}Th, and ^{40}K in both solid and liquid samples collected from the Yamuna Urea Fertiliser

Factory in Tarakandi, Jamalpur, Bangladesh. Six types of samples were analysed: (i) liquid wastewater stored within the factory, (ii) water from the Yamuna River near the liquid waste disposal point, (iii) liquid-waste-contaminated soil, (iv) normal soil adjacent to the factory, (v) the final product (urea), and (vi) urea dust from the factory. The samples were examined using gamma spectrometry with a high-purity germanium (HPGe) detector with 40% relative efficiency. The activity concentration of ^{226}Ra was determined based on the average concentrations of its decay products ^{214}Pb and ^{214}Bi, while that of ^{232}Th was calculated from ^{228}Ac and ^{208}Tl. The concentration of ^{40}K was measured directly. Analysis revealed that the average activity concentrations in the liquid waste samples were 3.64 ± 0.72 Bq/L for ^{226}Ra and 12.94 ± 2.02 Bq/L for ^{232}Th, with no detectable ^{40}K. In the liquid-waste-contaminated soil, the average activity concentrations of ^{226}Ra, ^{232}Th, and ^{40}K were 21.46 ± 3.18 Bq/kg, 63.00 ± 8.90 Bq/kg, and 311.95 ± 90.91 Bq/kg, respectively. In the normal soil, these values were 20.98 ± 3.55 Bq/kg, 61.76 ± 8.92 Bq/kg, and 645.47 ± 103.61 Bq/kg, respectively [60].

Ghosei et al. conducted a pilot study to measure the activity concentrations in soil, water, and fertiliser samples collected from areas around a urea fertiliser factory, a lagoon, and the Shitalakhya River in Narsingdi, Bangladesh. The analysis was performed using gamma spectrometry with a PC-based multi-channel analyzer (MCA) system. The activity concentrations of ^{226}Ra were found to range from 1.21 ± 0.42 to 7.35 ± 0.41 Bq/kg in water samples, 3.15 ± 0.31 to 10.27 ± 0.54 Bq/kg in soil samples, and 3.54 ± 0.32 to 90.64 ± 3.16 Bq/kg in fertiliser samples. For ^{232}Th, the concentrations ranged from 4.88 ± 0.46 to 15.81 ± 0.44 Bq/kg in soil, 1.22 ± 0.05 to 8.58 ± 0.36 Bq/kg in water, and 4.75 ± 0.26 to 26.37 ± 1.41 Bq/kg in fertilisers. The concentrations of ^{40}K varied between 24.95 ± 0.22 and 60.48 ± 0.55 Bq/kg across the samples [61].

Mugren et al. investigated the activity concentrations of ^{226}Ra, ^{232}Th, and ^{40}K in cement and phosphate fertilisers consumed in Saudi Arabia using γ-ray

spectrometry. Their findings indicated that in fertiliser samples, ^{226}Ra activity concentrations ranged from 9.2 ± 1.2 Bq/kg to 106.1 ± 6 Bq/kg, ^{232}Th ranged from 6.2 ± 2.3 Bq/kg to 42.6 ± 2 Bq/kg, and ^{40}K ranged from 45.5 ± 3.26 Bq/kg to 580.8 ± 13.1 Bq/kg [62].

Hussain et al. measured the specific activities of ^{238}U, ^{232}Th, and ^{40}K in fertilisers using a gamma-ray spectrometer equipped with a NaI(Tl) detector. Their results showed activity ranges of 12.845–88.584 Bq/kg for ^{238}U, 1.305–26.655 Bq/kg for ^{232}Th, and 11.597–2275.897 Bq/kg for ^{40}K. The radium equivalent activity (Ra_{eq}) varied from 0.893 to 175.25 Bq/kg, with average values below the global average. Leafy NPK fertilisers exhibited the highest Ra_{eq} values, while urea fertilisers showed no detectable radionuclides. The specific activity and absorbed dose rates at 1 meter above the ground surface (nGy/h) after agricultural application of NPK fertilisers were calculated, with the maximum dose rate representing only 0.15% of the global average outdoor terrestrial gamma radiation exposure [63].

Azeez et al. assessed the activity concentrations of radioactive nuclides in plant fertilisers used in agriculture in the Iraqi Kurdistan region using a high-purity germanium (HPGe) gamma spectrometer. Their study revealed that activity concentrations ranged from 0.1 to 135 Bq/kg for ^{226}Ra, 0.1 to 75 Bq/kg for ^{232}Th, 1 to 12,001 Bq/kg for ^{40}K, and 0 to 1 Bq/kg for ^{137}Cs. Some samples had radium equivalent activity exceeding the OECD-recommended limit of 371 Bq/kg, highlighting potential radiological hazards [64].

Hiwa et al. explored the impact of chemical fertiliser use on radioactivity levels in agricultural soils. Using gamma-ray spectrometry with a high-purity germanium (HPGe) detector, they measured the activity concentrations of ^{232}Th, ^{226}Ra, and ^{40}K in various soil samples. For virgin soils, the activity concentrations of ^{40}K, ^{232}Th, and ^{226}Ra ranged from 241.7 to 340.8 Bq/kg, 8.7 to 10.6 Bq/kg, and 10.5 to 16.2 Bq/kg, respectively. In agricultural soils, these values ranged from 247.7 to 338.3 Bq/kg for ^{40}K, 8.8 to 12.4 Bq/kg for ^{232}Th, and

11.9 to 18.2 Bq/kg for ^{226}Ra, highlighting the influence of fertiliser use on radionuclide levels [65].

Dipak et al. conducted a pioneering study on the alpha activity of commonly used building materials in West Bengal, India. Using a solid-state nuclear track detector, a highly sensitive tool for detecting alpha particles, they measured the alpha activities of materials collected from local markets in Kolkata. The recorded alpha activities ranged from 22.7 ± 2.5 Bq/kg to 590.6 ± 16.8 Bq/kg, with ceramic tiles exhibiting the highest alpha activity. This study contributes valuable data on environmental radiation exposure and its potential health impacts [32].

Didarul et al. conducted a study on soils and solid waste materials from industrial areas of Nasirabad, Chattogram, which are commonly used for land construction. The aim was to assess the radioactivity levels in these materials and the potential radiological hazards associated with their use. A total of 37 samples were collected, including 31 soil samples and 6 solid waste samples, from various industries. The activity concentrations of ^{232}Th, ^{226}Ra, and ^{40}K ranged from 8 ± 1.9 to 132 ± 18.32 Bq/kg (with an average of 22 Bq/kg), 10 ± 2.68 to 132 ± 15.95 Bq/kg (with an average of 41 Bq/kg), and 81 ± 22.67 to 930 ± 260.41 Bq/kg (with an average of 449 Bq/kg), respectively. The study also calculated several hazard indices, including the external hazard index (Hex), radium equivalent activity, internal hazard index, and activity concentration index, to evaluate the radiation risks. While the averages of the hazard indices were within safe limits, the activity concentration index showed elevated values [66].

Yassir Baqir et al. conducted an estimation of the specific activities of natural radionuclides ^{238}U, ^{232}Th, and ^{40}K in inorganic fertilizers using a gamma-ray spectrometer with a NaI(Tl) detector and a Rad Eye-B20 portable detector. The results from the NaI(Tl) detector revealed that the average activity concentrations of ^{238}U, ^{232}Th, and ^{40}K were 2.11 Bq/kg, 0.327 Bq/kg, and 95.792 Bq/kg, respectively, all of which were below the recommended limits. The

study also calculated the mean values for radiometric parameters, including Raeq, Hin, Hex, Iγ, and AEDE, which were 9.398 Bq/kg, 0.0354, 0.0247, 0.037, 0.0123 nGy/h, and 0.0065 mSv/y. In the samples, the maximum and minimum values of activity concentrations were found to be 0.2 and 0.4, respectively. The measurements from the Rad Eye-B20 portable detector showed the maximum values of surface contamination, dose rate, and general count rate were 0.415 Bq/cm², 0.161 μSv/h, and 1.054 counts per second (Cps), respectively, while the minimum values were 0.255 Bq/cm², 0.12 μSv/h, and 0.483 Cps. These values were slightly higher than the background measurements (0.21 Bq/cm², 0.12 μSv/h, and 0.42 Cps). The results from the Rad Eye-B20 detector were consistent with those from the NaI(Tl) detector, confirming that all radiological hazard measurements were within safe limits [67].

Alharbi et al. utilized sodium iodide gamma spectrometry to evaluate the levels of naturally occurring radionuclides such as ^{40}K, ^{226}Ra, and ^{232}Th in various brands of fertiliser from Saudi Arabia. Their results indicated that the average (range) activity concentrations for ^{226}Ra, ^{232}Th, and ^{40}K in nitrogen, phosphorus, and potassium fertilisers were 64 (35.81 - 120.71) Bq/kg, 17 (3.21 - 56.81) Bq/kg, and 2452 (744.91 - 4227.10) Bq/kg, respectively. In contrast, the average activity concentrations for ^{226}Ra, ^{232}Th, and ^{40}K in organic fertilisers were 43 Bq/kg, 11 Bq/kg, and 332 Bq/kg, respectively. The radium equivalent activity was determined to be below 371 Bq/kg, and all parameters related to dose were found to be within safe limits. The concentrations of natural radionuclides found in fertilisers from Saudi Arabia were comparable to those documented in several other countries. This study provides crucial baseline information regarding radiation exposure from fertilisers and its possible health implications [68].

Servitzoglou et al. conducted a study involving 100 samples from fertilisers, agricultural soils treated with fertilisers, and wheat grain soils collected from various farms in Greece. Using an HPGe detector, they determined the mean

activity concentrations for ^{238}U, ^{226}Ra, ^{232}Th, and ^{40}K to be 376, 192, 21, and 2621 Bq/kg, respectively. The study found that phosphate fertilisation did not significantly affect the natural radioactivity levels in the soil compared to non-fertilized soils, nor did it influence the natural radioactivity of wheat grains, with only ^{40}K being detected. However, the mean external dose rate of 212 nGy/h for fertilisers was notably higher than the 54 nGy/h measured for fertilised soils, which raised concerns about radiation safety for workers handling fertilisers. The maximum external dose rate of 1.14 mSv/y calculated for truck drivers involved in transportation was found to be close to the annual external dose limit of 1 mSv/y. Moreover, there are concerns for workers in the fertiliser storage and distribution sector, where the estimated maximum dose rate is 1.981 mSv/y, while the average value is 0.891 mSv/y [69].

Alzahrani et al. measured the specific activities of ^{226}Ra, ^{232}Th, and ^{40}K in phosphorite deposit samples from both surface and sub-surface layers in the Turayf, Thaniyat Turayf, and Umm Wual regions of north-western Saudi Arabia using a Sodium Iodide NaI(Tl) detector. The average activity concentrations in the phosphate rocks were found to be (13.11 ± 2.51) Bq/kg for ^{226}Ra, (39.10 ± 1.51) Bq/kg for ^{232}Th, and (241.71 ± 4.31) Bq/kg for ^{40}K. The calculated external γ-radiation dose experienced by workers in these phosphorite deposits was estimated to be 261 μSv/year, which is significantly lower than the internationally allowed dose limit of 21 mSv/year for occupational workers, as specified by ICRP-60 (1990). [70] .

Samad et al. conducted a study to detect probable radionuclides and assess their activity concentrations in raw materials (phosphate rock), final products (fertilizer), and waste samples from two phosphate fertilizer factories in Bangladesh: a Di-ammonium Phosphate (DAP) factory and a Triple Super Phosphate (TSP) factory. Seven types of samples were analysed, including liquid waste, waste-mixed river water, normal river water, phosphate rock, phosphate fertilizer, solid waste, and normal soil. Raw material samples were

exclusively collected from the TSP factory, while fertilizer, solid waste, and liquid waste samples were obtained from both factories. Additionally, normal soil and surface water samples from nearby areas were collected for comparison. The samples were analysed using gamma-ray spectrometry with a Hyper-Pure Germanium (HPGe) detector with 40% relative efficiency. The results revealed the presence of natural radionuclides, including ^{226}Ra, ^{232}Th, and ^{40}K, while no artificial radioactivity was detected. In some samples, ^{40}K was below the detection limit. The findings for the TSP factory showed average activity concentrations of ^{226}Ra, ^{232}Th, and ^{40}K in raw materials as 851.28 ± 7.12 Bq/kg, 19.64 ± 6.59 Bq/kg, and 54.08 ± 5.94 Bq/kg, respectively; in the final product as 211.91 ± 4.75 Bq/kg, 42.49 ± 10.57 Bq/kg, and ND (Not Detected); in solid waste as 187.491 ± 4.87 Bq/kg, 70.07 ± 11.77 Bq/kg, and 289.28 ± 40.25 Bq/kg; and in liquid waste as 6.26 ± 0.63 Bq/L, 10.01±1.39 Bq/L, and ND. For the DAP factory, the average activity concentrations of ^{226}Ra, ^{232}Th, and ^{40}K in the final product were 17.32 ± 3.93 Bq/kg, 69.75 ± 9.89 Bq/kg, and 48.47 ± 17.21 Bq/kg, respectively; in solid waste as 24.48 ± 4.14 Bq/kg, 164.621 ± 11.09 Bq/kg, and 191.53 ± 33.741 Bq/kg; and in liquid waste as 3.58 ± 1.04 Bq/L, 37.09 ± 3.31 Bq/L, and ND. The study also calculated the radium equivalent activity, radiation hazard index, and external annual effective dose for workers and the public due to these materials, comparing them with global average values [71].

Nour Khalifa Ahmed et al. investigated the radioactivity levels in samples of phosphate fertilizers and farm soils collected from cultivated land in the Qena Governorate of Upper Egypt. Soil samples were taken to a depth of up to 30 cm. The activity concentrations of background radionuclides, including ^{226}Ra, ^{232}Th, and ^{40}K, in these samples were determined using gamma-ray spectrometry. The results indicated that the concentrations of these radionuclides in phosphate fertilizers were 366.2 ± 10.51 Bq/kg for ^{226}Ra, 66.72 ± 7.31 Bq/kg for ^{232}Th, and 4 ± 2.61 Bq/kg for ^{40}K. For farm soil and soil from Nile islands, the corresponding

values were 13.71 ± 70 Bq/kg, 12.3 ± 4.61 Bq/kg, and 1233.2 ± 646.1 Bq/kg for farm soil, and 11.91 ± 6.71 Bq/kg, 10.51 ± 6.11 Bq/kg, and 1636.1 ± 416 Bq/kg for Nile Island soil. The radium equivalent activity, representative level index, and the absorbed dose in air for all samples were calculated. The findings were discussed and compared with data available in existing literature [72].

Based on the previous discussion, it is clear that different types of fertilizers may contain various radionuclides, and in order to protect the environment, it is necessary to calculate the concentration of these radionuclides and their radiation impacts. In our country, relatively little research has been conducted on this subject, and since 1997, no researchers have examined fertilizers to assess radionuclide concentrations; consequently, no hazard indexes have been published on this matter. I believe that there is now a significant opportunity to investigate the presence of all types of radionuclides in fertilizers, as well as the potential health risks they pose to humans.

Chapter 3: METERIALS AND METHODOLOGY

3.1 BASIC RESEARCH MATERIALS

The emission of nuclear radiation occurs when various radioactive materials, such as tritium, carbon, iodine, potassium, strontium, radium, uranium, thorium, etc., are present in soil and water. Living organisms are exposed to these radiations through their surroundings, the food they consume, and the water they drink. While radiation is harmful to all living organisms, a certain level of radiation can be tolerated. However, if the radiation level exceeds the tolerance threshold, it can adversely affect the human body, either temporarily or over a prolonged period. Living organisms receive internal radiation from the food and drinks they consume, and they are also exposed to external radiation from sources like cosmic rays, nuclear weapon tests, nuclear accidents, and manufactured products containing radionuclides. The concentration of radioactive elements in nature increases due to the gradual production of radioactive isotopes, including the continuous interaction between cosmic rays and atmospheric atoms, nuclear plant operations, nuclear weapon tests, and the presence of radionuclides in manufactured goods.

Following the consequences of the Chernobyl accident, many countries started paying attention to the calculation of internal and external radiation doses. In 1990, the International Commission on Radiological Protection (ICRP) recommended reducing the radiation level from 50 mSv/year to 20 mSv/year. Therefore, it is now crucial to determine the internal and external radiation dose levels in Bangladesh. Several researchers have already studied radiation dose levels in various sectors, including water, soil, building materials, and manufactured products [73].

Due to increased crop production worldwide, fertiliser production has also grown to meet the demands of farmers. However, a downside to this is the presence of more impurities containing radioactive isotopes. Fertiliser

industries use raw materials such as phosphate rock, phosphonium, and potassium compounds. Typically, fertilisers consist mainly of nitrogen, phosphorus, and potassium, which are essential elements for plant growth. The phosphorus component is derived from phosphate rocks, which contain numerous radionuclides [36]. Over time, the use of fertilisers leads to the contamination of soil with radionuclides and their radiation, which gradually exceeds natural levels. The widespread use of fertilisers is the primary cause of increased radionuclide levels in soil and underground water [36].

Consequently, these radionuclides enter the human body and become part of the food chain through soil and drinking water. There is also a high risk of significant accumulation of the radionuclide ^{226}Ra in the bone marrow, which can cause biological damage. Workers and farmers directly involved in agricultural production and distribution are at an increased risk of exposure to various radionuclides. Some articles indicate that workers in fertiliser factories, fertiliser distributors, and farmers are at high risk of exposure to radiation emitted by radionuclides present in fertiliser impurities. External exposure occurs directly through gamma rays, while internal exposure occurs through alpha particles resulting from the inhalation of radon and its decay products. This exposes the bronchial tissue to alpha radiation and increases the potential for radiogenic lung cancer [74]. Therefore, radiation released from fertilisers has the potential to cause cancer in individuals exposed to significant levels. Hence, monitoring the natural radioactivity in fertilisers is crucial from a radiation protection standpoint [41].

There is a growing global awareness of the radiation hazards associated with fertiliser materials as a potential source of risk to workers, the general public, and the environment. As a developing country, Bangladesh lacks a robust radiation protection system. In this study, the specific activities of ^{238}U, ^{232}Th, and ^{40}K, which are common radionuclides, were measured in commonly used fertiliser materials in Chittagong, Bangladesh. To measure specific activity of

radionuclide HPGe detector was used which is available in Atomic Energy Commission, in Chittagong.

3.2 EXPERIMENTAL INVESTIGATION

3.2.1 High Purity Germanium (HPGe) Detectors

Gamma rays can be detected by calculating the number of effects on matter. After colliding with an electron, it bounces off like a billiard ball, called the Compton Effect. Again, gamma rays can eject electrons from metal in the case of the photoelectric effect. As gamma rays sometimes hold more energy, they can produce one electron and another ion from a matter (called pair production). Above all processes, electrons can be free from metal and can move. That is called current flow. After amplifying the energy and direction of the original gamma ray, it can be calculated. Therefore high-purity germanium (HPGe) detectors such as semiconductor devices can detect gamma rays from various radioactive nuclides. Almost all radioactive matter emits gamma rays of different energies and intensities. One spectroscopy system can detect and analyse this additional emission [75].

Generally, the HPGe detector is a solid analogue used instead of the usual gas. This is a precious apparatus is used for gamma-ray spectrometry with high efficiency and reasonable resolution.

A single germanium crystal designed with a p-n diode structure is referred to as an HPGe detector. By reducing the impurity concentration in germanium to approximately 10^{10} atoms/cm^3 (equivalent to one impurity atom per 10^{13} germanium atoms), it is possible to achieve a depletion depth of around 10 mm. These germanium diode detectors, characterized by their large volume, are commonly called "intrinsic" or "high-purity" germanium detectors. The reliability of such detectors largely depends on their depletion depth, which increases with the square root of the material at a given voltage [76].

High-purity germanium is typically p-type due to residual acceptor impurities like aluminium or acceptor centres linked to lattice defects within the material.

This configuration is often described as an n^+-p-p^+ diode structure. The n^+ region is created by evaporating lithium onto a lapped germanium surface, followed by brief diffusion at high temperatures. The detector's depletion region is formed by reverse-biasing the n^+-p junction, while the p^+ contact on the opposite side is usually a diffused gold surface barrier junction. The outer n-type lithium contact is roughly 300 nm thick, and the inner gold surface barrier contact has about 40 mg/cm² of evaporated gold. This intrinsic region is sensitive to ionizing electromagnetic radiation, and under reverse bias, an electric field spans the depleted or intrinsic region [77].

Gamma rays are detected by HPGe detectors through their ionizing properties, where primary and secondary electron-hole pairs are formed as photons interact with the depleted volume. These ion pairs are swept to the respective p and n electrodes by the electric field. The total electron-hole pairs collected under the applied electric field create a voltage pulse proportional to the gamma-ray energy absorbed, which is processed by a charge-sensitive preamplifier. Ionization in the detector occurs via three processes: the photoelectric effect, Compton scattering, and pair production. At energies of 1.022 MeV, pair production becomes the dominant process. The spectrum of mono-energetic gamma rays typically consists of a full absorption peak, a Compton continuum, and pair production peaks at energies of 1.022 MeV. The relative contribution of each component to the spectrum depends on the energy of the gamma rays, the material of the detector, and its size [78]. HPGe detectors are manufactured in two basic geometries: planar detectors, where the electric field is uniform, and coaxial detectors, where the electric field decreases inversely with radial distance from the detector's axis. The gamma-ray detection efficiency and functionality of an HPGe detector are equivalent to those of a Ge (Li) detector with similar dimensions and shape. Due to germanium's low band gap and high sensitivity to temperature, these detectors must be cooled to minimize the thermal generation of charge carriers, thereby

reducing leakage current to an acceptable level. Without adequate cooling, noise from the leakage current significantly degrades the detector's energy resolution. Liquid nitrogen, with a temperature of 77 K, is commonly used as the cooling medium for these detectors. The detector is housed in a vacuum chamber, which is either attached to or inserted into a liquid nitrogen Dewar. This setup protects the sensitive surfaces of the detector from moisture and other condensable contaminants.

High-purity germanium is typically p-type due to residual acceptor impurities like aluminium or acceptor centres linked to lattice defects within the material. This configuration is often described as an n^+-p-p^+ diode structure. The n^+ region is created by evaporating lithium onto a lapped germanium surface, followed by brief diffusion at high temperatures. The detector's depletion region is formed by reverse-biasing the n^+-p junction, while the p^+ contact on the opposite side is usually a diffused gold surface barrier junction. The outer n-type lithium contact is roughly 300 nm thick, and the inner gold surface barrier contact has about 40 mg/cm² of evaporated gold. This intrinsic region is sensitive to ionizing electromagnetic radiation, and under reverse bias, an electric field spans the depleted or intrinsic region. Gamma rays are detected by HPGe detectors through their ionizing properties, where primary and secondary electron-hole pairs are formed as photons interact with the depleted volume. These ion pairs are swept to the respective p and n electrodes by the electric field. The total electron-hole pairs collected under the applied electric field create a voltage pulse proportional to the gamma-ray energy absorbed, which is processed by a charge-sensitive preamplifier. Ionization in the detector occurs via three processes: the photoelectric effect, Compton scattering, and pair production. At energies of 1.022 MeV, pair production becomes the dominant process. The spectrum of mono-energetic gamma rays typically consists of a full absorption peak, a Compton continuum, and pair production peaks at energies of 1.022 MeV. The relative contribution of each component to

the spectrum depends on the energy of the gamma rays, the material of the detector, and its size [79].

The global appeal of germanium as a semiconductor radiation detector can be credited to its superior charge transport characteristics, enabling the use of larger crystals without substantial carrier losses from trapping or recombination. In scenarios where only a limited number of gamma-ray energies is concerned, the higher efficiency, increased photo fraction, and reduced expense of sodium iodide may make it the more favourable choice. However, germanium detectors are favoured for analysing intricate gamma-ray spectra that involve numerous energies and peaks [80].

It also helps in identifying weak discrete energy sources that are layered over a broad continuum. To minimize thermally induced leakage currents, germanium must be consistently maintained at low temperatures (77K). The appeal of semiconductor detectors lies in their superior energy resolution compared to scintillation detectors (NaI, CsI, ZnS, etc.) and the enhanced stopping power of a solid material as opposed to a gas. In the case of germanium, approximately 3 eV of energy is required to create one electron-hole pair, while in a solid-state scintillation detector, 100 eV is necessary to form an ion pair, and 34 eV is needed in a gaseous ionization detector. Consequently, semiconductors generate a higher number of carriers for a specific energy absorption, and the statistical variations in that number are minimal when presented as a percentage of the total. The performance of an HPGe is generally characterized by energy resolution, relative efficiency, and the lower detection limit [81].

The depth of the depletion layer in a detector is directly related to its performance and inversely related to the impurity concentration in the detector material. Generally, a minimal amount of pure material is necessary to attain a significant depletion depth. The net impurity concentration in the HPGe detector is roughly 10^{10} atoms/cc. With germanium having a low energy gap (0.74 eV), the detector needs to be maintained at low temperatures to optimize

performance, thereby minimizing thermal leakage current to an acceptable range. Additionally, leakage current contributes to noise and diminishes the detector's energy quality. For optimal performance, HPGe detectors are typically operated at approximately 77K [82]. The detector is placed in a vacuum chamber, where liquid nitrogen dewier is used. In this condition, the reverse current is in the range of 10^{-9} to 10^{-12} amps [83]. Otherwise, leakage current-induced noise will destroy the energy resolution of the detector. The detector is mounted in a vacuum chamber, which is inserted into a liquid nitrogen dewar. At this temperature, reverse leakage current is in the range of 10^{-9} to 10^{-12} amp.

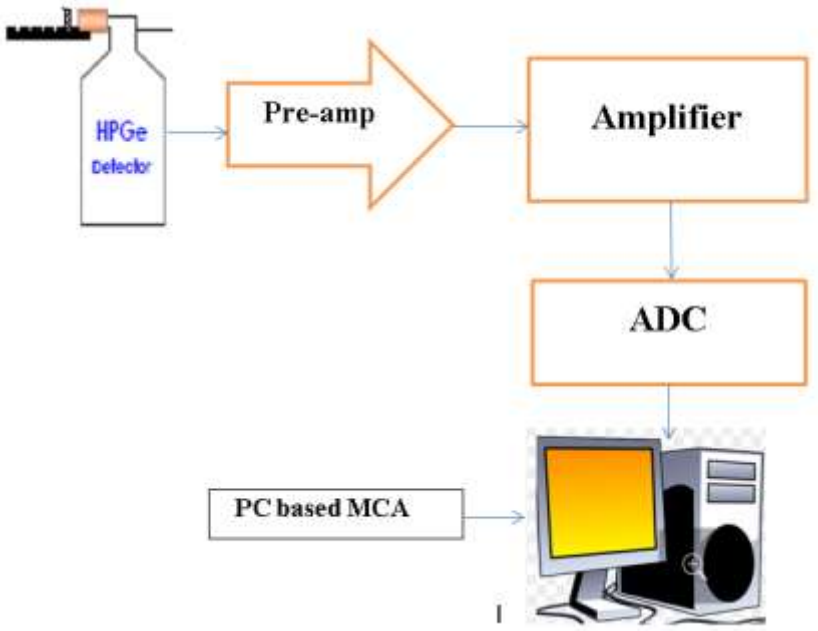

Fig. 3.1 Block diagram of a HPGe γ-ray detector.

3.2.2 Processing of detector and associated electronics

To provide significant information regarding radiation, nearly all radiation detectors create an electrical pulse for detection. A primary integration of three fundamental functions of a detector is used to process an electrical signal: amplification, shaping, and analysis. The process of enlarging the signal's magnitude is referred to as amplification, while shaping pertains to alterations in the form of the electrical signal, and analysis focuses on assessing pulses based on their area or height. The electronic circuit facilitates the amplification, shaping, and analysis of the detector's pulse. According to Fig 3.1 from the

detector, electrical signals are sent to a preamplifier, where both amplification and initial shaping occur. The preamplifier serves as an intermediary between the detector and the amplifier, transforming the ionization charge generated by the photon in the detector into a voltage signal. The voltage signal produced in the detector is directly proportional to the charge generated. A shielded wire connects the preamplifier to the detector, which is situated very close to the detector itself. This arrangement is necessary to reduce the distortion of the pulse caused by electrical "noise" in the cable and to ensure the detector remains adequately cooled, which is crucial for its functioning. After the electrical signal is generated from the detector and further amplified by the preamplifier, these signals proceed to the amplifier for final shaping and amplification. Once they reach the multi-channel analyser, the signals are categorized into groups based on height, and the count of pulses in each category is recorded [84].

3.2.3 Setup of HPGe Detector in Lab

The Atomic Energy Centre in Chattogram has a High Purity Germanium Detector (HPGe Detector) facility that is utilized to determine the levels of natural and anthropogenic activity concentrations in soil and solid waste samples. The laboratory is equipped with several tools, including an HPGe detector NATS, cylindrical plastic containers for holding samples, lead (Pb) shielding, a digital weighing balance, standards, and a PC-based data acquisition system. Figure 3.2 illustrates the complete setup with all the components.

3.2.4 P-Type HPGe Detector GCD-40 190

In this study the High Purity Germanium Detectors (HPGE) is extensively used for detecting and analysing Gamma-ray emissions from various fertiliser samples. The coaxial design of this detector enables energy range coverage from 10 keV to 10 MeV, ensuring efficient detection of radiation. The range of this HPGE detector is diverse and includes the following features:

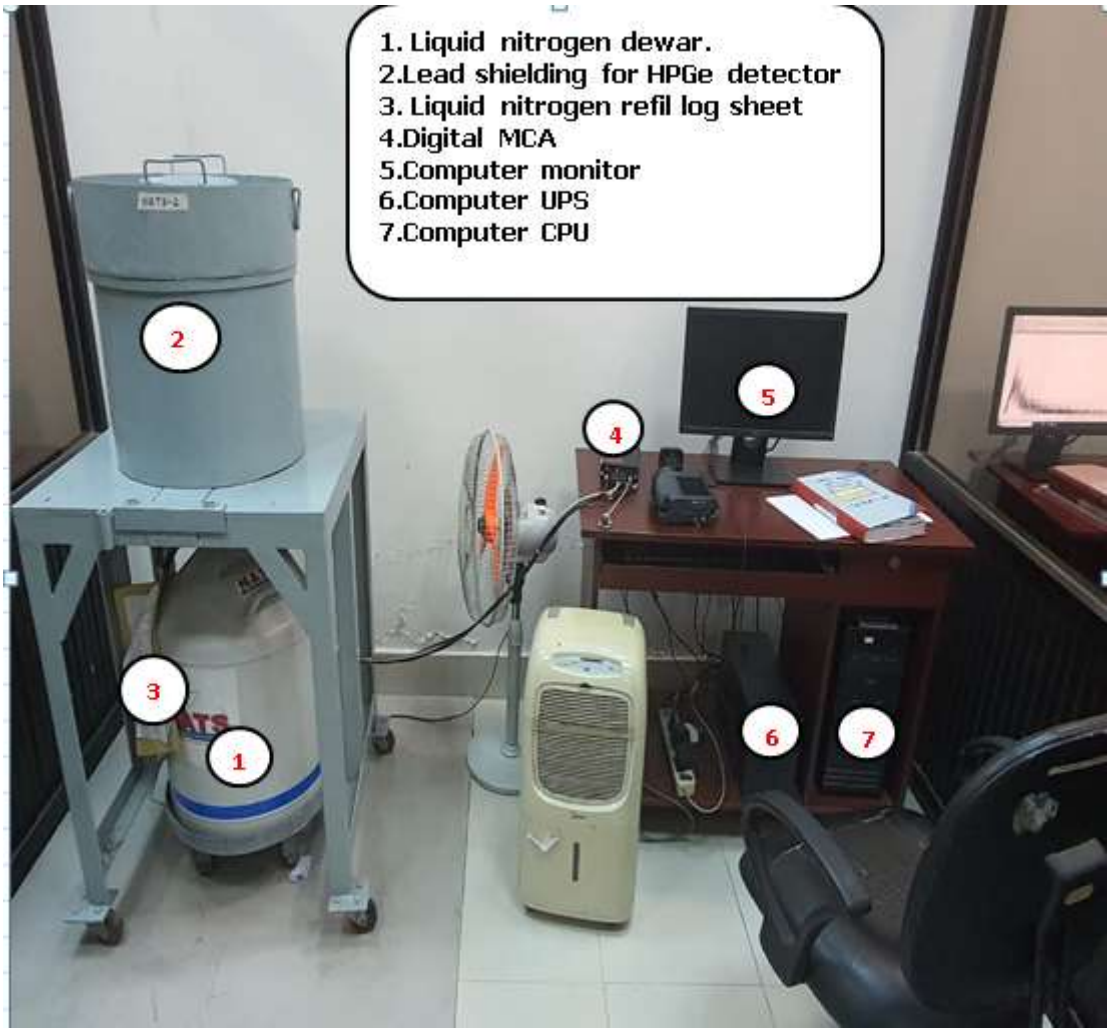

Fig. 3.2 Gamma Ray Spectrometry System

1. The relative efficiencies of the HPGe detector with ranging from 10% to 40% are available.

2. It has a Liquid Nitrogen and Electrically Cooled Cryostats.

3. The cryostats is portable.

4. Field Radionuclide Identification Systems compatible with both LN2 and Electrically Cooled configurations.

5. Specialized Systems specifically designed for Gaseous and Liquid Flow applications.

6. Wide energy range coverage from 10 keV to 10 MeV.

7. High efficiency in radiation detection.

8. High energy rate capability of up to 200,000 MeV/sec.

9. Excellent peak symmetry to ensure accurate analysis.

10. Availability of Low background and Ultra-low background materials for sensitive measurements.

In addition, this detector also can provide complete Signal Processing Electronics and analysis software that complement the HPGE systems. These additional components include:

a) HPGe coaxial detector options, including p-type and extended-range variants. b) Preamplifier with cooling input stage for optimized performance. c) Cryostat and Dewar vessel for temperature control. d) Spectrometric MCA (Multi-Channel Analyser) options, including Digital, Analog, and Hybrid Systems Emulation. e) Advanced Gamma Ray Analysis Software for comprehensive data analysis and interpretation.

3.2.5 Instrumental Set up of Gamma-ray Detection Unit Based on P-type HPGe Detector GCD-40 190 in the present work

Application: The purpose of the gamma-ray spectrometer is to convert the energy of gamma ray photons into electrical signals. It is built using a p-type high-purity germanium (HPGe) detector. These electrical signals have amplitudes proportional to the energy of the gamma rays and are meant to be processed in a multi-channel analyser (MCA) 527 or similar nuclear physics equipment. The DU is specifically designed for use in laboratory settings.

Complete set: 1.P-type high purity germanium (HPGe) semiconductor detector (SCD). 2. Preamplifier with cold input stage. 3. Vertical Cryostat.4. Related cables and connectors set (2m) 5. Dewar vessel 6. Multi-channel analyser MCA 527. 7. Software Spectra Line GP. 8. Software Effmaker

Technical characteristics: Main parameters and characteristics are measured in the normal conditions, i.e. at the following conditions:

- The ambient temperature should be (20±5) °C.

- ❖ Relative humidity must range from 45% to 75%, ensuring it is non-condensing.
- ❖ Atmospheric pressure should be maintained between 86 kPa and 106.7 kPa.
- ❖ The voltage supply bias is allowed to vary from the nominal value within ±2%.
- ❖ The bias for AC frequency must be less than 1% for 50Hz.
- ❖ The maximum allowable factor for high harmonics is 5%.
- ❖ There should be no external electric or magnetic fields, or they must remain within limits that do not affect the device's operation. Main parameters and characteristics are measured in the normal conditions influence the operation of the device.

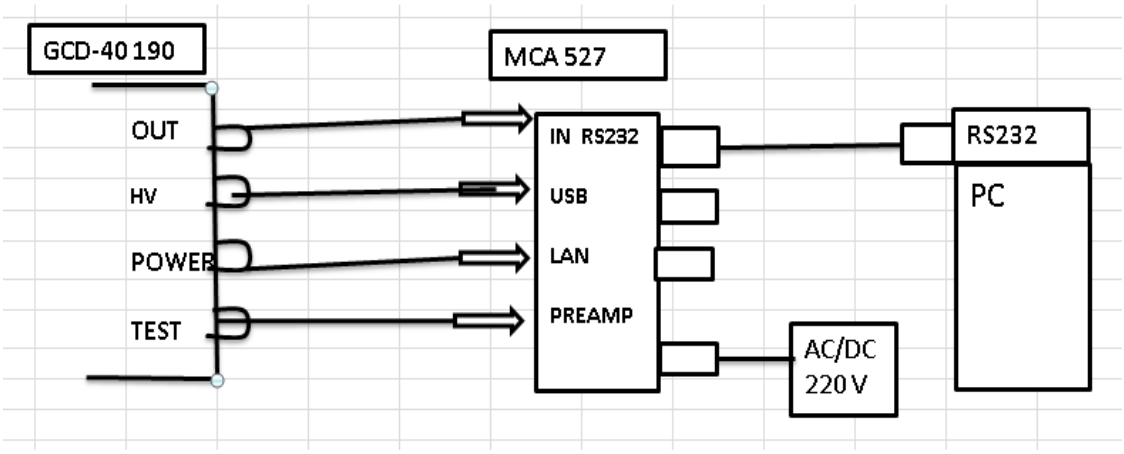

Fig. 3.3 Typical electric configurations diagram for spectroscopy system of HPGE

The Detection Unit, which operates using an HPGe SCD and employs liquid nitrogen cooling, comprises the cryostat, preamplifier, and Dewar vessel, as illustrated in fig. 3.3. The detector along with the input stage of the preamplifier is situated within the vacuum chamber of the cryostat and is cooled to a temperature near that of liquid nitrogen. The part of the preamplifier (PA) that does not require cooling is located outside of the vacuum space in a distinct section that is hermetically sealed with a cover. Four cables run from this section to link the DU to the spectrometric equipment. The cryostat is securely attached to the plug using three lock screws and is positioned on the neck of the

Dewar vessel. Inside the detector cryostat, there is a sensing element connected to the cooling path. This sensing element interfaces with a monitoring circuit that is incorporated into the PA electronics. The output signal from the monitoring circuit, known as HV inhibit, is transmitted through the POWER DC +12V cable and contact D 9-5 to the control input of the HV source in the spectrometric device. If the detector's temperature has not reached the required level (green LED does not light up), HV supply to the detector is prohibited. The supplied high voltage to the detector is switched off when the detector's temperature exceeds the acceptable level (e.g., due to LN2 evaporation).

At the end of the cable connected to the POWER DC ±12V connector, there are two light-emitting diode (LED) indicators: a green one indicating the detector temperature and a red one indicating high count rate. The green LED, known as the Detector Temperature indicator, shows when the detector temperature exceeds the critical level, while the red LED, known as the High-Rate indicator, shows an excess of the input count rate. The LED monitor can be affixed to surfaces using the included self-adhesive clip. The cryostat plug is equipped with a nipple for liquid nitrogen filling, while the output nipples are used for releasing nitrogen vapours during the filling process and operational assembly of the detector-Dewar vessel combination and filling the Detection Unit with liquid nitrogen. The DU cryostat and Dewar vessels are transported separately in a specialized package for long distances. Unpack the DU and Dewar vessels following the instructions in the Unpacking manual. Fill a warm Dewar vessel with approximately 20% liquid nitrogen.

Once the release of intense liquid nitrogen vapours subsides, insert the cooling rod of the cryostat into the Dewar vessel. Ensure that a rubber gasket is placed between the lower surface of the filling collar and the Dewar vessel. Secure the DU in the Dewar vessel using tie-rods during transportation for short distances and, if necessary, to maintain stability during measurements.

Allow 8 hours for the Dewar vessel to stabilize the thermal conditions of the detector after filling. Sequence for turning on the detection unit: Connect the standard cables to the appropriate connectors of the multi-channel analyser HYBRID. The multi-channel analyser HYBRID is designed for amplification, analogy filtration, registration, and accumulation of pulse signals, as well as visualization and processing of signal spectra on an IBM PC-type computer, originating from different ionizing radiation detection devices. After installing the Software Spectra Line GP apply a low voltage supply of ±12V to the preamplifier (PA). If the green diode lights up, it indicates that the detector's temperature has reached the optimal value, and the HV power supply can be switched on.

Apply the specified high voltage (as mentioned in section 3.1.5) to the detector, with a ramp rate not exceeding 50V/sec. Alter 30 minutes the detector and preamplifiers will be stabilize. Than total detection unit can begin operate [85].

3.2.6 Multi-Channel Analyser, MCA527

The MCA527 is a compact gamma spectroscopy system that combines a high-performance 16k Multi-Channel Analyser module with the capabilities of a laboratory-grade MCA. It can integrate high voltage supply for detector and preamplifier power, an internal coarse amplifier, and a digital filter. This module is specifically designed to meet the requirements of various applications, including international safeguards, environmental monitoring, nuclear waste treatment facilities, radioactive transport control, and similar fields.

It can provide extensive support for a wide range of detectors, and its 16k resolution is suitable for high-resolution gamma spectrometry when used with HPGe detectors. By utilizing digital filtering, the MCA527 can adjust the filter time constants to a broad range and is capable of accommodating diverse preamplifier signal shapes. The MCA software has complimentary application

programs that allow to operate the device as a versatile multi-channel analyser, multi-channel scalar, universal counter, or oscilloscope.

Furthermore, there is an optional feature available that allows the MCA527 to function as a multiplicity or neutron coincidences counter in List Mode, providing users with expanded functionality for their specific needs. In table 3.1 illustrates all key features of MCA527 and also benefits of various section of MCA is given.

Table 3.1 Key feature of MCA527

KEY FEATURE	BENEFIT
Channel resolution Up to 16k	With HPGE detectors high performance gamma spectroscopy
On board μSD-card holder very low power consumption of 0.7W	Able to perform long time autonomous field determination
Li-Ion batteries Equipped with high capacitive	Without external power (depends on detector 10h–25h operation time)
Easy-view front panel layout and Dimensions in compact format,	Excellent mobility and operability
High Voltage up to (+) or (-) 5000V supported	Large types of HPGE detectors can be applied
On list modes optionally firmware extension	As a multiplicity or neutron coincidence counter. The MCA527 can be used

3.2.7 Spectra Line GP Process

Spectra Line GP carries out a range of processes, including: i) Identification of informative intervals surrounding spectra markers and determination of peak positions. ii) Estimation of informative intervals by utilizing model functions and deriving parameters for all peaks through fitting. ii) Consideration of background levels. iv) Measurement of activity in specific zones, such as base measurements, zone-by-zone analysis, enhanced zone-by-zone evaluation, template methods, and smoothing techniques. v) Configuration of spectra processing boundaries.vi) Spectra Line GP operates on spectra based on the

following actions: a) Searching for informative intervals around peaks (spectra markers), automatically detecting peak positions, and allowing interactive mode and the inclusion of lines from a library. b) Approximating informative intervals using model functions and determining peak parameters through fitting. c) Defining the processing bounds for spectra. d) Taking into account the background signal. e) Calculating activity levels using various methods, including base measurements, zone-by-zone analysis, enhanced zone-by-zone evaluation, all-zone analysis, all-zone analysis with smoothing, template methods, and quasi-template methods. f) Extracting information on radionuclide activities and their ratios during the spectra processing procedure. g) Comparing different spectra. h) Conducting measurements of dose rates. i) Generating protocols for reporting and documentation purposes. j) Performing measurements of meteorological parameters in accordance with ISO 1192 [86].

Spectra Line GP also includes various operations with the analyser, such as: a) Starting and cleaning the analyser. b) Stopping the analyser based on real- or live-time measurements. c) Additional stop conditions based on criteria such as activity uncertainty values, peak area, peak area uncertainty, peak MDA, and zone integral count. d) Conducting sequential measurements. e) Viewing information about the analyser's status. f) Copying data into the spectrum window. c) Loading data into the analyser for analysis [86]

3.3 RESEARCH DESIGN

3.3.1 Sample Collection and Preparation

In this study it was collected a total of 39 fertiliser samples from both retail markets and farmers of 12 sub-district in Chattogram as shown in fig. 3.4, Bangladesh, to identify and quantify natural and anthropogenic radionuclides. Of these samples, 16 were organic fertilisers, and the remaining 33 were chemical fertilisers. Specifically, we collected 7 samples of triple superphosphate (TSP), 5 samples of di-ammonium phosphate (DAP), 8 samples of muriatic of potash (MOP), 1 sample of Q-potash, 4 samples of boron (BOR)

fertilisers, 1 sample of gypsum (GYP), 1 sample of single superphosphate (SSP), and 11 samples of organic (ORG) fertilisers. In fig 3.5 it is shown that collection of fertiliser samples from 12 sub-district of Chottogram district and preservation process in polybag.

Fig. 3.4. The site where the study was conducted [87]

The samples chosen were pulverized and filtered through a 1mm sieve to improve their homogeneity. Afterwards, to eliminate excess moisture, the samples were air-dried for several days, and then oven-dried at 110°C for 24 hours [66]. Subsequently, each sample was labelled with a unique identification number, date, and location, as shown in Fig. 3.5 following the complete removal of moisture, the samples were cooled down in a desiccator. Subsequently, each sample was transferred into a plastic container with a diameter of 5 cm and height of 8 cm, which was then, sealed air tightly. The samples were stored for duration of 1 month prior to conducting the main experimental procedures to attain secular equilibrium of short-lived members of the ^{226}Rn series and confine

the radon gas within the container [88]. Before radioactivity measurement, the samples were weighed using a high-precision laboratory balance machine.

Fig. 3.5 Sample collection from study area.

Fig. 3.6 Sample packaging, levelling and coding.

Fig. 3.7 Sample weighing by digital balance machine.

3.3.2 Specific Radioactivity measurement in lab by using HPGe detector

The HPGe detector is a highly sensitive device that utilizes a high-purity germanium crystal as the detecting element, which allows for the detection of gamma rays with energies ranging from 40 keV to 10 MeV. The preamplifier with cold input stage amplifies the signal from the detector, while the multi-channel analyser converts the analogy signal into a digital signal that can be analysed by a computer. The software programs Spectra line GP and Effmaker are used to analyse and process the data obtained from the HPGe detector. The parameters and characteristics of the HPGe detector are crucial to the accuracy of the measurements obtained. The ambient temperature for normal operation

is (20±5) °C, while the relative humidity should be between 45-75% and non-condensing. The atmospheric pressure should be between 86 and 106.7 KPa, and the voltage supply bias should be nominal and ≤±2%. The AC frequency bias should be ≤1 Maximum allowed factor for high harmonic 5%. The presence of any outer electric or magnetic field must be within the limits that do not influence the operation of the device [88].

Multi-channel analyser (MCA527) is acting to convert the gamma-ray energy into electrical signals proportional in amplitude. The complete set up of HPGe detector system in the lab is given following: -

a)Preamplifier with cold input stage b)P-type high purity germanium(HPGe) semiconductor detector(SCD) c) vertical Cryostat d)Related cables and connections set(2m) e)Dewar Vessel 301 f)Multi-channel analyser MCA527 f) Software Spectra line GP g) Software Effmaker [90].

To measure the activity of radionuclides in the samples, we used gamma ray spectroscopy with a liquid nitrogen-cooled coaxial p-type high-purity germanium (HPGe) detector (BSI, GCD 40190, S/N 2465-17) that had a sensitive area of 63.3 mm diameter and 61.3 mm depth. We operated the detector with an operating bias voltage of +2200 volts and achieved an energy resolution of 1.74 keV (FWHM) at the 1332 keV peak of ^{60}Co, as well as a relative efficiency of 43.1% for energy 1331 keV to NaI(Ti) peak of Compton ratio 71:1. The detector could detect photons with energies between 40 keV and 10,000 keV, and we shielded it with a 10 cm thick jacketed cylinder lead (206Pb) shield, which had a 5mm outer housing and a 1mm inner layer. We set up the detector so that the sample was placed on top of it. With associated electronics for data acquisition about the photo-peaks Multi-Channel Analyser (MCA 527, GBS electronic) connect a connecting system of a 16K (for full range gamma spectra analysis). Some highly configured desktop computer has been used where spectra Line Gamma Precision (GP) software package installed for measurements of spectrometry and linear spectra processing as shown in fig 3.7. Peaks

parameters, radionuclides identification, Spectra processing procedures include calibration, radionuclides activity estimation and activity calculation, typical for gamma spectrometry [91].

Fig. 3.8 Analysing the gamma-ray spectrum with Spectra-line GP software.

The detector system also contains a liquid nitrogen cooling, cryostat, preamplifier and Dewar vessel. In fig 3.9 illustrates the input stage of preamplifier and detector are placed in the vacuum chamber of the cryostat and has to keep cool until the temperature of the liquid nitrogen. The non-cooled part of the preamplifier is being kept out of the vacuum volume in a separate section.4 cables are used to connect the detector to the spectrometric equipment. With 3 lock screws the cryostat is fixed and is placed on the neck of the Dewar vessel illustrates in fig. 3.10. The detector accommodate one types of sensing element attached to the cooling part.

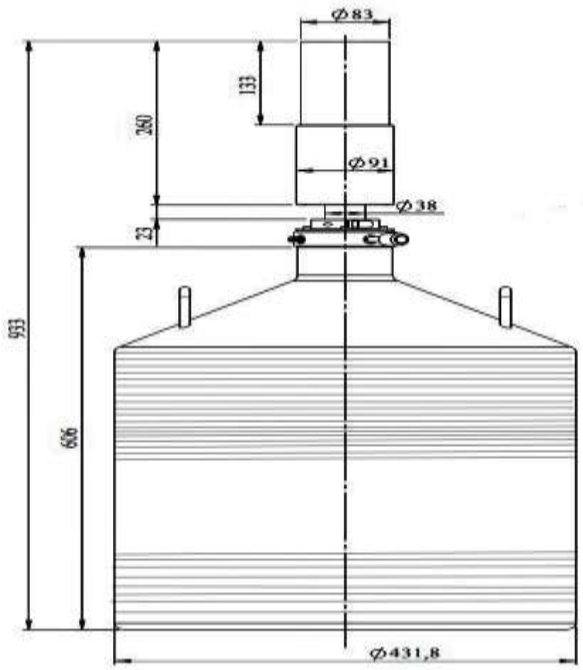

Fig 3.9 Schematic diagram of HPGe detector unit used in this study

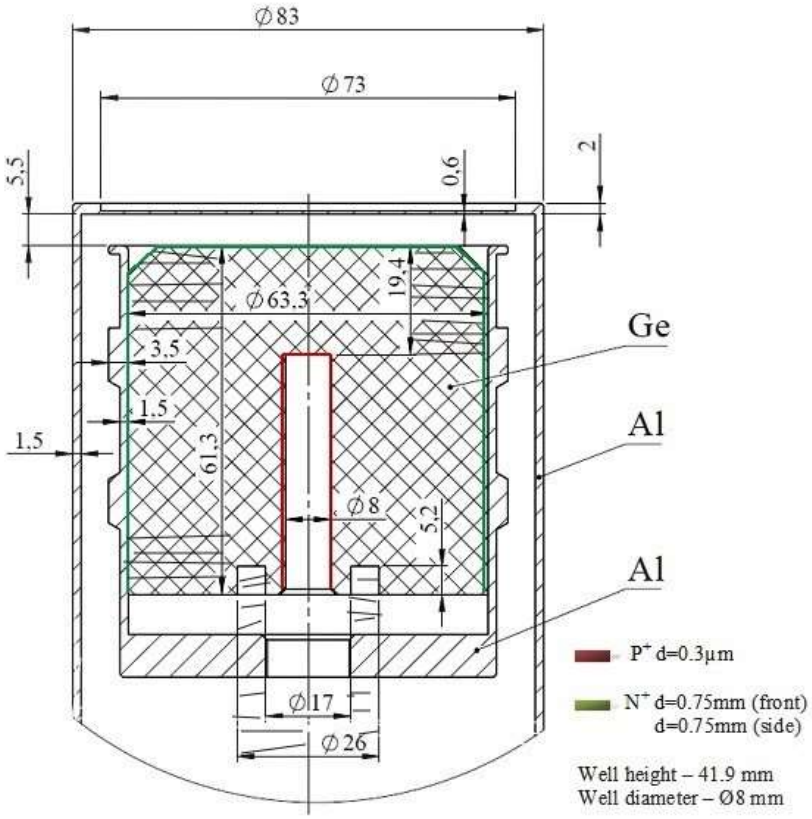

Fig. 3.10 Schematic diagram of HPGe detector crystal used in this study

A monitoring circuit is connecting to the sensing element which is incorporated into PA electronics. The monitoring circuit's output signal is connected via the cable POWER DC ±12V and it contact to the input of HV source in spectrometric device and acts [92].

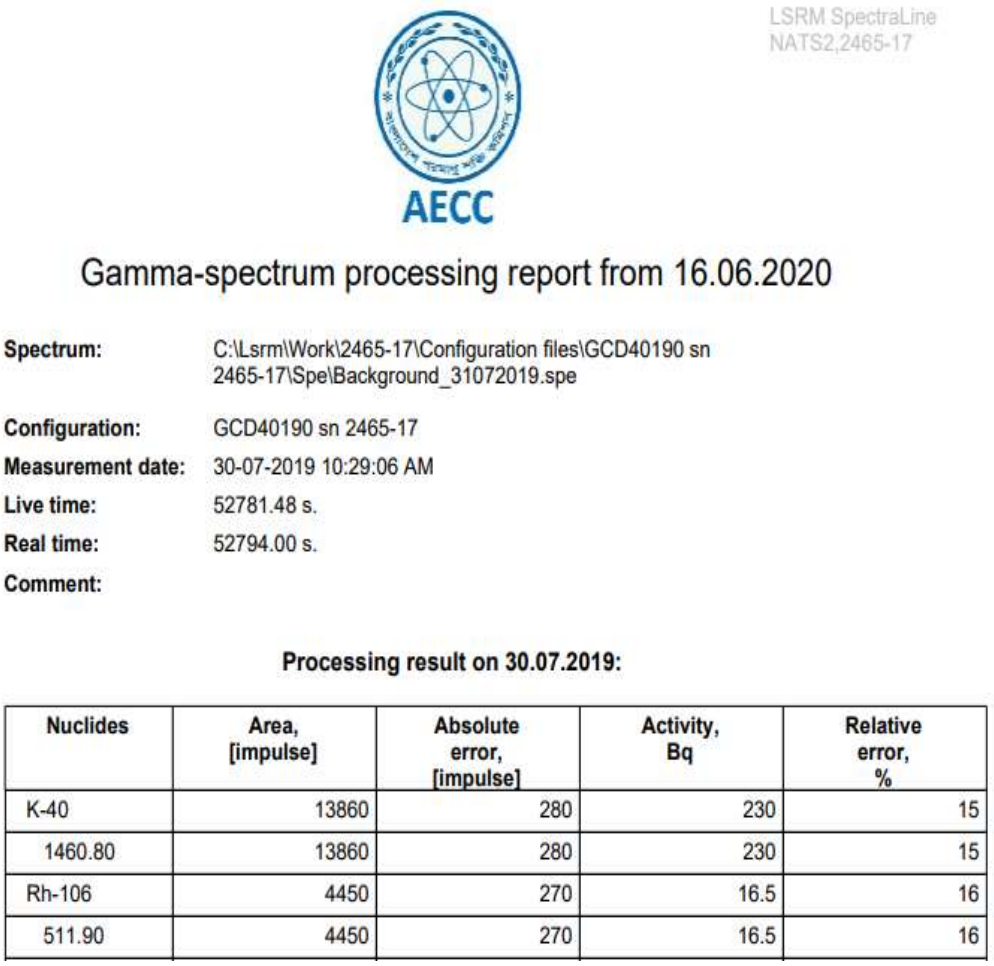

LSRM SpectraLine
NATS2,2465-17

AECC

Gamma-spectrum processing report from 16.06.2020

Spectrum: C:\Lsrm\Work\2465-17\Configuration files\GCD40190 sn 2465-17\Spe\Background_31072019.spe

Configuration: GCD40190 sn 2465-17
Measurement date: 30-07-2019 10:29:06 AM
Live time: 52781.48 s.
Real time: 52794.00 s.
Comment:

Processing result on 30.07.2019:

Nuclides	Area, [impulse]	Absolute error, [impulse]	Activity, Bq	Relative error, %
K-40	13860	280	230	15
1460.80	13860	280	230	15
Rh-106	4450	270	16.5	16
511.90	4450	270	16.5	16

Fig. 3.11 Gamma spectrum processing report of background.

In order to reduce the statistical counting error, the samples were counted for 60,000 s. To determine the background counts, an empty sealed plastic container was counted under the same conditions as the samples, and this value was subtracted from the counts of each sample to obtain the net counts. However, the data obtained from the measurement consists of a large number of pulse heights, of which only a small portion were utilized for analysis.

Fig: 3.12 Digital MCA 527.

A high-performance desktop computer equipped with the Spectra line Gamma Precision (GP) software package is utilized to perform spectrometry measurements and process linear spectra. The procedure for processing spectra includes identifying radionuclides, determining peak parameters, estimating radionuclide activity, and calculating activity. These procedures are performed in accordance with the specified conditions [90]. Prior to and following a set of sample readings, a background measurement of the detector was conducted by placing an empty marinelli beaker on the detector head for the same duration as the readings taken for soil and water samples. The average background measurement from a series of readings was deducted from each of the sample results. Before and during the read-out process, several operations involving the HPGe detector needed to be performed. These include: (i) calibrating the energy, (ii) assessing the energy resolution, (iii) calibrating the efficiency, and (iv) determining the lower limit of detection for each of the radionuclides identified. Throughout the readout duration, the dewar was replenished with liquid nitrogen once a week.

Eckert & Ziegler Analytics

CERTIFICATE OF CALIBRATION
Standard Reference Source

1380 Seaboard Industrial Blvd.
Atlanta, Georgia 30318
Tel 404-352-8677
Fax 404-352-2837
www.ezag.com

SRS Number: 104867
Source Description: 500 mL Sieved Macon Soil in 590G GA-MA Beaker
Product Code: 8501-EG-SOI
Customer: Bangladesh Atomic Energy Commission
P.O. Number: BD-60667-EZ, Item 2 (EZ-EG-SOI-Matx)

This standard radionuclide source was prepared from an aliquot measured gravimetrically from a master radionuclide solution calibrated with a germanium gamma-ray spectrometer system. Additional radionuclides were added gravimetrically from solutions calibrated by gamma-ray spectrometry, ionization chamber, or liquid scintillation counting. Calibration and purity were checked using germanium gamma-ray spectrometry. At the time of calibration no interfering gamma-ray emitting impurities were detected. The gamma-ray emission rates for the most intense gamma-ray lines are given. Eckert & Ziegler Analytics (EZA) maintains traceability to the National Institute of Standards and Technology (NIST) through a Measurements Assurance Program as described in USNRC Regulatory Guide 4.15, Revision 2, July 2007, and compliance with ANSI N42.22-1995, "Traceability of Radioactive Sources to NIST."

Reference Date : 01-October-2016 12:00 PM EST

MGS Mixture

Isotope	Gamma-Ray Energy, keV	Half-Life, d	Activity, Bq	Flux, s^{-1}	Uncertainty			Calibration Method
					u_A(%)	u_B(%)	U(%)	
Am-241	89.8	1.088E+05	5.613E+03	2.015E+03	0.1	1.8	3.6	4πLS
Cd-109	88.0	4.614E+02	7.380E+04	2.731E+03	0.5	2.0	4.1	HPGe
Co-57	122.1	2.717E+02	2.156E+03	1.845E+03	0.4	1.7	3.4	HPGe
Ce-135	165.9	1.376E+02	2.556E+03	2.045E+03	0.4	1.7	3.6	HPGe
Hg-203	279.2	4.689E+01	5.838E+03	4.762E+03	0.3	1.7	3.5	HPGe
Sn-113	391.7	1.151E+02	4.358E+03	2.832E+03	0.4	1.9	3.9	HPGe
Sr-85	814.0	6.485E+01	5.410E+03	2.832E	0.4	1.9	3.9	HPGe
Y-88	898.0	1.066E	7.137E+03	6.687+03	0.7	1.7	3.7	HPGe
Y-88	1836.1	----------	----------	7.080E+03	0.7	1.8	3.9	--------
Co-60	1173.2	1.925+03	3.488E+03	3.423E+03	0.7	1.8	3.9	HPGe
Co-60	1332.5	----------	----------	3.428E+03	0.7	1.8	3.9	---------

Mixed Gamma (MGS) master solution is EZA's eight isotope mixture which is calibrated quarterly and consists of Cd-109, Co-57, Ce-139, Hg-203, Sn-113, Cs-137, Y-88, and Co-60. *Uncertainty*: U-Relative expanded uncertainty, k=2. See NIST Technical Note 1297, "Guidelines for Evaluating and Expressing the Uncertainty of NIST. Measurement Results."**Calibration Methods: 4π LS-4π Liquid Scintillation Counting, HPGe High Purity Germanium Gamma-Ray Spectrometer, IC - Ionization Chamber.

EZA Certificate Program Rev.0,07-DEC-2015

Corporate Office
24937 Avenue Tibbitts Valencia, California 91355

Laboratory
1380 Seaboard Industrial Blvd, Arianta Georgia, 30318

Fig.3.13 Certificate of calibration of slandered calibration.

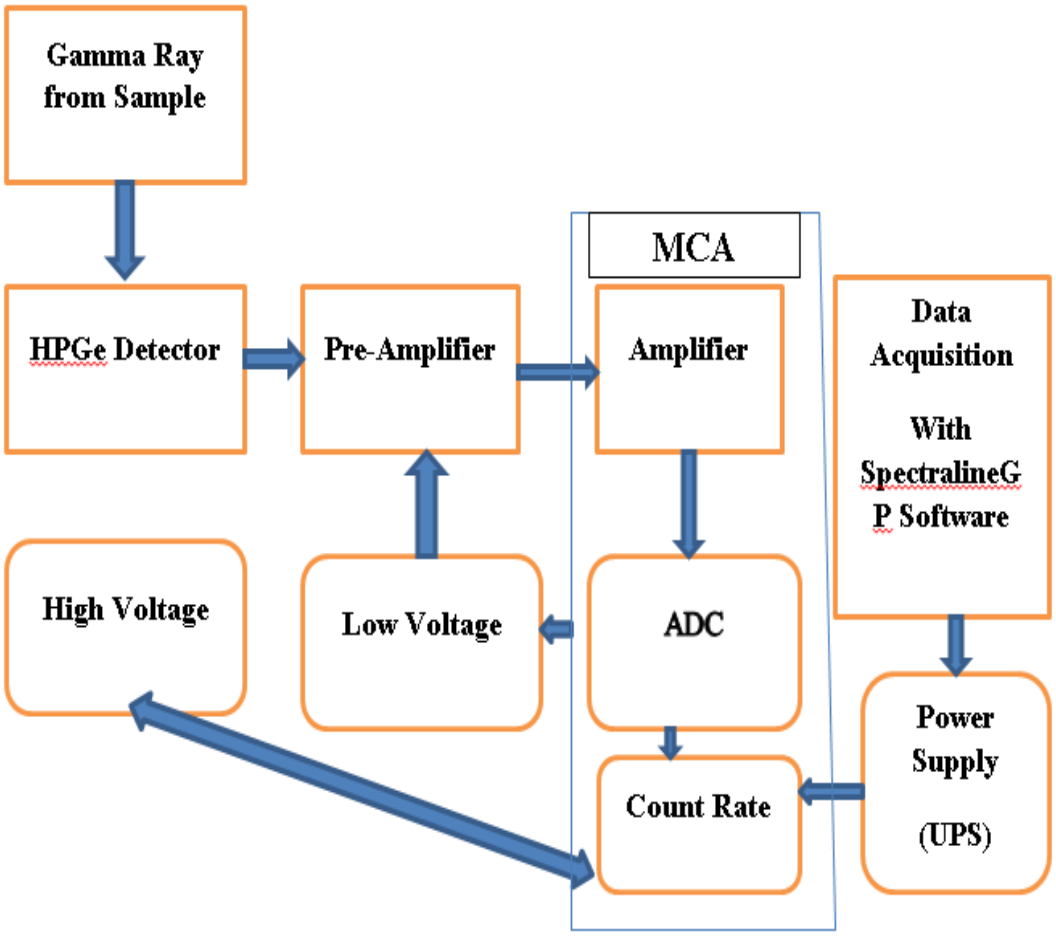

Fig. 3.14 Block diagram of electronic system for Gamma spectrometry

nitrogen once a week.

3.3.3 Pre-sets

The initial configuration of a detector before it is used is referred to as "pre-set." To achieve enough counts for accurate determination of activity in a sample with minimal activity, the live time pre-set can be adjusted. Both live time and real time are measured in seconds and fractions of seconds. These measurements are kept internally with a resolution of 20 milliseconds, as the detector clock increments in 20-millisecond intervals. Real time signifies the elapsed time or clock time. In contrast, live time indicates the duration during which the detector can accept additional pulses (i.e., when it is not processing), and it is calculated as real time minus dead time.

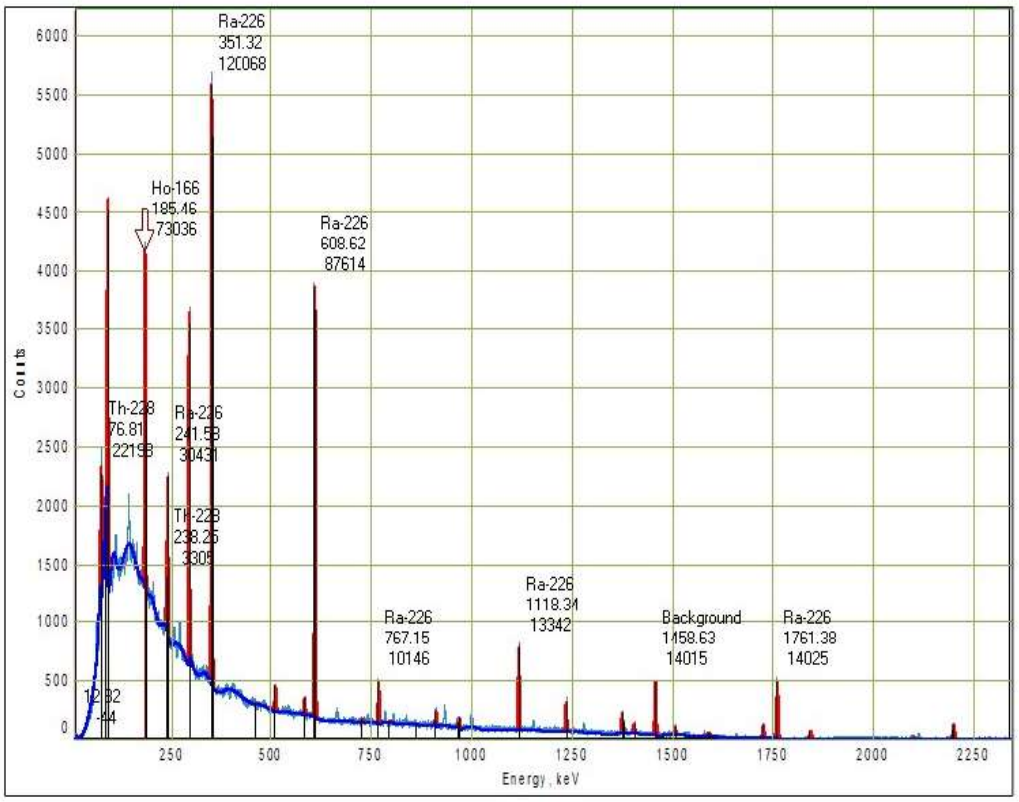

Fig. 3.15 Spectrum of TSP sample-05.

3.3.4 Pulse height analyser and counting technique

A simple discriminator that can be set above the noise level and can produce a standard logic pulse is the main part of a pulse height analyser. Nonetheless, a large body of data consists of a range of pulse heights, only a small portion of which is of interest. MCA is used to summarize the single channel analyser series, including narrow windows, which it can analyse. A multi-channel analyser is used to select an energy spectrum using a pulse analyser that works within many different intervals or channels. The analyser collects pulses at different voltages, which is a significant improvement over SCA spectrum analysis. After collecting all pulses for all voltage ranges, a spectrum can be generated for visual monitoring at the same time. In the form of final results or as raw data, MCA can provide an output signal [93]. This process of determining the performance characteristics of the analyser continues for a time period determined by the experiment. Once the data is stored, it can be

displayed on the monitor graphically. The display reads the memory contents versus memory locations, which is equivalent to the number of pulses versus energy.

As a result, the ADC is referred to as the main component in calculating the analyser's performance characteristics. For a certain time period, it is determined by the experiment conducted by the ADC. This data is then saved and displayed on the monitor as a graphical representation of the number of pulses versus energy [94].

3.3.5 Background effect

Some background signal is produced by all radiation signals. All sources of background signal can be divided into five categories.

i) Radionuclides in the surrounding materials. ii) All Radionuclide in air. iii) Radionuclide in the detector. iv) Interactions of cosmic ray to both the detector itself and also with the surrounded materials. v) The natural radioactivity of the accessory instrument supports and shielding placed of the detector.

Detectors can capture all cosmic radiation that penetrates the Earth's atmosphere along with the presence of natural radioactivity. The measurement of this background radiation can differ depending on the size and type of detector, as well as how the detector is shielded. Since the background intensity essentially indicates the lowest detectable level of radiation, it is essential to consider radiation sources with minimal activity in those applications. Given that the background level ultimately influences the minimum detectable radiation level, it is particularly important in applications involving radiation sources with low activity [95].

3.3.6 Shielding arrangement of the detector

The background radiation is causing damage to the gamma ray spectrometry device. Gamma rays can change the physical properties of the device if it is not properly shielded. From the various sources, radiation may be added during measurement. Another goal is to create strong isolation in laboratories by

providing detector shielding. Environmental radiation shielding of the detector is critical for low-level measurement.

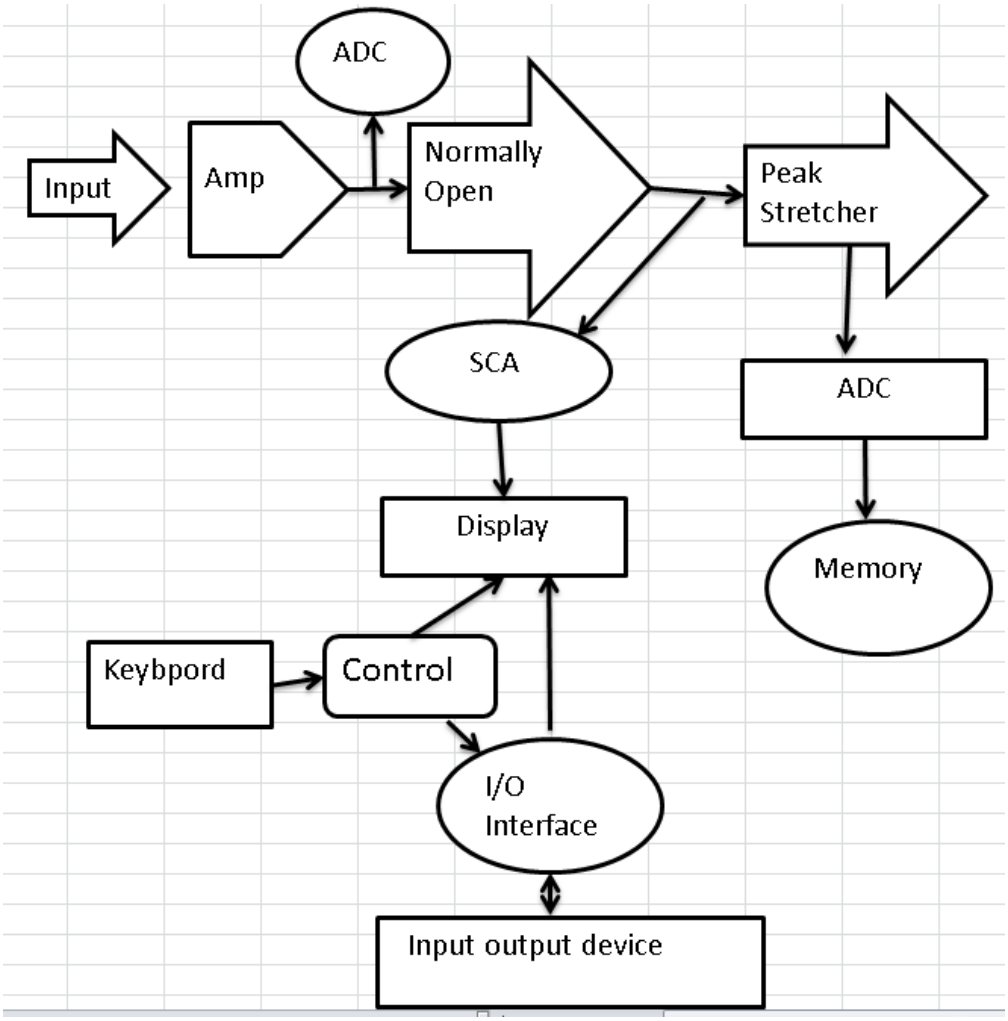

Fig. 3.16 Multi-channel analyser components.

The main function of a shielding arrangement is to reduce the background radiation that comes from cosmic and terrestrial sources. Almost all low-level radiation is emitted by the earth's surface, the cosmos, and artificial materials such as building materials and industrial materials. So erecting a shield, keeping a minimum distance from the source, and using sensitive materials that will successfully absorb unwanted radiations before they reach the detector are all necessary.

Mathematically, the shielding effectiveness is expressed as:

$$I = I_o \, e^{-\mu x} \qquad (3.1)$$

Where, μ = linear absorption co-efficient. x = thickness of the shielding material, I_0 = intensity of the beam.

Various kinds of shields are to be designed as if they can prevent radiation leakage. It is generally used for lead or steel with low activity. In the case of the photoelectric effect and pair production range, the absorption coefficient of lead material is higher than that of steel material. In this study, lead is used as a shielding material in the HPGe detector. Chief lead is more suitable than any other material due to its high density, large atomic number, and low price. As the atomic number of the shielding materials increases, backscatter within the shield decreases. Lead shields have significantly less backscatter than steel shields. As the internal dimension of the shield increases, the backscatter component decreases [96].

3.3.7 Peak area determination

The spectrum files and a list of the background, net area, counting uncertainty, full width at half maximum (FWHM), and net count rate for all peaks are analysed in the spectrum by the gamma vision program. For all library peaks in the analysis energy range, the programmer attempts to calculate the net peak area and centroid of the peak area centroid at that channel. Each peak is considered to be a singleton. An isolated peak is a singlet, i.e., in the spectrum.

For all library peaks in the analysis energy range, the programmer attempts to calculate the net peak area and centroid of a peak at that channel. At this step in the analysis, each peak is considered to be a singleton. An isolated peak is far away from other peaks, as if a significant background would be demonstrated on both sides of the singlet. After calculating the background, the net area is determined, and in this way, the centroid follows. The well-resolved peak area can be obtained by simply adding the data under the peak and subtracting the background underlying it. The areas of the components of unresolved multiples are obtained by performing non-linear least-squares fit to the data [97].

By using n points on each side of the peak, obtain the background under the peak that may be approximated by a straight line. The sum of the contents of each channel in between the background channels is called the gross area of the peak.

$$G = \sum_{i=l}^{h} C_i \qquad (3.2)$$

Where,

l = at the low energy side of the spectrum the centre channel of the background calculation width.

h= at the high-energy side of the spectrum the centre channel of the background calculation width.

C_i = the data value of channel i.

By using n points on each side of the peak, obtain the background under the peak that may be approximated by a straight line. The sum of the contents of each channel in between the background channels is called the gross area of the peak.

As the peaks get smaller, they are less sensitive to random fluctuations in the data and less sensitive to the difference between the spectrum peak shapes. The gross area minus the background in those channels is called the net area of the peak. The peak area calculation method (referred to as total summation) maintains precision as the peak gets smaller, is less sensitive to random fluctuations in the data, and is less sensitive to the differences between the spectrum peak shape and the calibrated peak shape. The net area of the peak is the gross area minus the background in those channels, as follows:

$$A = G - \left(\frac{N}{2n}\right)(B_1 + B_1) \ldots\ldots\ldots\ldots\ldots\ldots\ldots\ldots\ldots\ldots\ldots\ldots\ldots (3.3)$$

Where, N = number of channels in the peak,

n= Background channels number on each side of the peak,

B_1= sum over n channels below the peak

B_2 = sum over n channels above the peak

G = gross counts (integral) under the peak,

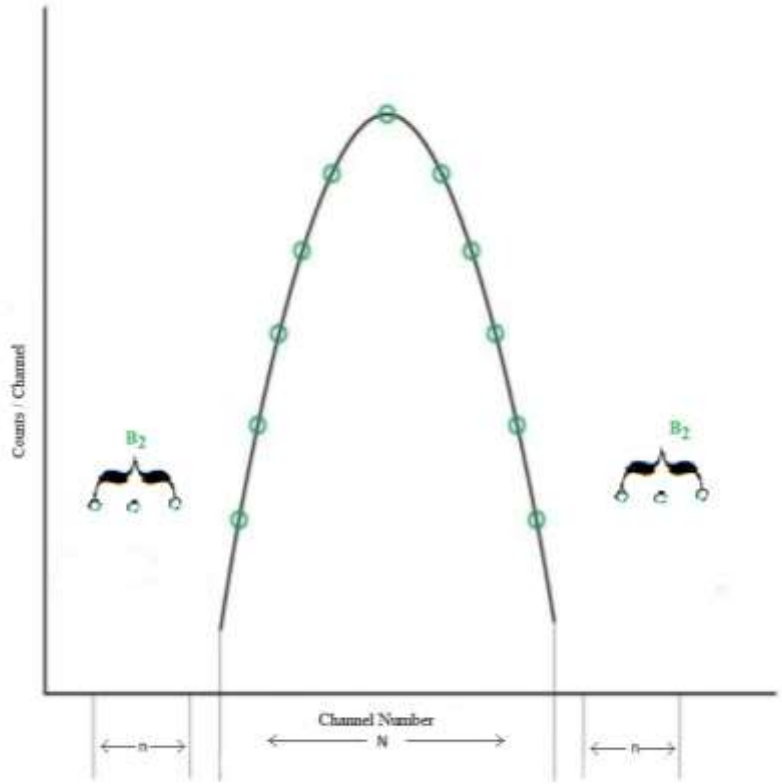

Fig. 3.17 Typical spectral peak with parameters used in peak area determination.

3.3.8 Peak uncertainty

The uncertainty in the gross area and the uncertainty in the background added in quadrature is called the counting uncertainty. The square root of the area is the uncertainty in the gross area.

As the background is a calculated number, so the uncertainty in the background is complex. The uncertainty in the channels used to calculate the end points of the background multiplied by the ratio of the number of channels in the peak to the number of channels used to calculate the background is called the background area uncertainty. For low counts and wide peaks per channel, there is high uncertainty in the calculated background.

$$bkg\ error = \left(\frac{(background\ area\ )(peak\ width)}{(width\ of\ low\ average + width\ of\ high\ average)}\right) \ldots\ldots\ldots\ldots (3.4\ )$$

Gross area error=√gross area

$$Net\ area\ error = \sqrt{(\text{gross area error})\ 2\ +\ (\text{background error}\ )2}$$

3.3.9 Peak centroid

The centre of moment of the peak is called the peak centroid. It is measured by calculating the weight of the channel number of the peak. As a result, the total number of channels multiplied by the sum of the channel contents The determination of the centroid is based on the data in the measured full-width at one 25^{th}(FW0.04) for the peak.

3.4 PRIOR TASKS TO BE ACCOMPLISHED

To get accurate measurements from a detector, first some basic tasks must be completed, and those are (i) energy resolution (the change of peak with energy); and (ii) energy calibration (the relationship between channels and energy). (iii) Calibration of efficiency

To make the performance of a detector fruitful in respect to the accuracy of measurements, there are some basic tasks to be accomplished first, including (i) energy calibration—the relationship between channels and energy. (ii) Energy resolution: the variation of peak width with energy; and (iii) Efficiency calibration—the relationship between the number of counts given by the detection and the actual disintegration rate. The peak-to-Compton ratio, peak shape, crystal dimension, and price are considered important characteristics. A detector's performance is evaluated based on its resolving power and higher-value efficiency. The resolution of a detector gradually decreases as its volume increases. The detector's performance improves as efficiency increases and energy resolution decreases, with all parameters describing the function of gamma-ray energy. There are various factors that influenced calibration, and they are a) sample density effect b) Source effect/ detector distance c) energy shifts with the change of the source. d) Atypical peak widths e) Inaccurate decay corrections. f) Live time correction errors g) True coincidence summing h) Pile-up losses.

3.4.1 Energy Calibration

Calibration refers to the relationship between gamma ray energy and peak position in the spectrum. The energy calibration is accomplished by measuring the spectrum of the standard gamma ray source and peak position with energy. For energy calibration in this study, e.g. ^{60}Co, ^{137}Ba and ^{152}Eu different source energies were used. The resulting spectrum from that source, the gamma-ray energies, and channel number are collected in the table [98].

To achieve good statistical exactness for the peaks, in practice more essential to measure the spectrum to be used for the calibration. The respective channel numbers and the calibrated energy are stored in memory, and after searching the peaks, the peak position of a channel is determined. With a channel number, the gamma energy follows a linear relationship, and the straight line equation is formed by the gamma energy regarding the channel number.

$$Y = aX + b \tag{3.5}$$

X = Channel number, a and b are constants, Y = Energy of the source in keV

Table: 3.2 Data for energy calibration of the HPGe γ-ray detector

Name of sources	Energy	Channel No
Am-241	59.373	93.387
Cd-109	87.793	137.976
Co-57	121.852	191.739
Ce-139	136.405	214.247
Cs-137	661.719	1038.446
Co-60	1173.206	1840.951
Co-60	1332.462	2090.818
K-40	1460.691	2292.005
Y-88	1846.872	2997.909

3.4.2 Energy resolution

As an important parameter of a detector, energy resolution is calculated to show the ability of a detector to identify the separation of two adjacent peaks in

a gamma-ray spectrum. Any specific peak is measured using full width half maximum (FWHM) [77].

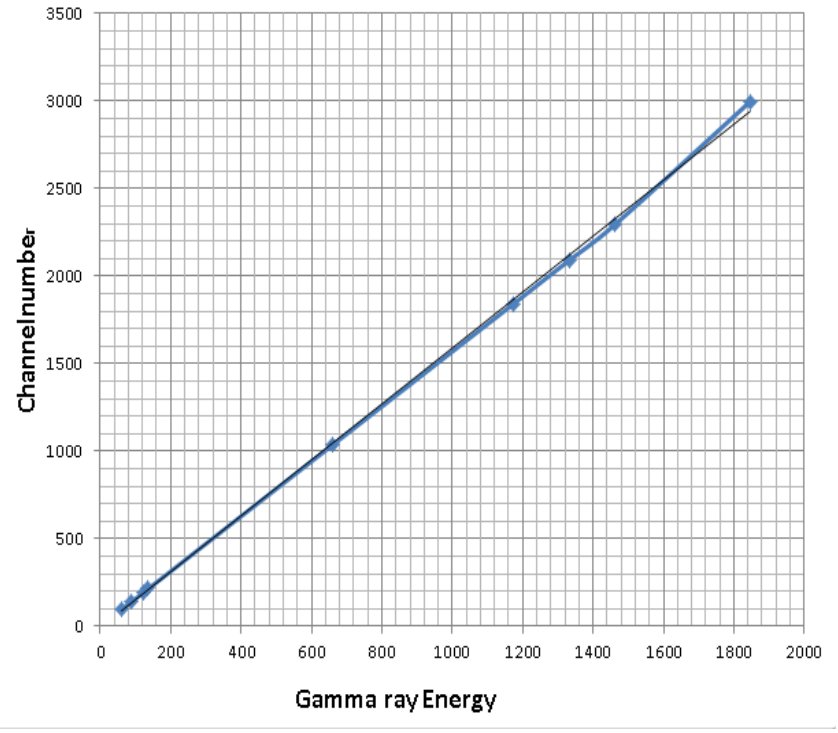

Fig. 3.18 Energy calibration curve of HPGe γ- ray detector.

For these two reasons, good resolutions are important.

1. The gamma rays, which are close in energy and measurable separately. As soon as the centroids of good shapes peak at 3 FWHM apart, then all peaks are distinctly separated. As a Gaussian shape, FWHM = 2.38FWHM at the one-fiftieth maximum level with equal areas in each peak, there is a negligible overlap.

It is a less critical and connected spectrum with small peaks on an unstable background for high resolution viewing. A peak with few counts in it will centralize those counts into only a few channels, and those channels will stand out more separately above the background continuum, enabling more reliable detection and measurement. This latter point may be a good enough reason for making germanium into sodium iodide to get greater efficiency in counting [99].

The resolution is given by the following equation:

$$\text{Resolution} = \text{FWHM(in channel)} \times \frac{\text{Energy difference of two gamma ray peak}}{\varepsilon_\gamma \times P_\gamma \times t \times m} \quad (3.6)$$

$$\text{Resolution} = \frac{E_2 - E_1}{C_2 - C_1} \quad (3.7)$$

$$\text{Resolution} = 11 \times \frac{1332.51 - 1173.23}{6671 - 5871} = 2.1 \quad (3.8)$$

3.4.3 Efficiency Calibration

Gamma rays are produced by the source, and the overall count of gamma rays is recorded by a detector, which is known as the detector's efficiency. The efficiency refers to a detector's capacity to absorb a significant amount of gamma ray energy. For a specific gamma ray, a detector's efficiency is influenced by its dimensions, design, the materials utilized within the detector, and the distance separating the detector from the source. Additionally, the counting system can be affected by the environment in which it is located. This variation is related to both the physical alterations of the counting mechanism and the surrounding conditions. Therefore, the geometry of the counting system is kept constant throughout the experiment. It is important to observe general precautions while conducting efficiency calibration since precise calibration of a detector's efficiency in relation to gamma ray energy is essential for detecting activity in the activated sample. For gamma ray detectors, various kinds of efficiency exist, such as a. absolute efficiency and b. intrinsic efficiency [100].

3.4.4 Absolute efficiency

With the help of a source in all directions, produced gamma rays are counted by the detector, and the efficiency is called the ratio of counted gamma rays to produced gamma rays. [101]It depends on the distance between the detector and the source and also on the detector's solid angle.

$$\varepsilon_{abs} = \frac{Number\ of\ \text{counts}\ recorded}{Number\ of\ gamma\ rays\ insident\ on\ the\ detector} \quad (3.9)$$

ε_{abs}= Number of counts recorded Number of gamma rays emitted by the source into all directions.

3.4.5 Intrinsic Efficiency

It is defined as the ratio of the number of pulses recorded by the detector to the number of gamma rays striking the detector. The intrinsic efficiency can be obtained from the following relation:

$$\varepsilon_{in} = \frac{Number\ of\ pulses\ recorded}{Number\ of\ gamma\ rays\ insident\ on\ the\ detector} \quad (3.10)$$

The relation between intrinsic efficiency and absolute efficiency is given by the following equation:

$$\varepsilon_{in} = \varepsilon_{abc}\ x\frac{4\pi}{\Omega\ x\ f} \quad (3.11)$$

Where, f = percentage yield for any source and Ω is the solid angle subtended by the detector at the source position.

3.4.6 Full energy photo-peak efficiency

In practical gamma spectrometry full energy photo-peak efficiency is the most significance parameter and it can be determined with the ratio of the number of counts detected in a peak to the number emitted by the source [101].

$$\varepsilon\ (\%) = \frac{R}{S\ x\ I_Y} \quad (3.12)$$

Where S is the source strength in disintegration per second and Iγ gamma-ray intensity and R is the full-energy peak count rate in counts per second. So, this efficiency can also be defined by the number of detected counts per number of disintegrations in the source as

$$\varepsilon(\%) = \frac{\text{Detecteds counts}}{\text{Prfesent activity of the sample, AtxGamma intensity, } I_Y} \quad (3.13)$$

The dependence of the photo-peak efficiency on energy is described by some analytical functions proposed by a few groups [67–70]. The most frequently used function is the polynomial fit. In practical gamma spectroscopy, the full energy peak is the most significant parameter. In this experiment, an accurate calibration of efficiency is necessary. As the overall uncertainty of the

measurement will be limited by the uncertainty of the efficiency value, a very careful efficiency calibration should be performed. The efficiency of the HPGe detector can be determined using different calibrated standards like ^{60}Co, ^{137}Ba, ^{152}Eu and ^{137}Cs sources.

A calibrated source is specified by its activity on a certain date. The present activity of the source can be obtained from the following relation:

$$A_t = A_0 e^{-\lambda t} \quad (3.14)$$

A_0 is the initial activity of the source.

A_t is the final activity of the source.

t is the decay time.

λ= decay constant= $\ln 2/T_{1/2} = 0.693/ T_{1/2}$; here $T_{1/2}$= half-life of the source.

Using standard calibrated sources separately for a counting time sufficient for a peak area equal to or greater than 10,000 spectra, they were acquired at various distances above the surface of the detector. The energies of the gamma-rays emitted from radioactive sources ranged from 81 keV to 1408 keV. This is completed by using a detector of suitable size or by choosing a detector material of a high atomic number. This is completed by employing a detector made of a high atomic number material or of a suitable size.

3.4.7 The minimum detectable activity

The minimum detectable activity (MDA in $Bqkg^{-1}$) of the gamma-ray measurement system employed in this study was determined using equation 3.15.

$$MDA = \frac{C_F \times \sqrt{B}}{\varepsilon I_\gamma t m} \quad (3.15)$$

In this equation, C_F represents the statistical coverage factor for a 95% confidence level, B denotes the background counts within the region of interest for each radionuclide, ε signifies the absolute efficiency of the HPGe detector, I_γ is the probability of gamma emission, t indicates the measuring time (86,400 s), and m refers to the sample mass in kg.

3.5 RADIOLOGICAL PARAMETERS

3.5.1 Measurement of Activity Concentration

The activity levels of ^{226}Ra (^{238}U) and ^{232}Th were determined using gamma peaks from their respective progeny. Specifically, the activity concentration of ^{226}Ra (^{238}U) was measured using the characteristic gamma peaks of its progeny: ^{214}Pb (351.93 keV), ^{214}Bi (1120.28 KeV and 1764.491 KeV)[46]. In addition, the activity of ^{232}Th was estimated by utilizing the gamma-ray lines of ^{212}Pb (238.63 keV), ^{228}Ac (911.20 keV), and ^{208}Tl (583.191 keV). Meanwhile, the activity concentrations of ^{40}K were determined through the detection of a single transition photo peak with an energy of 1460.821 keV [54]. In order to reduce ambiguity when evaluating the activity of the multi-photo-peaks progenies of ^{226}Ra and ^{232}Th, a weighted mean approach was employed [102]. The activity concentration of the desired radionuclides was determined through the use of Equation (3.17) [103].

$$A = \frac{N}{\varepsilon_Y \, I_Y \, T_s \, M_s} \tag{3.17}$$

where A represents the specific activity (Bqkg^{-1}), N denotes the net count within a photo peak, ε_γ indicates the efficiency of the detector for the related peak, I_γ is the probability of gamma emission[63]ability, T_s refers to the sample's counting duration in seconds, and Ms signifies the mass of the sample in kilograms.

To achieve more precise results, the overall uncertainty of the specific activity for each sample analysed was calculated by considering several factors: detector efficiency (5%), assessment of the photo peak area (2-7%), gamma-ray emission probability (<0.2%), and the weight of the sample (0.01%).All other related parameters, as mentioned before in Chapter-1, were calculated accordingly.

Chapter 4: RESULTS AND DISCUSSION

4.1 GENERAL

The concentration of radionuclides in widely used chemical and organic fertilizers in Chattogram, Bangladesh, was assessed using a high-purity germanium (HPGe) gamma-ray spectroscopic system at the Atomic Energy Centre in Chattogram. This study included 39 samples of fertilizer from nine different types to identify the presence and concentration levels of radionuclides. The activity concentrations and uncertainties for the detected radionuclides, including ^{226}Ra, ^{232}Th, and ^{40}K, are presented in Table 4.1(a-e), while the average activity concentration of radionuclides across all fertilizer samples is shown in Table 4.2.

4.2 SPECIFIC ACTIVITY

Table 4.3 reveals that the specific activities of ^{226}Ra in Triple Superphosphate (TSP) fertiliser range from 98±10.8 to 460±55.2 Bqkg^{-1}, averaging 304.6±6.1 Bqkg^{-1}. The average concentration of ^{232}Th is 19.1±3.5 Bqkg^{-1}, which is found to be within the normal range as compared to the findings of a previous study by Alam et al. [44]. Notably, the concentrations of ^{238}U and ^{232}Th series radionuclides in our examined TSP fertilisers are significantly lower than the typical concentrations reported in the UNSCEAR 2008 report [104]. Furthermore, the presence of ^{40}K in TSP remains below the 40 Bqkg^{-1}. So, more experiments are essential for monitoring properly the presence of ^{226}Ra in TSP fertiliser. Otherwise, it may be harmful for various living organism. Especially, as shown in table 4.3, in seven samples of TSP where the specific activity of ^{226}Ra was found to be higher than 300 (Bqkg^{-1}). But the ^{232}Th concentration was detected as lower comparatively than ^{226}Ra. The concentrations of ^{226}Ra and ^{232}Th in di-ammonium phosphate fertilisers range from 1.4±0.7 to 6.9±1.3 Bqkg^{-1} and from 7±1.6 to 33±5.6 Bqkg^{-1}, respectively, with an average of 4.8 ± 1.1 Bqkg^{-1} and 20 ± 3.6 Bqkg^{-1}, respectively as shown in table 4.4

Table 4.1 Specific Activity concentrations of ^{226}Ra, ^{232}Th and ^{40}K in all fertiliser samples in Bqkg^{-1}.

Sample code	Specific activity			Sample code	Specific activity		
	^{226}Ra	^{232}Th	^{40}K		^{226}Ra	^{232}Th	^{40}K
(a) TSP Fertiliser				(b) DAP Fertilisers			
TSP-1	320 ± 35.2	8.6 ± 2.6	< 40	DAP-1	1.4 ± 0.7	< 2.8	< 40
TSP-2	460 ± 55.2	26 ± 4.9	< 40	DAP-2	3.8 ± 1.1	33 ± 5.6	< 40
TSP-3	400 ± 48	16 ± 3.4	< 40	DAP-3	5 ± 1.1	< 2.8	< 40
TSP-4	104 ± 10.4	18 ± 3.3	< 40	DAP-4	6.9 ± 1.3	7± 1.6	< 40
TSP-5	98 ± 10.8	20 ± 3.6	< 40	DAP-5	6.8 ± 1.3	< 2.8	< 40
TSP-6	400 ± 40	26 ± 12	< 40	DAP Avg	4.8 ± 1.1	20 ± 3.6	-
TSP-7	350 ± 52.5	< 2.8	< 40	(d) Boron Fertiliser			
TSP Avg.	304.6 ± 6.1	19.1 ± 3.5	-	BOR-1	8 ± 3.2	< 2.8	< 40
(c) MOP Fertiliser				BOR-2	< 1.2	7 ± 1.7	< 40
MOP-1	< 1.2	< 2.8	10600 ± 1484	BOR-3	5.7 ± 2.9	< 2.8	< 40
MOP-2	8 ± 2.3	< 2.8	10300 ± 1442	BOR-4	11.4 ± 1.9	10 ± 2.2	< 40
MOP-3	< 1.2	< 2.8	9800 ± 1372	BOR Avg.	8.4 ± 2.7	8.6 ± 1.9	
MOP-4	2 ± 0.8	< 2.8	10700 ± 1070	(e) Organic Fertiliser			
MOP-5	< 1.2	< 2.8	11000 ± 1100	ORG-1	< 1.2	7 ± 1.8	< 40
MOP-6	< 1.2	< 2.8	11100 ± 1110	ORG-2	55 ± 9.9	68 ± 8.8	320 ± 48
MOP-7	< 1.2	< 2.8	10700 ± 1070	ORG-3	< 1.2	3.4 ± 1.4	700 ± 105
MOP-8	< 1.2	< 2.8	10500 ± 735	ORG-4	138 ± 17.9	< 2.8	1250 ± 187.5
MOP-9	< 1.2	< 2.8	8100 ± 1134	ORG-5	29 ± 7.3	< 2.8	3440 ± 275.2
Q-Potash	< 1.2	< 2.8	12400 ± 1240	ORG-6	12 ± 3.6	31	< 40
MOP Avg.	5 ± 1.52	-	10520 ± 1175.7	ORG-7	4.3 ± 2.2	< 2.8	< 40
(f) Gypsum and SSP Fertilisers				ORG-8	4.6 ± 1.3	9.1 ± 2.2	410 ± 65.6
GYP	242 ± 29.1	< 2.8	< 40	ORG-9	9 ± 3.6	< 2.8	< 40
SSP	84 ± 15.1	60 ± 13.2	710 ± 78.1	ORG-10	4.8 ± 1.1	9.4 ± 1.7	< 40
				ORG-11	8 ± 4	< 2.8	< 40
				ORG Avg	33.6 ± 5.8	19.2 ± 4.4	1224 ± 136.3

The concentrations of ^{226}Ra and ^{232}Th in di-ammonium phosphate fertilisers range from 1.4±0.7 to 6.9±1.3 Bqkg^{-1} and from 7±1.6 to 33±5.6 Bqkg^{-1}, respectively, with an average of 4.8 ± 1.1 Bqkg^{-1} and 20 ± 3.6 Bqkg^{-1}, respectively as shown Table 4.4.

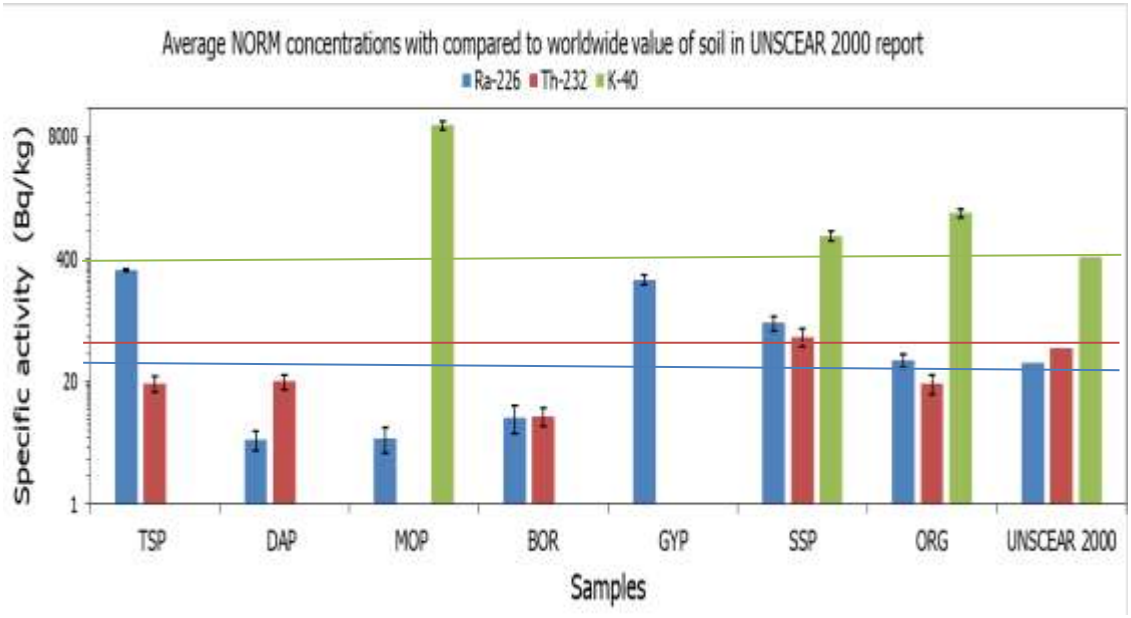

Fig. 4.1.Average specific activity in studied samples compared to the worldwide average activity in soil reported by UNSCEAR 2000 [105].

Our study found that the concentrations of ^{226}Ra and ^{232}Th in DAP were relatively lower than those reported in the studies by Loan et al. [106], El-Taher et al. [107],and Samad et al. [108]. Although some of the DAP and TSP simples have ^{232}Th below the minimum detectable limit (2.8 Bqkg^{-1}), and in three DAP samples and one TSP samples have ^{232}Th, all of the samples we studied have ^{40}K levels below the detectable limit (40 Bqkg^{-1}) [109]111].

Table 4.2. Average specific Activity concentrations of ^{226}Ra,^{232}Th, and ^{40}K in TSP, MOP, Q-Potash, DAP, GYP, SSP, Organic and BORON fertiliser samples in Bqkg^{-1}.

Fertiliser Type	^{226}Ra Activity (Bqkg^{-1})	^{232}Th Activity((Bqkg^{-1})	^{40}K Activity (Bqkg^{-1}-)
TSP Avg.	304.6 ± 6.1	19.1 ± 3.5	< 40
MOP Avg.	5 ± 1.52	< 2.8	10520±1175.7
Q-Potash	< 1.2	< 2.8	12400±1240
DAP Avg.	20±3.61	4.78±1.1	< 40
GYP	242 ± 29.1	< 2.8	< 40
SSP	84±15	60±13.2	710±±76.1
ORG Avg.	33.6 ± 5.8	19.2 ± 4.4	1224±136.26
BOR Avg.	8.55±1.96	8.366±2.66	< 40

The gamma-ray spectroscopy analysis results for the Muriate of Potash samples are presented in Table 4.5. The findings indicate that 40K is the radionuclide with the highest abundance, showing an average specific activity of 10,520±1175.7 Bqkg−1, while the minimum and maximum values are recorded at 8100±1134 and 12,400±1240 Bqkg−1, respectively. This elevated level of 40K in MOP fertilizer is linked to the fact that potassium constitutes 60% of its makeup [110].Except MOP-2 and MOP-4 samples rest of the six samples had 226Ra below the detectable limit (1.2 Bqkg-1). All MOP sample had 232Th below the detectable limit (2.8 Bqkg-1). It was found the presence of 226Ra and 232Th in MOP samples 17.0 ± 3.6 Bqkg-1 and 6.2 ± 1.6 Bqkg-1 in the analysis of Alam et al. [44].

Table 4.3. Activity concentrations of ^{226} Ra, ^{232}Th, and ^{40}K in TSP fertiliser samples in Bqkg^{-1}.

TSP Fertiliser	Specific Activity		
TSP	^{226} Ra (Bqkg^{-1})	^{232}Th (Bqkg^{-1})	^{40}K (Bqkg^{-1})
TSP-1	320 ± 35.2	8.6 ± 2.6	< 40
TSP-2	460 ± 55.2	26 ± 4.9	< 40
TSP-3	400 ± 48	16 ± 3.4	< 40
TSP-4	104 ± 10.4	18 ± 3.3	< 40
TSP-5	98 ± 10.8	20 ± 3.6	< 40
TSP-6	400 ± 40	26 ± 12	< 40
TSP-7	350 ± 52.5	< 2.8	< 40
TSP Avg.	304.6 ± 6.1	19.1 ± 3.5	

The presence of primordial radionuclides, specifically ^{226}Ra and ^{232}Th, in Boron fertilisers is shown in table 4.6 with lower concentrations compared to other fertiliser types, with an average of 8.4 ± 2.7 and 8.6 ± 1.9 Bqkg^{-1}, respectively, while ^{40}K remains undetected.

The data analysed for 11 varieties of organic fertilizers, largely sourced from animal manure and plant compost, are shown in table 4.7. The findings indicate that the average radioactivity per unit mass in the samples corresponding to ^{226}Ra, ^{232}Th, and ^{40}K is 33.6±5.8, 19.2±4.4, and 1224±136.3 Bqkg^{-1}, respectively. Despite being made from combustible natural materials, the average

concentration of ^{40}K in these organic fertilizers exceeds the population-weighted average noted for soil (420 $Bqkg^{-1}$) in the UNSCEAR 2000 report. [105].

Table 4.4. Activity concentrations of ^{226} Ra, ^{232}Th, and ^{40}K in DAP fertiliser samples in $Bqkg^{-1}$.

DAP Fertiliser	Specific Activity		
DAP	^{226}Ra ($Bqkg^{-1}$)	^{232}Th ($Bqkg^{-1}$)	^{40}K ($Bqkg^{-1}$)
DAP-1	1.4 ± 0.7	< 2.8	< 40
DAP-2	3.8 ± 1.1	33 ± 5.6	< 40
DAP-3	5 ± 1.1	< 2.8	< 40
DAP-4	6.9 ± 1.3	7± 1.6	< 40
DAP-5	6.8 ± 1.3	< 2.8	< 40
DAP Avg.	4.8 ± 1.1	20 ± 3.6	

As can be seen in the table 4.5. Gypsum fertiliser the specific concentration of ^{226}Ra were 242 ± 29.1 $Bqkg^{-1}$ which are almost seven times higher than the world recommended value of ^{226}Ra concentration(35 $Bqkg^{-1}$) reported by the United Nations Scientific Committee on the Effects of Atomic Radiation [105].

Table 4.5. Activity concentrations of ^{226} Ra, ^{232}Th, and ^{40}K in MOP fertiliser samples $Bqkg^{-1}$.

MOP fertiliser	Specific Activity		
MOP	^{226} Ra ($Bqkg^{-1}$)	^{232}Th ($Bqkg^{-1}$)	^{40}K ($Bqkg^{-1}$)
MOP-1	< 1.2	< 2.8	10600± 1484
MOP-2	8 ± 2.3	< 2.8	10300± 1442
MOP-3	< 1.2	< 2.8	9800 ± 1372
MOP-4	2 ± 0.8	< 2.8	10700± 1070
MOP-5	< 1.2	< 2.8	11000± 1100
MOP-6	< 1.2	< 2.8	11100± 1110
MOP-7	< 1.2	< 2.8	10700± 1070
MOP-8	< 1.2	< 2.8	10500 ± 735
MOP-9	< 1.2	< 2.8	8100 ± 1134
Q-Potash	< 1.2	< 2.8	12400± 1240
MOP Avg.	5 ± 1.52	< 2.8	10520 ± 1175.7

In the one sample of single superphosphate fertilisers presence of ^{226}Ra radionuclide concentration is 84 ± 15.1 $Bqkg^{-1}$ that is not elevated level of world

recommended value. In the SSP sample, presence of ^{232}Th is 60 ± 13.2 Bqkg^{-1} which is also alarming but lower value of analysis of Alam et al [44].

Table 4.6. Activity concentrations of ^{226} Ra, ^{232}Th, and ^{40}K in BORON fertiliser samples in Bqkg^{-1}.

Sample code	Specific activity		
Boron Fertiliser	^{226} Ra (Bqkg^{-1})	^{232}Th (Bqkg^{-1})	^{40}K(Bqkg^{-1})
BOR-1	8 ± 3.2	< 2.8	< 40
BOR-2	< 1.2	7 ± 1.7	< 40
BOR-3	5.7 ± 2.9	< 2.8	< 40
BOR-4	11.4 ± 1.9	10 ± 2.2	< 40
BOR Avg.	8.4 ± 2.7	8.6 ± 1.9	

Fig. 4.1 displays the average specific activity of NORM found in the studied samples and compares it with the worldwide average specific activity of NORM in soil reported in the UNSCEAR 2000 report [105].

Most of the samples exhibit hazardous radionuclide levels that are lower than the UNSCEAR 2000 standard, with the exception of MOP fertilizers, where ^{40}K is detected at a higher concentration. The concentrations recorded, however, remain within the acceptable international radioactivity limits set by the IAEA, which stipulate 1000 Bqkg^{-1} for radionuclides from the ^{238}U and ^{232}Th series, and 10,000 Bqkg^{-1} for ^{40}K [69]. Conversely, the Q-potash sample has shown a ^{40}K concentration (12400±1240 Bqkg^{-1}) that exceeds the exemption threshold. This finding suggests that additional research is essential to gather more accurate data and to implement regulatory actions if necessary. In Table 4.2, the average specific activity concentrations of ^{226} Ra, ^{232}Th, and ^{40}K in different samples are presented, allowing for a comparison of all radioactive nuclides. It is evident that the average specific activity concentrations of ^{226} Ra are greater in TSP samples, while they are lower in MOP samples. Simultaneously, the average specific activity concentrations of ^{232}Th are predominantly higher in SSP samples. However, the average concentration of ^{40}K is notably elevated in MOP

fertilizers, with organic fertilizers showing an average of 1224±136.26 Bqkg^{-1}, while the SSP sample's average is yet to be specified for further investigation.

Table 4.7 Specific activity concentrations of ^{226}Ra, ^{232}Th, and ^{40}K in organic fertiliser samples in Bqkg^{-1}.

Organic Fertiliser	Specific activity		
Sample code	^{226} Ra	^{232}Th	^{40}K
ORG-1	< 1.2	7 ± 1.8	< 40
ORG-2	55 ± 9.9	68 ± 8.8	320 ± 48
ORG-3	< 1.2	3.4 ± 1.4	700 ± 105
ORG-4	138 ± 17.9	< 2.8	1250 ± 187.5
ORG-5	29 ± 7.3	< 2.8	3440 ± 275.2
ORG-6	12 ± 3.6	31	< 40
ORG-7	4.3 ± 2.2	< 2.8	< 40
ORG-8	4.6 ± 1.3	9.1 ± 2.2	410 ± 65.6
ORG-9	9 ± 3.6	< 2.8	< 40
ORG-10	4.8 ± 1.1	9.4 ± 1.7	< 40
ORG-11	8 ± 4	< 2.8	< 40
ORG Ave	33.6 ± 5.8	19.2 ± 4.4	1224 ± 136.3

Table 4.8. Specific activity concentrations of ^{226} Ra, ^{232}Th, and ^{40}K in Gypsum and SSP fertiliser samples in Bqkg^{-1}.

Fertiliser	Specific activity		
	^{226} Ra	^{232}Th	^{40}K
GYP	242 ± 29.1	< 40	< 40
SSP	84 ± 15.1	60 ± 13.2	710 ± 78.1

4.3 RADIUM EQUIVALENT ACTIVITY

As previously mentioned, radium equivalent activity serves as a commonly used hazard index that allows for the comparison of the activity concentrations of radium, thorium, and potassium found in the samples. The index value is calculated using Equation 1.2 and is visually represented in Fig 4.2 as well as in Table 4.9. The findings indicate that the average Ra^{eq} concentrations in MOP fertilizers are almost twice the recommended limit of 370 Bqkg^{-1}.[66][111]. In contrast, other types of fertilisers exhibit Ra_{eq} levels within the safe range, indicated as the green zone. The primary factor leading to the surpassing of

recommended Ra_{eq} limits is the elevated concentration of ^{40}K in MOP. Conversely, the lower average Ra_{eq} of organic fertilisers, at 83.07±12.69 $Bqkg^{-1}$, suggests that opting for these types of fertilisers is a sensible decision. Our findings advocate for the use of radiation protection when dealing with MOP Fertiliser.

Table 4.9. The average radium equivalent activity (Ra_{eq}), external hazard index (H_{ex}), Internal hazard Index, H_{in}, γ-radiation hazard and index, I_γ in different fertiliser.

Fertiliser Type	Ra equivalent activity Bq/Kg	External Hazard index, H_{ex}	Internal hazard index, H_{in}	γ-radiation hazard index, I_γ
TSP	327.98±40.32	0.89±0.11	1.71±0.21	1.10±0.14
DAP	16.22±3.15	0.04±0.01	0.06±0.01	0.06±0.01
MOP	811.04±90.83	2.19±0.25	2.19±0.25	3.51±0.39
BOR	12.39±3.40	0.03±0.01	0.05±0.01	0.04±0.01
GYP	242.00±29.04	0.65±0.08	1.31±0.16	0.81±0.10
SSP	224.47±40.01	0.61±0.11	0.83±0.15	0.82±0.14
ORG	83.08±12.69	0.22±0.03	0.29±0.05	0.32±0.05
Mean value	245.31±31.35	0.66 ±0.08	0.92±0.12	0.95±0.12

As we can see in the Fig. 4.9. The average value Ra_{eq} were 327.98±40.32 $Bqkg^{-1}$ in TSP which were very close to world recommended value. In Gypsum and SSP Ra_{eq} value also noticeable but for organic samples 83.08±12.69 $Bqkg^{-1}$ activity showed tolerable.

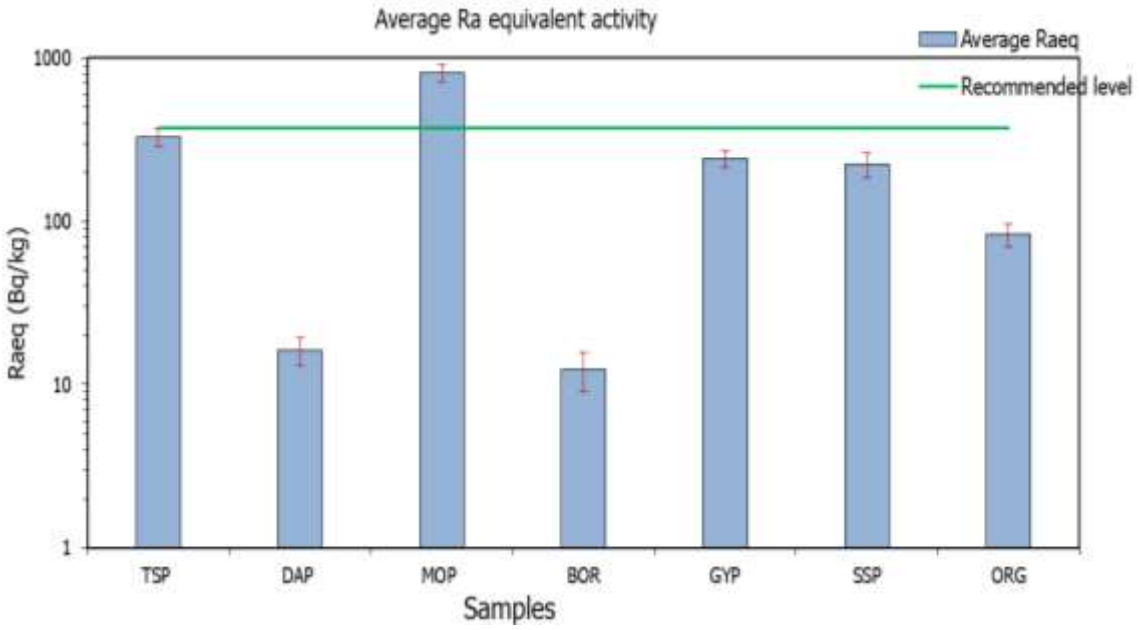

Figure 4.2. Average radium equivalent activity (Ra_{eq}) in different fertiliser samples.

From table 4.9 the lower average value of Ra_{eq} were found 16.22±3.15 $Bqkg^{-1}$ in BORON fertiliser samples but higher range was found 811.04±90.83 $Bqkg^{-1}$ in MOP fertiliser samples which is greater than world recommended value. In DAP fertilizer the presence of average value of Ra_{eq} is 16.22±3.15 that is the lowest value. But the average value of Ra_{eq} of seven types of fertilisers are 245.31±31.35 $Bqkg^{-1}$ was calculated. In Fig. 4.2 shows the presentation of average radium equivalent activity (Ra_{eq}) in different fertiliser samples where it is clearly shown that the height of MOP column is higher than any other fertilisers.

4.4. HAZARD INDICES

The radiological risks in the samples analysed were evaluated using various hazard parameters, which included the external hazard index (H_{ex}), internal hazard index (H_{in}), and γ-radiation hazard index (I_γ) as advised by the Organization for Economic Co-operation and Development (OECD) and the European Commission [111][112].

As indicated in Table 4.9, the computed values for Hex, Hin, and Iγ clearly demonstrate that MOP fertilizers surpassed the recommended limit (≤1) for all

of these indices, while TSP and GYP exceeded the non-violent threshold for Hin due to their elevated levels of 226Ra. Furthermore, Iγ values calculated for different types of fertilizers to assess gamma radiation hazards are illustrated in Fig. 4.9 [113][65].

The results from the hazard parameter assessments reveal that MOP fertilizers have surpassed the acceptable margin (≤1) [48]. These findings suggest that the production and use of fertilizers that exceed the recommended levels ought to be regulated in accordance with radiation protection guidelines.

In this study table 4.10 seven TSP samples is analysed where TSP-4 and TSP-5 samples shows above 126 $BqKg^{-1}$ Ra equivalent activity and in the sample TSP-02, highest activity Ra equivalent activity is found that is 497.18± 62.26 $BqKg^{-1}$. External hazard index in 4 sample below the 1 but it is remarkable that in 3 samples of TSP H_{ex} is greater than world recommended value. Another hazard parameter internal hazard index is found greater than 2 in 3 samples and average value of H_{in} are 1.709±0.206 which is greater than recommended value 1. Radioactivity level index in the TSP samples is shown in table 4.10 where range of I_y are 0.42 ± 0.05 to 1.663 ± 0.20.

Table 4.10. The average radium equivalent activity (Ra_{eq}), external hazard index (H_{ex}), Internal hazard index (H_{in}), Radioactivity level index, I_γ in TSP fertiliser.

Type	Ra equivalent activity, $BqKg^{-1}$	External Hazard index, H_{ex}	Internal hazard index, H_{in}	Radioactivity level index, I_γ
TSP-1	332.29 ±38.88	0.89±0.10	1.762± 0.2	1.109 ± 0.13
TSP-2	497.18 ± 62.26	1.34 ±0.16	2.586± 0.32	1.663 ± 0.20
TSP-3	422.88±52.81	1.14 ±0.14	2.223± 0.27	1.41± 0.17
TSP-4	129.74±15.033	0.35± 0.04	0.631±0.068	0.43 ± 0.05
TSP-5	126.6 ± 15.92	0.342±0.04	0.606± .072	0.42 ± 0.05
TSP-6	437.18±44.83	1.181 ± 0.121	2.26± 0.229	1.46± 0.15
TSP-7	350 ± 52.5	0.945±0.14	1.891± 0.28	1.166± 0.175
TSPAvg.	327.98± 40.32	0.886 ± 0.10	1.709±0.206	1.097 ± 0.135

5 DAP fertiliser samples was taken in this study where except DAP-02 sample, Ra equivalent activity in each sample was found to be greater than 16 $BqKg^{-1}$ (shown Table 4.11). The H_{ex} and H_{in} is less than the world recommended value 1. Except DAP-2 sample, the value of Radioactivity level index (I_γ) of each sample are below 0.1.

In table 4.12 all of the investigated MOP samples showed higher values of radium equivalent activity than the recommended worldwide mean value 370 $Bqkg^{-1}$. For having high concentration of ^{40}K elevated in each and every sample all hazard parameter ($H_{ex,}$ H_{in} and I_γ) are also higher than 1. The range of Ra_{eq} is 623.7 ± 87.32 to 854.7 ± 85.47 and average is 811.04± 90.83 $Bqkg^{-1}$. The range of External hazard values from 1.68±0.23 to 2.28±0.23 and average is 2.18±0.24 which is double than world recommended value 1. Again, in All MOP sample internal hazard index (H_{in}) starts from 1.68 ±0.23 to 2.235 ±0.22 where average value is 2.192 ±0.24.

Table 4.11. The radium equivalent activity (Ra_{eq}), external hazard index (H_{ex}), Internal hazard index (H_{in}), Radioactivity level index, I_γ in DAP fertiliser.

DAP fertiliser Sample	Ra equivalent activity, Bq/Kg	External Hazard index, H_{ex}	Internal hazard index, H_{in}	Radioactivity level index, I_γ
DAP-1	1.4 ±0.7	0.01 ±0.002	0.007±0.004	0.004±0.002
DAP-2	50.99 ±9.08	0.13 ±0.02	0.148±0.27	0.177±0.031
DAP-3	5 ±1.1	0.01 ±0.002	0.027±0.005	0.0166±0.003
DAP-4	16.91 ±3.61	0.04 ±.009	0.064±0.013	0.058±0.012
DAP-5	6.8 ±1.2	0.02 ±0.0035	0.0367±0.007	0.022±0.004
DAP Avg.	16.22 ±3.15	0.044 ±0.008	0.0567±0.011	0.055±0.01

The value of Radioactivity level index, I_γ also alarming at the case of all MOP samples where the range of I_γ from 2.7±0.37 to 3.57±0.35 and average 3.51±0.39. That's why in future with MOP sample need more experiment for clarification.

Table 4.12 The radium equivalent activity (Ra_{eq}), external hazard index (H_{ex}), internal hazard index (H_{in}), Radioactivity level index, I_γ in MOP fertiliser.

MOP Fertiliser	Ra equivalent activity, $Bqkg^{-1}$.	External Hazard index , H_{ex}	Internal hazard index, H_{in}	Radioactivity level index, I_γ
MOP-1	816.2±114.268	2.203±0.31	2.203 ±0.31	3.533±0.49
MOP-2	801.1± 105.64	2.162±0.3	2.184 ±0.31	3.46±0.49
MOP-3	754.6± 105.64	2.03±0.28	2.037 ±0.28	3.266±0.46
MOP-4	825.9 ± 83.19	2.23±0.22	2.235 ±0.22	3.57±0.35
MOP-5	847 ± 84.7	2.28±0.23	2.28 ±0.22	3.666±0.36
MOP-6	854.7 ± 85.47	2.30±0.23	2.31 ±0.23	3.7±0.37
MOP-7	823.9 ± 82.39	2.22±0.22	2.224±0.22	3.56±0.35
MOP-8	808.5 ± 56.59	2.18±0.15	2.182 ±0.15	3.5±0.39
MOP-9	623.7 ± 87.32	1.68±0.23	1.68 ±0.23	2.7±0.37
MOP Avg.	811.04± 90.83	2.18±0.24	2.192 ±0.24	3.51±0.39

The calculated results of Ra_{eq} of all organic samples are shown in table 4.13. where all value lower than world recommended value 370 $Bqkg^{-1}$ and range from 4.3±2.15 to 293.88±28.44 $Bqkg^{-1}$. External hazard values varied from 0.01±0.01 to 0.79±0.08 and internal hazard index varies from 0.02±0.01 to 1.005±0.13 where average value is 0.251. Radioactivity level index is started from 0.20±0.1 and higher range is 1.24±0.12.

Table 4.13. The average radium equivalent activity (Ra_{eq}), external hazard index (H_{ex}), Internal Hazard Index H_{in}, Radioactivity level index I_γ in organic fertiliser.

Organic fertiliser	Ra equivalent activity, $Bqkg^{-1}$.	External Hazard index, He_x	Internal hazard index, H_{in}	Radioactivity level index, I_γ
Org-1	10.582±2.253	0.0285±0.007	0.028±0.0068	0.037±0.008
Org-2	171.29±26.693	0.462±0.072	0.646±0.0959	0.61±0.95
Org-3	58.762±10.02	0.158±0.27	0.158±0.027	0.25±0.041
Org-4	234.25±32.37	0.632±0.087	1.005±0.13	0.87±0.122
Org-5	293.88±28.44	0.79±0.08	0.87±0.1	1.24±0.12
Org-6	56.33±16.89	0.15±0.05	0.18±0.06	0.20± 0.1
Org-7	4.3±2.15	0.01±0.01	0.02±0.01	0.01±0.01
Org-8	49.183±9.46	0.13±0.03	0.15±0.03	0.20±0.04
Org-9	9±3.6	0.02±0.01	0.05±0.02	0.03±0.01
Org-10	18.242±3.47	0.05±0.01	0.06±0.01	0.06±0.01
Org-11	ND	0.02±0.01	0.04±0.02	0.03±0.01
ORG Avg	83.07±12.69	0.22±0.03	0.29±0.05	0.32±0.05

4.5 EXPOSURES, DOSE RATES AND CANCER RISK

Fertilisers that have elevated levels of radionuclides present a possible risk of public exposure, given their prevalent use in agriculture. Consequently, it is essential to evaluate the exposure rate and the associated equivalent dose linked to these fertilisers. This study calculates the air-absorbed gamma dose rates for indoor (D_{in}) and outdoor (D_{out}) exposure, which are then displayed in Table 8.14 and illustrated in figures 4.7 and 4.8. The findings suggest that fertilisers with high radionuclide contents may expose the public to potential risks due to their significant use in farming. The average D_{out} values for various types of fertilisers varied from 5.48 ± 1.52 to 439.15 ± 49.17 $nGyh^{-1}$, with most chemical fertilisers—excluding DAP and BOR—registering higher levels than the global average of 50 nGy h^{-1}. The Din values for different fertilisers ranged from 10.48 ± 2.92 to 853.04 ± 95.51 $nGyh^{-1}$, where TSP, MOP, GYP, and SSP fertilisers surpassed the world average (84 $nGyh^{-1}$). The annual effective dose equivalents for outdoor ($AEDE_{outdoor}$) and indoor ($AEDE_{indoor}$) exposures were determined using Equations (6) and (7), with the results shown in Table 4.14 and represented in Figs. 4.6 and 4.7. With the exception of ORG, DAP, and BOR fertilisers, all the others exceeded the UNSCEAR 2000 limit of 0.07 mSv y^{-1} [105].

Figure 4.3 offers a visual comparison of D_{out} and $AEDE_{outdoor}$ alongside the respective global average values, clearly demonstrating that the majority of chemical fertilizers present values that are up to ten times greater than the global average. Table 4.14 and Figure 4.7 show the recorded data for $AEDE_{indoor}$, revealing that fertilizers such as TSP, MOP, GYP, and SSP yield higher indoor dose outcomes, with $AEDE_{indoor}$ alone surpassing the ICRP-103 guideline limit ($1mSvy^{-1}$) for the total annual effective dose [117]. Consequently, this study strongly advises that further organizations replicate this research to enhance the findings, facilitating the regulation of both the production and unintentional usage of these fertilizers for the safety of the public and the environment. Table

Table 4.14. Air absorbed dose rate and Annual effective dose equivalent at indoor and outdoor, and excess lifetime cancer risk at outdoor.

Sample	Air absorbed dose rate(D), $nGyh^{-1}$		Annual effective dose equivalent (AEDE), $mSv\ y^{-1}$		ELCR $\times 10^{-3}$
	D_{out}	D_{in}	$AEDE_{outdoor}$	$AEDE_{indoor}$	
TSP-1	153.03±17.82	303.86±35.22	0.19±0.02	1.49±0.17	0.66
TSP-2	228.22±28.48	451.8±56.22	0.28±0.03	2.22±0.27	0.98
TSP-3	194.46±24.21	385.6±47.86	0.24±0.03	1.89±0.23	0.83
TSP-4	58.92±6.76	115.48±13.13	0.07±0.01	0.57±0.06	0.25
TSP-5	57.36±7.155	112.16±13.88	0.07±0.01	0.55±0.07	0.25
TSP-6	200.51±20.52	396.6±40.52	0.25±0.03	1.95±0.19	0.86
TSP-7	161.7±24.26	322±48.3	0.20±0.03	1.58±0.24	0.69
TSP Avg.	150.6±18.46	298.21±36.45	0.18±0.02	1.46±0.18	0.65
DAP-1	0.65±0.32	1.29±0.64	0.001±0.0003	0.01±0.003	0.003
DAP-2	21.69±3.88	39.79±7.15	0.03±0.01	0.20±0.04	0.09
DAP-3	2.31±0.49	4.60±0.97	0.003±0.0006	0.02±0.01	0.01
DAP-4	7.42±1.58	14.05±2.98	0.01±0.002	0.07±0.01	0.03
DAP-5	3.14±0.60	6.26±1.19	0.004±0.001	0.03±0.01	0.01
DAP Avg.	7.04±1.37	13.20±2.59	0.01±0.002	0.07±0.01	0.03
MOP-1	442.02±61.88	858.60±120.20	0.54±0.08	4.21±0.59	1.90
MOP-2	433.21±61.17	841.66±118.86	0.53±0.08	4.13±0.58	1.86
MOP-3	408.66±57.21	793.80±111.13	0.50±0.07	3.89±0.55	1.75
MOP-4	447.114±44.99	868.54±87.41	0.55±0.06	4.26±0.43	1.92
MOP-5	458.70±45.87	891.00±89.10	0.56±0.06	4.37±0.44	1.97
MOP-6	462.87±46.29	899.10±89.91	0.57±0.06	4.41±0.44	1.99
MOP-7	446.19±44.62	866.70±86.67	0.55±0.05	4.25±0.43	1.92
MOP-8	437.85±30.65	850.50±59.54	0.54±0.04	4.17±0.29	1.88
MOP-9	337.77±47.29	656.10±91.85	0.41±0.06	3.22±0.45	1.45
Q-Potash	517.08±51.71	1004.40±100.44	0.63±0.06	4.93±0.49	2.22
MOP Avg.	439.15±49.17	853.04±95.51	0.54±0.06	4.18±0.47	1.88
BOR-1	3.70±1.48	7.36±2.94	0.005±0.001	0.04±0.02	0.02
BOR-2	4.05±1.05	7.37±1.92	0.005±0.001	0.04±0.01	0.02
BOR-3	2.63±1.32	5.24±2.62	0.003±0.002	0.03±0.01	0.01
BOR-4	11.55±2.21	21.93±4.18	0.014±0.003	0.11±0.02	0.05
BOR Avg.	5.48±1.52	10.48±2.92	0.007±0.002	0.05±0.01	0.02
GYP	111.80±13.42	222.64±26.72	0.14±0.02	1.09±0.13	0.48
SSP	104.66±18.22	200.79±34.76	0.13±0.02	0.98±0.17	0.45
ORG-1	4.47±1.07	8.14±1.95	0.01±0.001	0.04±0.01	0.02
ORG-2	77.98±12.07	148.98±22.91	0.10±0.02	0.73±0.11	0.33
ORG-3	31.24±5.20	60.44±10.00	0.04±0.01	0.30±0.05	0.13
ORG-4	115.88±16.11	228.21±31.69	0.14±0.02	1.12±0.16	0.50
ORG-5	156.85±14.83	305.32±28.96	0.20±0.02	1.50±0.14	0.67
ORG-6	24.27±7.28	45.14±13.54	0.03±0.01	0.22±0.07	0.10
ORG-7	1.97±0.99	3.96±1.98	0.002±0.001	0.02±0.01	0.01
ORG-8	24.72±4.65	47.45±8.90	0.03±0.01	0.23±0.04	0.11
ORG-9	4.16±1.66	8.28±3.31	0.01±0.002	0.04±0.02	0.02
ORG-10	7.90±1.51	14.76±2.83	0.01±0.001	0.07±0.01	0.03
ORG-11	3.700±1.85	7.36±3.68	0.004±0.002	0.04±0.02	0.02
ORG Avg.	41.20±6.11	79.82±11.80	0.05±0.01	0.40±0.06	0.18

4.14 also outlines the ELCR calculated using equation 3.10, based on the values of the outdoor annual effective dose. The ELCR for all samples varies from 0.003×10^{-3} to 2.22×10^{-3}, with an average of 0.68×10^{-3}, which is more than twice the world average of 0.3×10^{-3} depicted in Figure 4.8.

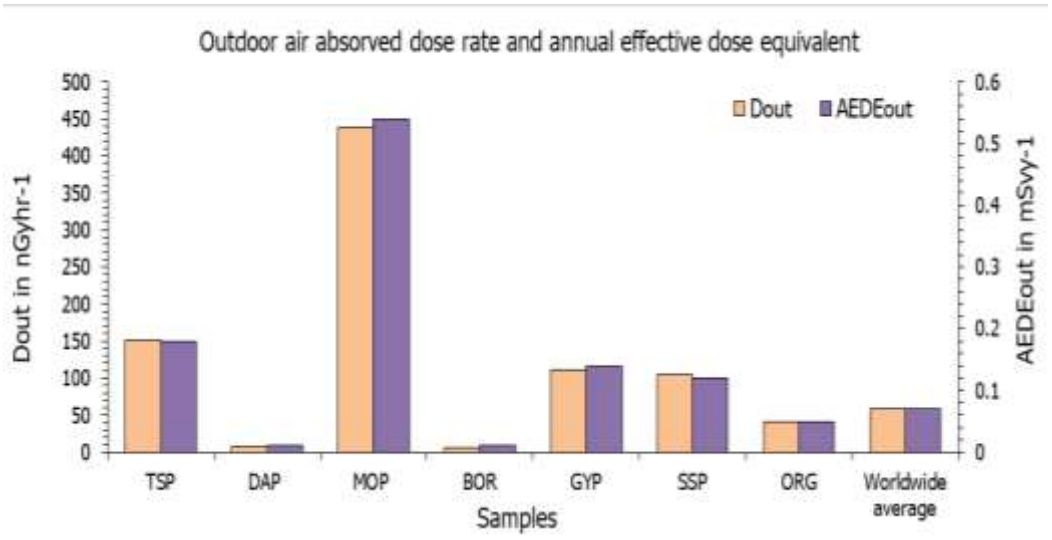

Fig. 4.3 Outdoor air absorbed dose rate and annual effective dose equivalent

From the experiment value of Table 4.15 represents all value of Air absorbed dose rate (D_{out}) presents in TSP samples where range is 57.36±7.155 to 228.22±28.48 $nGyh^{-1}$ which comparatively higher than recommended value. In each sample of TSP D_{out} shows that elevated value which is harmful for living organic body. Now in TSP sample air absorbed dose rate (D_{in}) varies from 298.21±36.45 to 396.6±40.52 $nGyh^{-1}$. In TSP samples annual effective dose equivalent $AEDE_{outdoor}$ range from 0.07±0.01to 0.28±0.03, where average is 0.18±0.02 and $AEDE_{indoor}$ 0.55±0.07 to 2.22±0.27. Again, the average value of excess lifetime cancer risk at outdoor 0.65×10^{-3}.

The table 4.16 represents all value of Air absorbed dose rate and Annual effective dose equivalent at indoor and outdoor, and excess lifetime cancer risk at outdoor. In DAP samples the lower range value of D_{out} is 0.65±0.32 in sample DAP-1 and higher range is 21.69±3.88 $nGyh^{-1}$ and the average value of D_{in} is 13.20±2.59. The average value of $AEDE_{outdoor}$ and $AEDE_{indoor}$ are 0.01±0.002 and 0.07±0.01 respectively where highest value of ELCR is 0.86×10^{-3}. Table 4.17

shows that highest value of D_{out} in the MOP samples is 517.08±51.71 $nGyh^{-1}$ where lower value is 337.77±47.29 $nGyh^{-1}$ and the average value of D_{in} is 853.04±95.51 $nGyh^{-1}$. Again, the $AEDE_{outdoor}$ value range from 0.41±0.06 to 0.57±0.06 and average value is 0.54±0.06. Again, the average value of $AEDE_{indoor}$ in MOP samples is 4.18±0.47 which is higher than recommended level 1 $mSvy^{-1}$. The average ELCR value is 1.88×10^{-3} which above the recommended value of 10^{-5}. In Q Potash fertiliser value of D_{out} and D_{in} are 517.08±51.71, 853.04±95.51 $nGyh^{-1}$ which exceed the average value of D_{out} and D_{in} of MOP samples.

Table 4.15. Air absorbed dose rate and Annual effective dose equivalent at indoor and outdoor, and excess lifetime cancer risk at outdoor in TSP fertiliser.

Sample	Air absorbed dose rate(D), $nGyh^{-1}$		Annual effective dose equivalent (AEDE), mSv y^{-1}		ELCR $\times10^{-3}$
	D_{out}	D_{in}	$AEDE_{outdoor}$	$AEDE_{indoor}$	
TSP-1	153.03±17.82	303.86±35.22	0.19±0.02	1.49±0.17	0.66
TSP-2	228.22±28.48	451.8±56.22	0.28±0.03	2.22±0.27	0.98
TSP-3	194.46±24.21	385.6±47.86	0.24±0.03	1.89±0.23	0.83
TSP-4	58.92±6.76	115.48±13.13	0.07±0.01	0.57±0.06	0.25
TSP-5	57.36±7.155	112.16±13.88	0.07±0.01	0.55±0.07	0.25
TSP-6	200.51±20.52	396.6±40.52	0.25±0.03	1.95±0.19	0.86
TSP-7	161.7±24.26	322±48.3	0.20±0.03	1.58±0.24	0.69
TSP Avg.	150.6±18.46	298.21±36.45	0.18±0.02	1.46±0.18	0.65

In all sample of MOP samples value of $AEDE_{outdoor}$ and $AEDE_{indoor}$ are also calculated, and their average value are 0.54±0.06, 4.18±0.47 mSv y^{-1} respectively. The highest ELCR result is 2.22 $\times10^{-3}$ where lowest value is 1.75 $\times10^{-3}$ that is elevate value than any other value presence in samples.

Table 4.16. Air absorbed dose rate and Annual effective dose equivalent at indoor and outdoor, and excess lifetime cancer risk at outdoor in DAP fertiliser.

Sample	Dout($nGyh^{-1}$)	Din($nGyh^{-1}$)	$AEDE_{outdoor}$	$AEDE_{indoor}$
DAP-1	0.65±0.32	1.29±0.64	0.001±0.0003	0.01±0.003
DAP-2	21.69±3.88	39.79±7.15	0.03±0.01	0.20±0.04
DAP-3	2.31±0.49	4.60±0.97	0.003±0.0006	0.02±0.01
DAP-4	7.42±1.58	14.05±2.98	0.01±0.002	0.07±0.01
DAP-5	3.14±0.60	6.26±1.19	0.004±0.001	0.03±0.01
DAP Avg.	7.04±1.37	13.20±2.59	0.01±0.002	0.07±0.01

Table 4.17. Air absorbed dose rate and Annual effective dose equivalent at indoor and outdoor, and excess lifetime cancer risk at outdoor in Muriate of Potash Fertiliser.

Sample	Air absorbed dose rate(D), ($nGyh^{-1}$)		Annual effective dose equivalent (AEDE), ($mSv\ y^{-1}$)		
	D_{out}	D_{in}	$AEDE_{outdoor}$	$AEDE_{indoor}$	$ELCR\times10^{-3}$
MOP-1	442.02±61.88	858.60±120.20	0.54±0.08	4.21±0.59	1.9
MOP-2	433.21±61.17	841.66±118.86	0.53±0.08	4.13±0.58	1.86
MOP-3	408.66±57.21	793.80±111.13	0.50±0.07	3.89±0.55	1.75
MOP-4	447.114±44.99	868.54±87.41	0.55±0.06	4.26±0.43	1.92
MOP-5	458.70±45.87	891.00±89.10	0.56±0.06	4.37±0.44	1.97
MOP-6	462.87±46.29	899.10±89.91	0.57±0.06	4.41±0.44	1.99
MOP-7	446.19±44.62	866.70±86.67	0.55±0.05	4.25±0.43	1.92
MOP-8	437.85±30.65	850.50±59.54	0.54±0.04	4.17±0.29	1.88
MOP-9	337.77±47.29	656.10±91.85	0.41±0.06	3.22±0.45	1.45
Q-Potash	517.08±51.71	1004.40±100.44	0.63±0.06	4.93±0.49	2.22
MOP Avg.	439.15±49.17	853.04±95.51	0.54±0.06	4.18±0.47	1.88

Table 4.18. Air absorbed dose rate and Annual effective dose equivalent at indoor and outdoor, and excess lifetime cancer risk at outdoor in Boron Fertiliser.

Sample	Air absorbed dose rate(D), ($nGyh^{-1}$)		Annual effective dose equivalent (AEDE), ($mSv\ y^{-1}$)		
	D_{out}	D_{in}	$AEDE_{outdoor}$	$AEDE_{indoor}$	ELCR ×10-3
BOR-1	3.70±1.48	7.36±2.94	0.005±0.001	0.04±0.02	0.02
BOR-2	4.05±1.05	7.37±1.92	0.005±0.001	0.04±0.01	0.02
BOR-3	2.63±1.32	5.24±2.62	0.003±0.002	0.03±0.01	0.01
BOR-4	11.55±2.21	21.93±4.1	0.014±0.003	0.11±0.02	0.05
BORAvg.	5.48±1.52	10.48±2.9	0.007±0.002	0.05±0.01	0.02

Table 4.19. Air absorbed dose rate and Annual effective dose equivalent at indoor and outdoor, and excess lifetime cancer risk at outdoor in Gypsum, Simple Super Phosphate and Organic Phosphate fertiliser.

Fertiliser Type	Air absorbed dose rate(D), ($nGyh^{-1}$)		Annual effective dose equivalent (AEDE), ($mSv\ y^{-1}$)		ELCR
	D_{out}	D_{in}	$AEDE_{outdoor}$	$AEDE_{indoor}$	$\times 10^{-3}$
GYP	111.80±13.42	222.64±26.72	0.14±0.02	1.09±0.13	0.48
SSP	104.66±18.22	200.79±34.76	0.13±0.02	0.98±0.17	0.45
ORG-1	4.47±1.07	8.14±1.95	0.01±0.001	0.04±0.01	0.02
ORG-2	77.98±12.07	148.98±22.91	0.10±0.02	0.73±0.11	0.33
ORG-3	31.24±5.20	60.44±10.00	0.04±0.01	0.30±0.05	0.13
ORG-4	115.88±16.11	228.21±31.69	0.14±0.02	1.12±0.16	0.5
ORG-5	156.85±14.83	305.32±28.96	0.20±0.02	1.50±0.14	0.67
ORG-6	24.27±7.28	45.14±13.54	0.03±0.01	0.22±0.07	0.1
ORG-7	1.97±0.99	3.96±1.98	0.002±0.001	0.02±0.01	0.01
ORG-8	24.72±4.65	47.45±8.90	0.03±0.01	0.23±0.04	0.11
ORG-9	4.16±1.66	8.28±3.31	0.01±0.002	0.04±0.02	0.02
ORG-10	7.90±1.51	14.76±2.83	0.01±0.001	0.07±0.01	0.03
ORG-11	3.700±1.85	7.36±3.68	0.004±0.002	0.04±0.02	0.02
$ORG_{Avg.}$	41.20±6.11	79.82±11.80	0.05±0.01	0.40±0.06	0.18

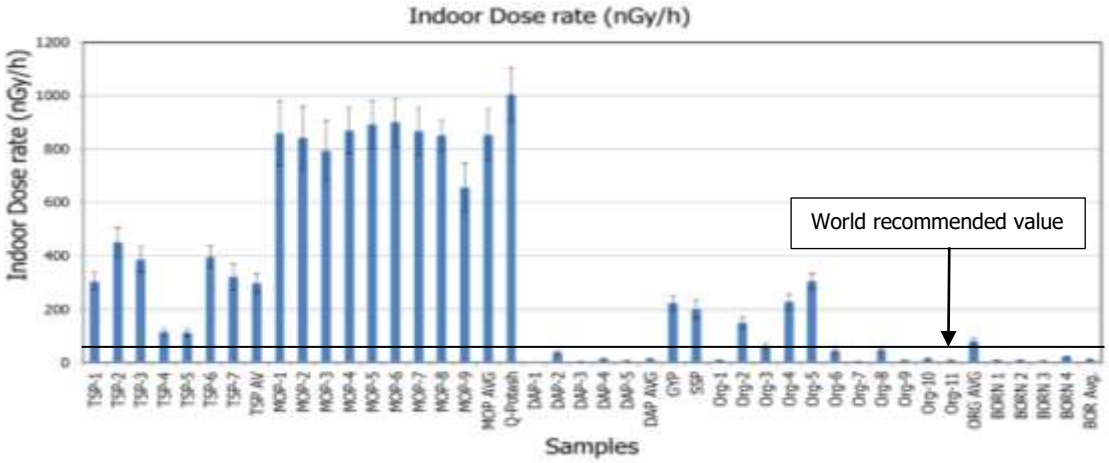

Fig. 4.4. Indoor dose rate in fertiliser samples.

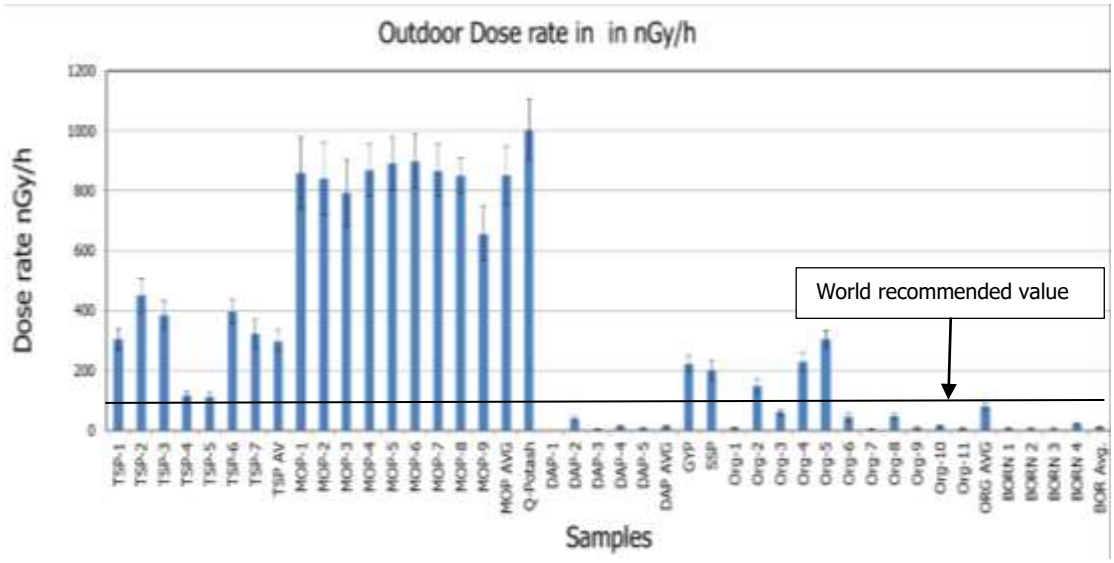

Fig. 4.5. Outdoor dose rate in fertiliser samples.

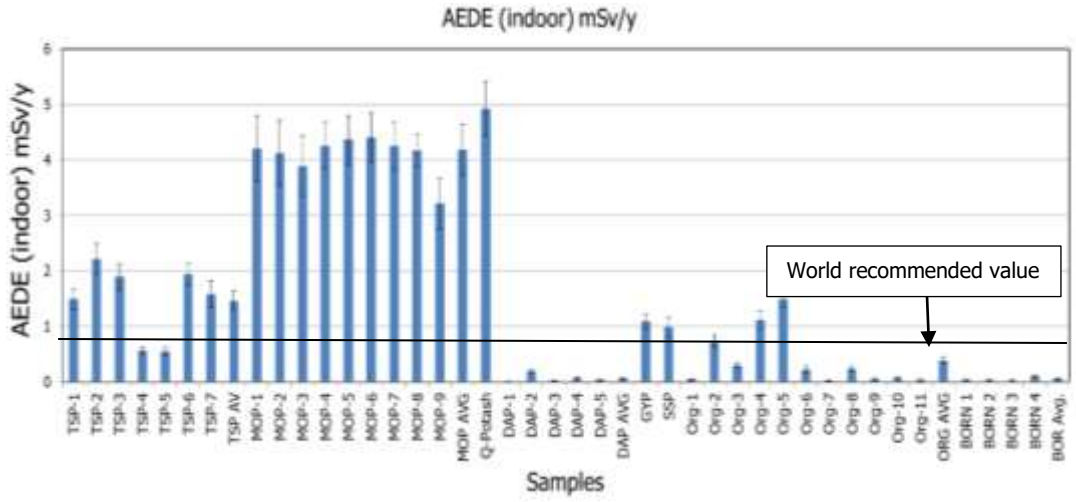

Fig. 4.6 Annual effective dose equivalent at indoor in fertiliser samples.

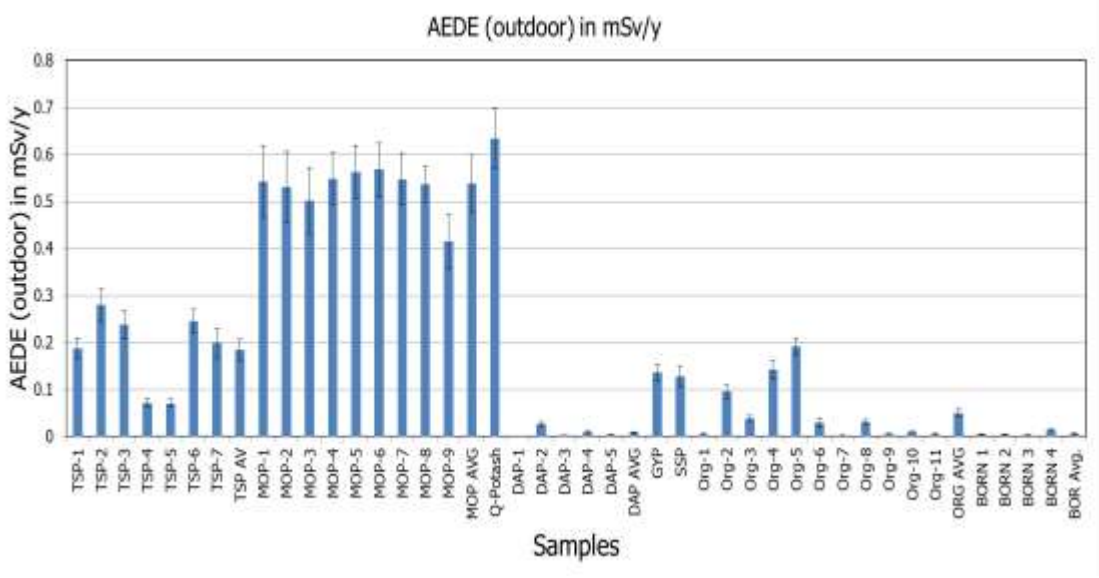

Fig. 4.7. Annual effective dose equivalent at outdoor in Fertiliser samples.

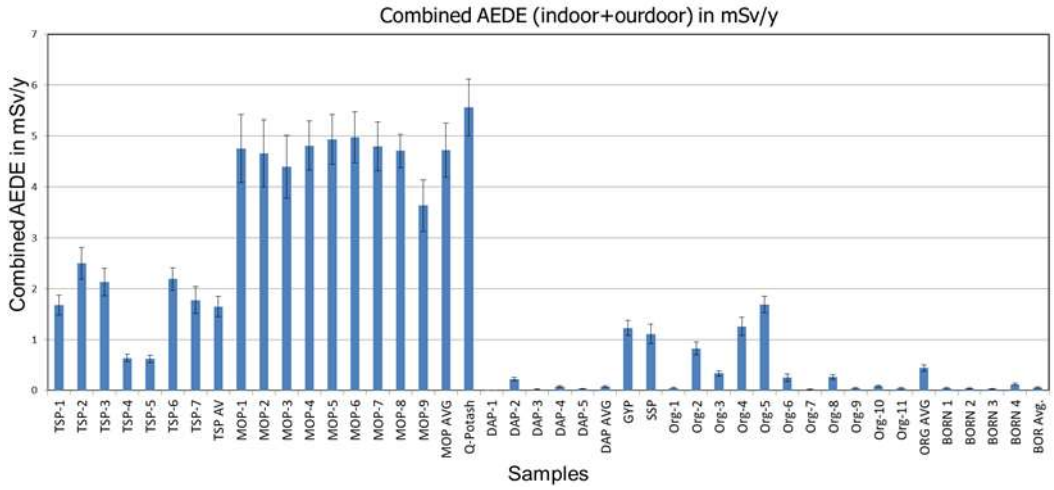

Fig. 4.8. Combined AEDE (outdoor and indoor) in fertilizer sample.

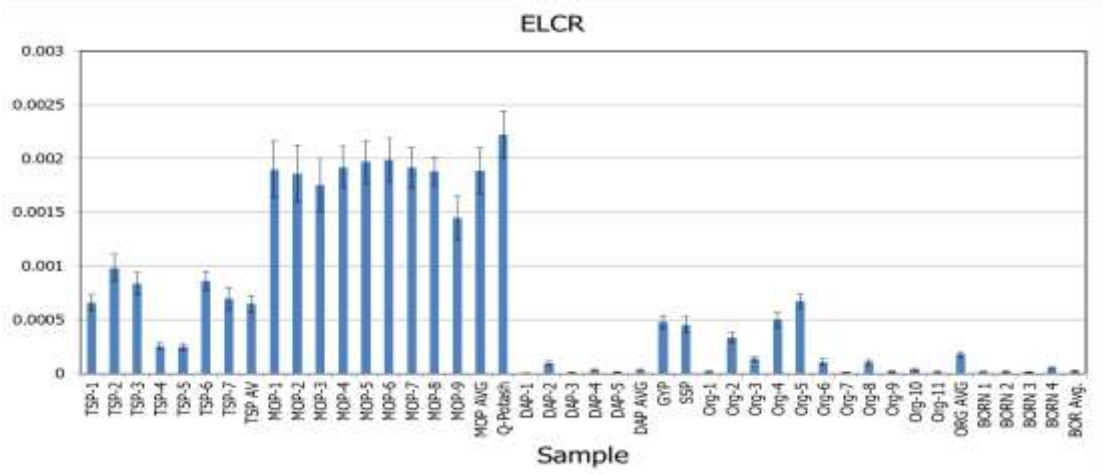

Fig. 4.9 ELCR in Fertiliser samples.

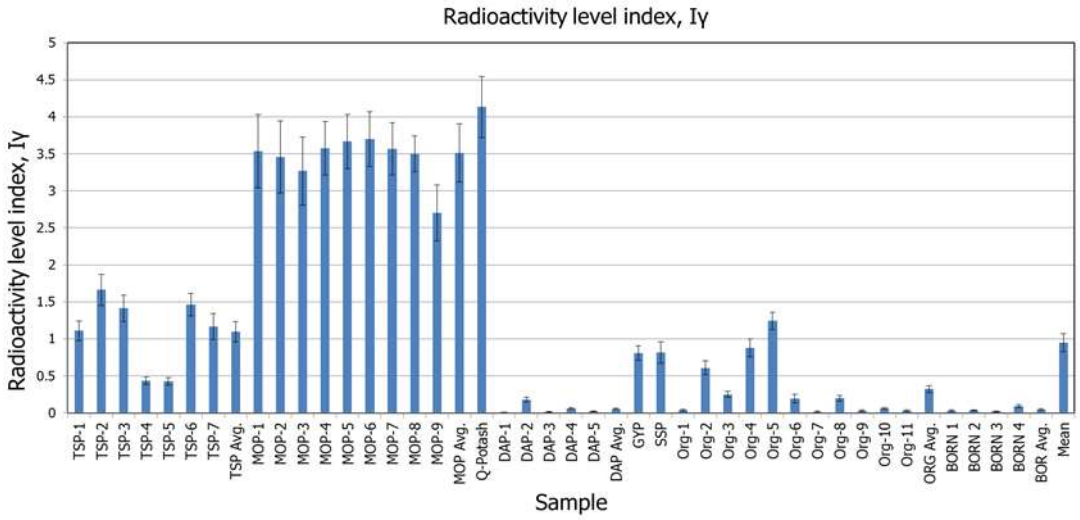

Fig. 4.10 Radioactivity level index in fertilizer samples.

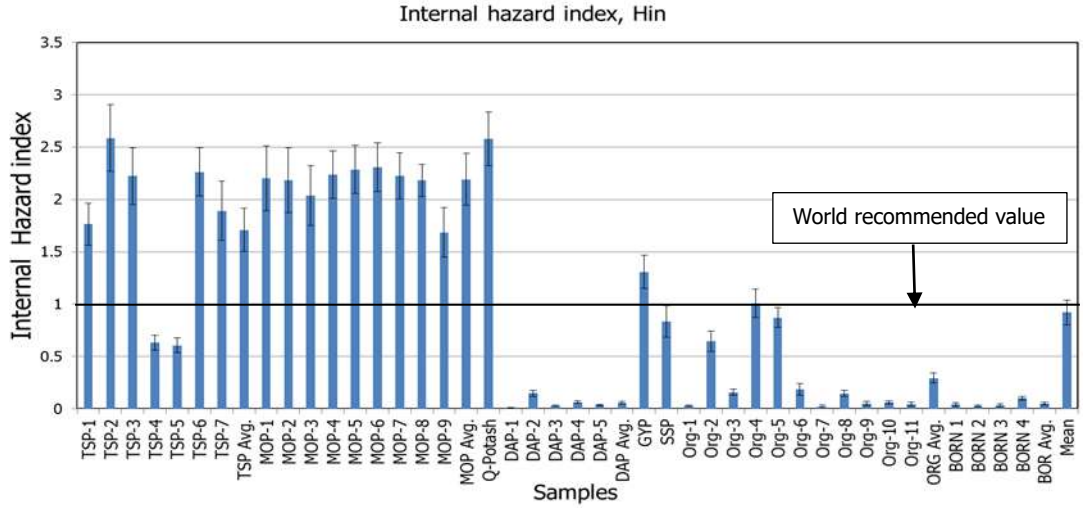

Fig.4.11 Internal hazard index in fertilizer samples.

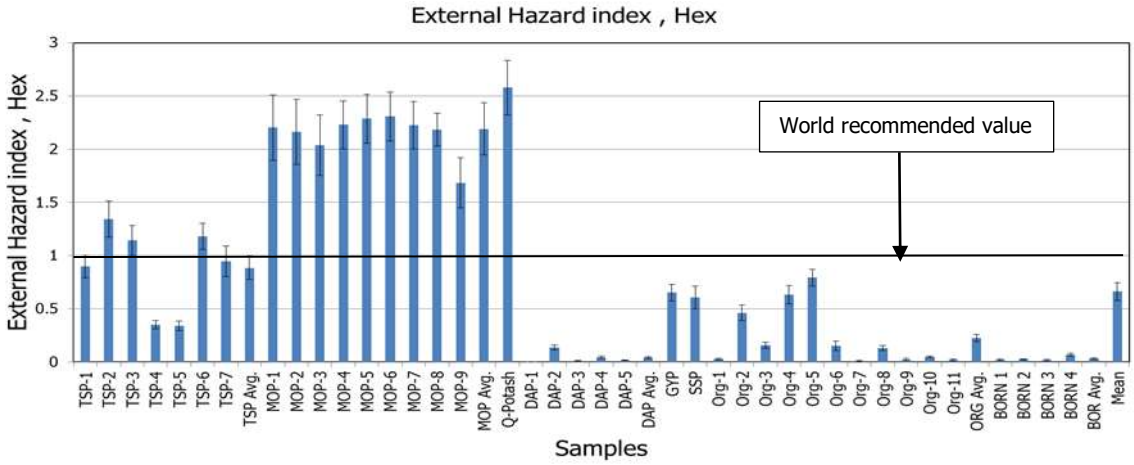

Fig. 4.12. External Hazard Index in Fertilizer sample

Chapter 5: CONCLUSION

5.1. GENERAL

This study centres on identifying and measuring the activity levels of naturally occurring radionuclides from the ^{226}Ra and ^{232}Th decay series, along with 40K in both chemical and organic fertilizers. The TSP fertilizer showed average activity concentrations of 304.57 ± 36.0 Bqkg^{-1} for 226Ra and 19.1 ± 6.8 Bqkg^{-1} for ^{232}Th, while the MOP fertilizer displayed an average activity concentration of $10,311.11 \pm 1168$ Bqkg^{-1} for ^{40}K. In the organic fertilizer samples tested, the mean concentrations were found to be 17.35 ± 3.1 Bqkg^{-1} for ^{226}Ra, 7.20 ± 1.74 Bqkg^{-1} for ^{232}Th, and 437.14 ± 42.58 Bqkg^{-1} for ^{40}K.

At the conclusion of the experiment, the average absorbed dose rates were recorded at 91.39 nGyh^{-1}. Moreover, the estimated combined annual effective dose equivalent (in both indoor and outdoor settings) was 0.322 mSv year^{-1}. The mean radium equivalent activity was calculated to be 190.15 ± 26.74 Bqkg^{-1}, which is significantly lower than the recommended threshold of 370 Bqkg^{-1}. The internal hazard index, external hazard index, and radioactivity level index calculated for the fertilizer samples were 0.56 ± 0.034, 0.54 ± 0.08, and 0.69 ± 0.10, respectively. Based on the calculated hazard indices, the excess lifetime cancer risk was found to exceed the global average in most chemical fertilizers, with the exception of DAP and BOR, while organic fertilizers had ELCR values that were lower than the global average. The results obtained suggest that there are no significant radiation risks posed by natural radionuclides in the fertilizer samples analysed. Nonetheless, the heightened level of 40K in MOP indicates a need for enhanced regulatory oversight. Ultimately, this investigation strongly advocates for the use of organic fertilizers owing to their relatively lower hazard parameters compared to the accepted levels. The data extracted highlights that potash fertilizers (MOP) have a somewhat elevated concentration of ^{40}K compared to the regulatory exemption threshold, even

though the amount of ^{226}Ra in phosphate fertilizers remains beneath the regulatory exemption limit [115], its concentration is 3 to 10 times higher than the average concentration in soil reported by UNSCEAR 2000 [105]. One type of phosphate fertiliser (SSP) exhibits an elevated concentration of ^{232}Th in comparison to the UNSCEAR 2000 report [105]. Apart from two samples that showed elevated levels of ^{40}K, organic fertilisers display nearly typical radioactivity concentration levels. However, the radium equivalent activity for organic fertilisers stays below the safety threshold. The findings from this study indicate that organic fertilisers are associated with relatively lower radiological risks compared to chemical fertilisers, even though both categories remain within the acceptable safety limits. This research is anticipated to serve as an important resource for exploring the cumulative impacts of fertilisers on soil and crops, as well as enhancing the foundational data for environmental radiation monitoring. It is advised to carry out additional studies periodically to support regulatory oversight if required. Furthermore, investigating the transfer factor of radionuclides from fertilisers to soil and then to crops can improve the safety information concerning the widespread usage of chemical fertilisers.

5.2. KEY FINDINGS

Using HPGe detector after investigation from 39 fertiliser samples the key findings are as follows:

1. The specific activities of ^{226}Ra in Triple Superphosphate fertilizer range from 98 ± 10.8 to 460 ± 55.2 $Bqkg^{-1}$, with an overall average of 304.6 ± 6.1 $Bqkg^{-1}$.

2. The average concentration of ^{232}Th detected in Triple Superphosphate fertilizer is 19.1 ± 3.5 $Bqkg^{-1}$.

3. In the sample of Triple Superphosphate fertilizer, the concentration of 40K was found to be undetectable.

4. The measured levels of ^{226}Ra and ^{232}Th in di-ammonium phosphate (DAP) fertilizers vary from 1.4 ± 0.7 to 6.9 ± 1.3 Bq kg^{-1}, averaging 4.8 ± 1.1 Bqkg^{-1}, and from 7 ± 1.6 to 33 ± 5.6 Bq kg^{-1}, with an average of 20 ± 3.6 Bq kg^{-1}, respectively.

5. The Muriate of Potash contains ^{40}K, showing an average specific activity of (10,520 ± 1175.7) Bq kg^{-1}, with minimum and maximum values of (8100 ± 1134) and (12,400 ± 1240) Bq kg^{-1}, respectively.

6. The levels of radionuclides 226Ra and 232Th in Boron fertilizers have averages of 8.4 ± 2.7 and 8.6 ± 1.9 Bq kg^{-1}, respectively.

7. In organic fertilizer, the average radioactivity per unit mass for the samples due to ^{226}Ra, ^{232}Th, and ^{40}K is recorded as 33.6 ± 5.8, 19.2 ± 4.4, and 1224 ± 136.3 Bq kg^{-1}, respectively.

8. The findings indicate a concerning situation as the average Ra_{eq} concentrations in MOP fertilizers are nearly twice the recommended limit of 370 Bq kg^{-1}, whereas the average Ra_{eq} concentrations of the other fertilizers remain below the recommended threshold.

9. The calculated Hex, H_{in}, and I_{γ} hazard indices for all fertilizer samples are below the recommended level (≤1), except for all MOP fertilizers.

10. The average D_{out} across various fertilizers was found to range from 5.48 ± 1.52 to 439.15 ± 49.17 $nGyh^{-1}$, while Din values for different types of fertilizers span from 10.48 ± 2.92 to 853.04 ± 95.51 $nGyh^{-1}$.

11. The annual effective dose equivalent for outdoor and indoor exposure, except for organic, DAP, and Boron fertilizers, exceeded the limit of 0.07 $mSvy^{-1}$ as reported by UNSCEAR 2000.

12. The ELCR for all samples varies from 0.003 × 10^{-3} to 2.22 × 10^{-3}, with an average of 0.68 × 10^{-3}, which is over twice the world average of 0.3 × 10^{-3}. **5.3**

5.3 LIMITATION OF THIS STUDY

Although the optimum carefulness and precautions were taken in each and every step of this research, even then some uncertainties might have been

included in our measurements due to some unavoidable limitations discussed below.

1. Ingredients of fertilisers differ from type to type and hence different in qualities and effects. While preparing the samples its essential to think about how different things are there within the group which is a prior task and might not be possible always to accomplish properly.
2. The efficiency of a HPGe detector for detecting gamma radiation can vary with the energy of the gamma rays and the geometry of the sample. Efficiency calibration curves are typically used to correct for these effects, but variations in sample shape and size might introduce uncertainties in the measurements.
3. HPGe detectors are sensitive to background radiation, which includes cosmic rays and natural radioactive sources present in the environment. Background radiation can contribute to the overall counts detected by the detector and may introduce uncertainties in the measured radioactivity concentration of the sample.
4. Precise vitality calibration of the HPGe detector is fundamental for accurately distinguishing and measuring the gamma-ray energies radiated by radionuclides within the test. Calibration vulnerabilities or mistakes can influence the exactness of the calculated radioactivity concentrations.

Recommendation for further study: In this study it is established that some of the fertiliser samples are found to be contaminated with ^{226}Ra, ^{232}Th and ^{40}K. So, at the time of handling, transporting and using in the field this contamination might cause harmful effect in the surrounding environment and day by day it will be increased. Here are some potential points for the scope of future research:

1. The present study has been conducted on 39 fertiliser samples collected from retail market of Chittagong district. But in future it will be better collecting

fertiliser samples from all possible districts of Bangladesh to assess radionuclide concentrations in fertilisers to get an overall status of the problem.

2. From various journal it has been found that radionuclide can be transfer from fertiliser to soil and from soil to it can be transfer again to plant, crop. So, after taking plant or crop as a food there is a great probability to transfer radionuclide from fertiliser to crop via soil. So, further research on soil, crops and plants is highly recommended to know about the uptake, accumulation and translocation of radionuclides from fertilisers to different crops commonly grown in Bangladesh. Analyse the transfer factors and bioaccumulation levels of radionuclides in different parts of plants to assess the potential radiation exposure through the food chain.

3. Investigate how the accessibility and transportation of radionuclides in fertilised soils and their subsequent absorption by plants can be affected by other parameters, such as soil composition, pH, organic matter concentration and others.

4. It is necessary to carry out a long-term study to evaluate the persistence and accumulation of radionuclides brought on by repeated fertiliser applications in soil and plants. Assess the effects of changing radionuclide concentrations on soil fertility, plant health and potential radiation risks over time.

6. Conduct a thorough evaluation of the radioactive exposure that results from consuming fertilised crops. To assess radiation doses and associated health concerns for the population, taking the variables including food practices, crop consumption habits and local food processing methods into account.

7. Have to investigate potential decreasing techniques to lower radioactive levels in fertilisers or limit plant absorption. To lower the amounts of radionuclides in agricultural systems, this could involve developing fertiliser treatment techniques, soil enhancements or agronomic practices.

8. It is needed to verify whether Bangladeshi fertilisers adhere to the advised safety norms, compare the radionuclide concentrations in them to those in other

countries' regulations and standards. To guarantee the safe use of fertilisers, pinpoint any areas where regulatory measures may need to be reinforced.

9. Conduct studies to assess the level of public awareness and knowledge regarding the potential radiation hazards associated with fertiliser use. Develop educational materials and outreach programs to raise awareness among farmers, consumers and other stakeholders about safe fertiliser practices and the potential risks of radionuclide contamination.

While setting future research goals, it is important to take into account the unique requirements and priorities of Bangladesh's agricultural sector as well as the existing regulatory framework. Additionally, collaborating with pertinent government agencies, agricultural institutions and environmental organizations can significantly amplify the influence and practicality of the research findings.

Reference:

[1] T. M. Missimer, C. Teaf, R. G. Maliva, A. Danley-Thomson, D. Covert, and M. Hegy, "Natural Radiation in the Rocks, Soils, and Groundwater of Southern Florida with a Discussion on Potential Health Impacts," *Int. J. Environ. Res. Public Health*, vol. 16, no. 10, 2019, doi: 10.3390/ijerph16101793.

[2] J.M. Clem, G.De Angelis, P. Goldhagen, and J. W. Wilson, "New calculations of the athmospheric cosmic radiation field - Results for neutron spectra," *Radiat. Prot. Dosimetry*, vol. 110, no. 1–4, pp. 423–428, 2004, doi: 10.1093/rpd/nch175.

[3] K.Rozanski and K.Froehlich,"Radioactivity and earth sciences: understanding the natural environment," *Int. At. Energy Agency Bull.*, vol. 38, no. 2, pp. 9–15, 1996.

[4] G. Keller and H. Muth, "Natural Radiation Exposure," pp. 1–24, 1990, doi: 10.1007/978-3-642-83802-6_1.

[5] L. E. Feinendegen, "Biological Effects of Low Doses of Ionizing Radiation: Damage versus Protection," *Mol. Nucl. Med.*, pp. 747–761, 2003, doi: 10.1007/978-3-642-55539-8_33.

[6] "Uranium Series - Radium Series - Nuclear Power." https://www.nuclear-power.com/nuclear-power/reactor-physics/atomic-nuclear-physics/radioactive-decay/radioactive-decay-chain/radioactive-series-radioactive-cascade/uranium-series/ (accessed Nov. 20, 2024).

[7] K. Kromer *et al.*, "Atomic mass determination of uranium-238," *Phys. Rev. C*, vol. 109, no. 2, Feb. 2024, doi: 10.1103/PHYSREVC.109.L021301.

[8] "Nuclear Power for Everybody-What is Nuclear Power." https://www.nuclear-power.com/ (accessed Nov. 20, 2024).

[9] "Radiation Basics|US EPA." https://www.epa.gov/radiation/radiation-basics?utm_source=chatgpt.com (accessed Dec. 23, 2024).

[10] J.A.Reisz,N.Bansal,J.Qian, W. Zhao, and C. M. Furdui, "Effects of Ionizing

Radiation on Biological Molecules—Mechanisms of Damage and Emerging Methods of Detection," *Antioxid. Redox Signal.*, vol. 21, no. 2, p. 260, Jul. 2014, doi: 10.1089/ARS.2013.5489.

[11] H. J. Jiang, T. C. Underwood, J. G. Bell, S. Ranjan, D. Sasselov, and G. M. Whitesides, "Mimicking Lighting-Induced Electrochemistry on the Early Earth," *Proc. Natl. Acad. Sci.*, vol. 120, p. 2017, 2017, doi: 10.1073/pnas.

[12] "Why Space Radiation Matters - NASA." https://www.nasa.gov/missions/analog-field-testing/why-space-radiation-matters/?utm_source=chatgpt.com (accessed Dec. 23, 2024).

[13] J. H. L. Mott and J. M. Daniel, "Interactions of Electromagnetic Radiation and Subatomic Particles with Matter – Part 2," *Clin. Oncol.*, vol. 33, no. 7, pp. 455–460, 2021, doi: 10.1016/j.clon.2021.02.005.

[14] "Radiation Interactions with Tissue | Radiology Key." https://radiologykey.com/4-radiation-interactions-with-tissue/?utm_source=chatgpt.com

[15] "Radiation - Pair Production, Photons, Electrons | Britannica." https://www.britannica.com/science/radiation/Pair-production?utm_source=chatgpt.com (accessed Dec. 23, 2024).

[16] K.Ram, *Nuclear Measurement Techniques,Affiliated East-West Press, 1986*. 1986.

[17] V. Tsapaki *et al.*, *Annals of the ICRP Annals of the ICRP Annals of the ICRP*, vol. 188, no. 24. 2021.

[18] "Dosimetry and Biological Effects of Ionizing Radiation," *Handb. Nucl. Chem.*, pp. 1647–1684, 2003, doi: 10.1007/0-387-30682-X_39.

[19] J.Talapko *et al.*, "Health Effects of Ionizing Radiation on the Human Body," *Med.*, vol. 60, no. 4, pp. 1–17, 2024, doi: 10.3390/medicina60040653.

[20] "Backgrounder On Biological Effects Of Radiation|NRC.gov." https://www.nrc.gov/reading-rm/doc-collections/fact-sheets/bio-effects-radiation.html?utm_source=chatgpt.com (accessed Dec. 23, 2024).

[21] P. L. Privalov and C. Crane-Robinson, "Role of water in the formation of macromolecular structures," *Eur. Biophys. J.*, vol. 46, no. 3, p. 203, Apr. 2016, doi: 10.1007/S00249-016-1161-Y.

[22] A. J. Gonzalez, "Biological effects of low doses of ionizing radiation : A fuller picture," *IAEA Bull.*, vol. 36, no. 4, pp. 37–45, 1994.

[23] J. F.Ward, "DNA Damage Produced by Ionizing Radiation in Mammalian Cells: Identities, Mechanisms of Formation, and Reparability," *Prog. Nucleic Acid Res. Mol. Biol.*, vol. 35, no. C, pp. 95–125, 1988, doi: 10.1016/S0079-6603(08)60611-X.

[24] J.D.Watson and F.H.C.Crick, "MOLECULAR STRUCTURE OF NUCLEIC ACIDS," *Nature*, vol. 173, no. 4356, pp. 737–738, 1953.

[25] H. F. . Lodish *et al.*, "Molecular cell biology," 2021.

[26] D. Bootsma and J. H. J. Hoeijmakers, "DNA repair and mutagenesis," *Trends Genet.*, vol. 12, no. 2, p. 79, 1996, doi: 10.1016/0168-9525(96)81408-9.

[27] U.Nations, U. Nations, S. Committee, and A. Radiation, "Sources and effects of ionizing radiation," vol. I, no. c, 2018, doi: 10.18356/f48d655d-en.

[28] U.N.S.C. on the E. of A. Radiation, "Sources and Effects of Ionizing Radiation, United Nations Scientific Committee on the Effects of Atomic Radiation (UNSCEAR) 1993 Report: Report to the General Assembly, with Scientific Annexes," Sep. 1993, doi: 10.18356/2C4203DC-EN.

[29] J. A. Reisz, N. Bansal, J. Qian, W. Zhao, and C. M. Furdui, "Effects of Ionizing Radiation on Biological Molecules—Mechanisms of Damage and Emerging Methods of Detection," *Antioxid. Redox Signal.*, vol. 21, no. 2, p. 260, Jul. 2014, doi: 10.1089/ARS.2013.5489.

[30] M. Douglass, "Eric J. Hall and Amato J. Giaccia: Radiobiology for the radiologist," *Australas. Phys. Eng. Sci. Med.*, vol. 41, no. 4, pp. 1129–1130, Dec. 2018, doi: 10.1007/S13246-018-0684-1.

[31] P.Haridasan, *Unscear 2013 Report*, vol. 36, no. 3. 2013. doi: 10.4103/0972-0464.137601.

[32] D.Ghosh, A. Deb, S. Bera, R. Sengupta, and K. K. Patra, "Assessment of alpha activity of building materials commonly used in West Bengal, India," *J. Environ. Radioact.*, vol. 99, no. 2, pp. 316–321, 2008, doi: 10.1016/j.jenvrad.2007.08.002.

[33] G.Silini, *The United Nations Scientific Committee on the Effects of Atomic Radiation (UNSCEAR)*, vol. 1, no. 4. 1981. doi: 10.1093/oxfordjournals.rpd.a079988.

[34] M.S. Linet *et al.*, "Cancer risks associated with external radiation from diagnostic imaging procedures," *CA. Cancer J. Clin.*, vol. 62, no. 2, pp. 75–100, 2012, doi: 10.3322/caac.21132.

[35] T. G. Members, "Low-dose_TG_rept_for_web.pdf," 2004.

[36] N.N. Jibiri and K. P. Fasae, "Activity concentrations of 226Ra, 232Th and 40K in brands of fertilisers used in Nigeria," *Radiat. Prot. Dosimetry*, vol. 148, no. 1, pp. 132–137, 2012, doi: 10.1093/rpd/ncq589.

[37] BER, "Socio-Economic Indicators of Bangladesh," *Bangladesh Econ. Rev. 2020*, vol. 22, pp. 14–15, 2020,

[38] F.A. Sunny, T. T. P. Karimanzira, W. Peng, M. S. Rahman, and H. Zuhui, "Understanding the determinants and impact of the adoption of technologies for sustainable farming systems in water-scarce areas of Bangladesh," *Front. Sustain. Food Syst.*, vol. 6, 2022, doi: 10.3389/fsufs.2022.961034.

[39] B.N. Thien, V. N. Ba, N. T. T. Vy, and T. T. H. Loan, "Estimation of the soil to plant transfer factor and the annual organ equivalent dose due to ingestion of food crops in Ho Chi Minh city, Vietnam," *Chemosphere*, vol. 259, p. 127432, 2020, doi: 10.1016/j.chemosphere.2020.127432.

[40] N.F. Kadhim, Y.A. Baqir, and L. Najam, "Radiation hazard of Chemical Fertilizers used in Growing Agriculture Crops in Iraq," *J. Radiat. Nucl. Appl.*, vol. 5, no. 2, pp. 127–134, 2020, doi: 10.18576/jrna/050207.

[41] N.M.Hassan, N.A. Mansour, M. Fayez-Hassan, and S. Fares, "Assessment

of radiation hazards due to exposure to radionuclides in marble and ceramic commonly used as decorative building materials in Egypt," *Indoor Built Environ.*, vol. 26, no. 3, pp. 317–326, 2017, doi: 10.1177/1420326X15606507.

[42] EC et al.,"IAEA Safety Standards for protecting people and the environment. Safety Series Requirements, No. GSR Part 3," 2014, http://ec.europa.eu/dgs/communication/services/visual_identity/index_en.htm

[43] P. P. Haridasan, A. C. Paul, and M. V. M. Desai, "Natural radionuclides in the aquatic environment of a phosphogypsum disposal area," *J. Environ. Radioact.*, vol. 53, no. 2, pp. 155–165, 2001, doi: 10.1016/S0265-931X(00)00121-1.

[44] M.N.Alam,M.I.Chowdhury,M.Kamal,S.Ghose,H.Banu,andD.Chakraborty, "Radioactivity in chemical fertilizers used in Bangladesh," *Appl. Radiat. Isot.*, vol. 48, no. 8, pp. 1165–1168, 1997, doi: 10.1016/S0969-8043(97)00019-5.

[45] S.M. El-Bahi, A. Sroor, G.Y. Mohamed, and N.S. El-Gendy, "Radiological impact of natural radioactivity in Egyptian phosphate rocks, phosphogypsum and phosphate fertilizers, "*Appl. Radiat. Isot.*, vol. 123, pp. 121–127, 2017, doi: 10.1016/j.apradiso.2017.02.031.

[46] M.A.M. Uosif,A.M.A. Mostafa,R.Elsaman, and E.Moustafa, "Natural radioactivity levels and radiological hazards indices of chemical fertilizers commonly used in Upper Egypt," *J. Radiat. Res. Appl. Sci.*, vol. 7, no. 4, pp. 430–437, 2014, doi: 10.1016/j.jrras.2014.07.006.

[47] N.M.Hassan,N.A.Mansour,M. Fayez-Hassan, and E. Sedqy, "Assessment of natural radioactivity in fertilizers and phosphate ores in Egypt," *https://doi.org/10.1016/j.jtusci.2015.08.009*, vol. 10, no. 2, pp. 296–306, 2018, doi: 10.1016/J.JTUSCI.2015.08.009.

[48] "Radiological protection principles concerning the natural radioactivity of

building materials - Publications Office of the EU." https://op.europa.eu/en/publication-detail/-/publication/988f3243-5259-43a5-b621-fbff662deeb0/language-en (accessed May 01, 2023).

[49] M. M. M. Siraz *et al.*, "Evaluation of transfer factors of 226Ra, 232Th, and 40K radionuclides from soil to grass and mango in the northern region of Bangladesh," *Environ. Monit. Assess.*, vol. 195, no. 5, p. 579, May 2023, doi: 10.1007/S10661-023-11223-8/METRICS.

[50] D.R.Fisher and F.H.Fahey, "Appropriate use of effective dose in radiation protection and risk assessment," *Health Physics*, 2017. https://www.ncbi.nlm.nih.gov/pmc/articles/PMC5878049/

[51] "https://www.who.int/news-room/questions-and-answers/item/radiation-andhealth?gad_source=1&gclid=Cj0KCQiAoKeuBhCoARIsAB4WxteunUxCUSNKPH1PFUhuwZJx-0Y6HFcPleW5bmUPmh7MsIjoWdKF-gUaAi-0EALw_wcB."

[52] A. Alengebawy, S.T.Abdelkhalek, S. R. Qureshi, and M. Q. Wang, "Heavy Metals and Pesticides Toxicity in Agricultural Soil and Plants: Ecological Risks and Human Health Implications," *Toxics*, vol. 9, no. 3, pp. 1–34, Mar. 2021, doi: 10.3390/TOXICS9030042.

[53] N.M.Hassan, N.A.Mansour,M. Fayez-Hassan, and E. Sedqy, "Assessment of natural radioactivity in fertilizers and phosphate ores in Egypt," *J. Taibah Univ. Sci.*, vol. 10, no. 2, pp. 296–306, 2016, doi: 10.1016/j.jtusci.2015.08.009.

[54] N.M. Hassan, B. U. Chang, and S. Tokonami, "Comparison of Natural Radioactivity of Commonly Used Fertilizer Materials in Egypt and Japan," *J. Chem.*, vol. 2017, 2017, doi: 10.1155/2017/9182768.

[55] R.W.D.Garcêz, J.M.Lopes,M.A.F.Lima, and A. X. da Silva, "Determination of Ra-226, Ra-228 and K-40 specific activities in samples of mineral fertilizers marketed in the city of Rio de Janeiro, Brazil," *Appl. Radiat. Isot.*,

vol. 141, no. June 2019, pp. 199–202, 2018,
doi: 10.1016/j.apradiso.2018.04.013.

[56] Adel G.E.Abbady1, A.El-Taher2, A.M.M.Yousef1, and and A.Abbady1, "Radioactivity in Chemical and Organic Fertilizer Used in Egypt," *VII Radiat. Phys. Prot. Conf.*, no. November, pp. 27–30, 2004,

[57] J. H. Jebur and A. R. H. Subber, "Natural radioactivity of some local and imported fertilizer in Basrah Governorate/Iraq," *Arch. Phys. Res.*, vol. 5, no. 5, pp. 18–22, 2014,
http://scholarsresearchlibrary.com/ABR-vol1-iss2/ABR-2010-1-2-87-90.pdf

[58] M. M. Makweba and E. Holm, "The natural radioactivity of the rock phosphates, phosphatic products and their environmental implications," *Sci. Total Environ.*, vol. 133, no. 1–2, pp. 99–110, 1993, doi: 10.1016/0048-9697(93)90115-M.

[59] H.A.Yousef, G.M.Saleh,A.H.El-Farrash,and A. Hamza, "Radon exhalation rate for phosphate rocks samples using alpha track detectors," *J. Radiat. Res. Appl. Sci.*, vol. 9, no. 1, pp. 41–46, 2016,
doi: 10.1016/j.jrras.2015.09.002.

[60] M.A. Samad, M.I. Ali, D. Paul, and S. M. A. Islam, "An Environmental Impact Study of Jamuna Urea Fertilizer Factory at Tarakandi in Jamalpur with Radiological Indices," *J. Environ. Sci. Nat. Resour.*, vol. 4, no. 2, pp. 27–33, 2011.

[61] S. Ghose, M. Akhter, S. M. A. Islam, M. Shahabuddin, and M. M. Rahman, "Assessment of radioactive pollution around a fertilizerfactory complex in the North-Eastern part of Bangladesh," *Radioprotection*, vol. 48, no. 4, pp. 575–591, 2013, doi: 10.1051/radiopro/2013074.

[62] K. S. Al Mugren and A. El-Taher, "Risk assessment of some radioactive and elemental content from cement and phosphate fertilizer consumer in Saudi Arabia," *J. Environ. Sci. Technol.*, vol. 9, no. 4, pp. 323–328, 2016, doi: 10.3923/jest.2016.323.328.

[63] R. O. Hussain and H. H. Hussain, "Investigation the natural radioactivity in local and imported chemical fertilizers," *Brazilian Arch. Biol. Technol.*, vol. 54, no. 4, pp. 777–782, 2011, doi: 10.1590/s1516-89132011000400018.

[64] H. H. Azeez, S. T. Ahmad, and H. H. Mansour, "Assessment of radioactivity levels and radiological-hazard indices in plant fertilizers used in Iraqi Kurdistan Region," *J. Radioanal. Nucl. Chem.*, vol. 317, no. 3, pp. 1273–1283, 2018, doi: 10.1007/s10967-018-6001-3.

[65] H. H. Azeez, H. H. Mansour, and S. T. Ahmad, "Effect of using chemical fertilizers on natural radioactivity levels in agricultural soil in the Iraqi Kurdistan Region," *Polish J. Environ. Stud.*, vol. 29, no. 2, pp. 1059–1068, 2020, doi: 10.15244/pjoes/106032.

[66] M. D. A.Mojumder, M. Ahmed, M. Kamal, M. B. Hossen, and M. A. Rashid, "The Activity Concentrations, Radiation Contamination, and Hazards from Wastes and Soil Samples in Nasirabad Industrial Area, Chattogram, Bangladesh," *J. Environ. Prot. (Irvine,. Calif).*, vol. 11, no. 10, pp. 767–778, 2020, doi: 10.4236/jep.2020.1110047.

[67] N. F. Kadhim, "Estimation of the Radiation Hazards Indices of Organic Fertilizers Using NaI (Tl) Gamma Spectrometer," vol. 144, no. March, pp. 126–140, 2020.

[68] W. R. Alharbi, "Natural Radioactivity and Dose Assessment for Brands of Chemical and Organic Fertilizers Used in Saudi Arabia," vol. 2013, no. March, pp. 344–348, 2013.

[69] N. G. Servitzoglou, S. Stoulos, D. Katsantonis, M. Papageorgiou, and A. Siountas, "Natural radioactivity studies of phosphate fertilizers applied on Greek Farm soils used for wheat cultivation," *Radiat. Prot. Dosimetry*, vol. 181, no. 3, pp. 190–198, 2018, doi: 10.1093/RPD/NCY009.

[70] J. H. Alzahrani, W. R. Alharbi, and A. G. E. Abbady, "Radiological Impacts of Natural Radioactivity and Heat Generation by Radioactive Decay of Phosphorite Deposits from Northwestern Saudi Arabia," *Aust. J.*

Basic Appl. Sci., vol. 5, no. 6, pp. 683–690, 2011.

[71] M. A. Samad, M. A. Haydar, M. I. Ali, D. Paul, M. M. R. Bhuiyan, and S. M. A. Islam, "A Study on the Radioactivity Level in Raw Materials, Final Products and Wastes of the Phosphate Fertilizer Industries in Bangladesh, " *J. Environ. Prot. (Irvine,. Calif).*, vol. 03, no. 10, pp. 1393–1402, 2012, doi: 10.4236/jep.2012.310158.

[72] N. K.Ahmed andA. G. M. El-Arabi, Natural radioactivity in farm soil and phosphate fertilizer and its environmental implications in Qena governorate, Upper Egypt, " *J.Environ. Radioact.*, vol. 84, no. 1, pp. 51–64, 2005, doi: 10.1016/j.jenvrad.2005.04.007.

[73] ICRP, "ICRU and ICRP Draft Joint Report Operational Quantities for External Radiation Exposure," vol. 20, no. 10, 2017.

[74] IAEA, "IAEA Safety Standards Safety Assessment for Facilities and Activities," vol. 4.

[75] R. F. Casten and C. W. Beausang, "Gamma-Ray Spectroscopy,"*Encycl. Phys. Sci. Technol.*, pp. 433–454, 2003, doi: 10.1016/B0-12-227410-5/00273-8.

[76] N.Connor,"What is High Purity Germanium Detector HPGe Definition," *Radiation Dosimetry*, 2019. https://www.radiation-dosimetry.org/what-is-high-purity-germanium-detector-hpge-definition/ (accessed Apr. 27, 2023).

[77] R. Methodology,"Hyper-Pure Germanium Detector," *Radioisot. Radiat. Methodol.*, no. practically Li, pp. 1–20.

[78] W. H. Geist and P. A. Santi, *Nondestructive Assay of Nuclear Materials for Safeguards and Security*.

[79] M.U.Khandaker,"High purity germanium detector in gamma-ray spectrometry: High-Purity Germanium detector," *Int. J. Fundam. Phys. Sci.*, vol. 1, no. 2, pp. 42–46, Jun. 2011, doi: 10.14331/ijfps.2011.330011.

[80] R. L.Murray and W. H. Zinn, *Introduction to Nuclear Engineering*, vol. 23,

no. 1. 1955. doi: 10.1119/1.1933896.

[81] H.Spieler,"Semiconductor Detector Systems Clardon press.OXFORD," 2005.

[82] Ge. Lutz, "Semiconductor radiation detectors. Device Physics," *Science*, 1999. https://inspirehep.net/literature/513731 (accessed Apr. 27, 2023).

[83] G. F. Knoll, "Radiation Detection and Measurement 4th Edition, Wiley," 2008. https://www.wiley.com/enus/Radiation+Detection+and+Measurement,+4th+Edition-p-9780470131480 (accessed Apr. 27, 2023).

[84] Mirion Technologies, "High-Resolution Gamma-Ray Spectroscopy with HPGe Detectors," 2020. https://www.mirion.com/learning-center/lab-experiments/high-resolution-gamma-ray-spectroscopy-with-hpge-detectors-lab-experiments (accessed Apr. 27, 2023).

[85] "HPGe Detectors & Spectrometers | BSI.LV." https://bsi.lv/en/products/hpge-detectors-spectrometers/ (accessed Jun. 08, 2023).

[86] "SpectraLine Software. Linear Spectra Processing. User 's Manual .," 2015.

[87] Banglapedia, "Chittagong District-Banglapedia," *Banglapedia - the National Encyclopedia of Bangladesh*, 2014. http://en.banglapedia.org/index.php/Chittagong_District.

[88] A. A. Md Sirajul Islam, M. M. Hossain Miah, M. Ahmed, S. Hossain, and M. U. Khandaker, "The presence of terrestrial radionuclides in the Karnaphuli and Halda river sediments and concomitant hazards to the dwellers," *Int. J. Environ. Anal. Chem.*, vol. 00, no. 00, pp. 1–11, 2021, doi: 10.1080/03067319.2021.1912339.

[89] G. F. Knoll, "Radiation detection and measurement," p. 830, 2010.

[90] "GBS Elektronik MCA-527 User Manual (Page 42 of 71) | ManualsLib." https://www.manualslib.com/manual/1526544/Gbs-Elektronik-Mca-

527.html?page=42#manual (accessed Apr. 30, 2023).

[91] "Software | BSI.LV." https://bsi.lv/en/products/software/analytical-software-package-spectralinegp/ (accessed May 01, 2023).

[92] S. Usb *et al.*, "A mca527," vol. 49, no. 0, pp. 21–22.

[93] "The Operation and Construction of Pulse-Height Spectrometers," vol. 3, pp. 116–310, Jan. 1980, doi: 10.1016/b978-0-444-99777-7.50007-0.

[94] N. Electronics,"Detectors,nuclear electronics,"no.December,pp.1–21, 2010.

[95] I.Radulescu,A.M.Blebea-Apostu,R.M.Margineanu,andN.Mocanu, "Background radiation reduction for a high-resolution gamma-ray spectrometer used for environmental radioactivity measurements, "*Nucl. Instruments Methods Phys.Res.Sect.AAccel.Spectrometers,Detect.Assoc. Equip.*, vol. 715, no. July, pp. 112–118, 2013, doi: 10.1016/j.nima.2013.03.024.

[96] "Hpge detector shieiding adjustment " Trnková L . Rulík P .," pp. 164–166.

[97] H. Persson and K. Phillips, "Peak Area Consistency Evaluation in Gamma Spectrometry," *EPJ Web Conf.*, vol. 253, p. 07002, 2021, doi: 10.1051/epjconf/202125307002.

[98] J. T. Li *et al.*, "Energy calibration of HPGe detector using the high-energy characteristic γ rays in 13C formed in 6Li + 12C reaction,"*Nucl. Sci. Tech.*, vol. 31, no. 5, pp. 1–7, May 2020, doi: 10.1007/s41365-020-00758-x.

[99] T. S. Reshid, "Calculation of excitation function of some structural fusion material for (n, p) reactions up to 25 MeV," *J. Fusion Energy*, vol. 32, no. 2, pp. 164–170, 2013, doi: 10.1007/s10894-012-9541-5.

[100] S. Harb and K. S. Din,"Study of Efficiency Calibrations of HPGe Detectors for Radioactivity Measurements of Environmental Samples,"*Proc.3rd Environ. Phys. Conf.*, pp. 207–218, 2008.

[101] A. Parmentier *et al.*,"Absolute efficiency calibration of a coaxial HPGe

detector for quantitative PGAA and T-PGAA," *J. Phys. Conf. Ser.*, vol. 1055, no. 1, 2018, doi: 10.1088/1742-6596/1055/1/012010.

[102] T. Barua *et al.*,"The presence of radioactive and metal contaminants in wild mushrooms grown in Chattogram hill tracts, Bangladesh," *J. Radioanal. Nucl. Chem.*, vol. 322, no. 1, pp. 173–182, 2019, doi: 10.1007/s10967-019-06579-6.

[103] S. Yasmin *et al.*,"The presence of radioactive materials in soil, sand and sediment samples of Potenga sea beach area, Chittagong, Bangladesh: Geological characteristics and environmental implication," *Results Phys.*, vol. 8, pp. 1268–1274, 2018, doi: 10.1016/j.rinp.2018.02.013.

[104] F. Carini,"Radionuclides,"*Chem. Anal. Food Tech. Appl.*, pp. 757–783, 2012, doi: 10.1016/B978-0-12-384862-8.00023-6.

[105] M. Charles, *UNSCEAR Report 2000: Sources and Effects of Ionizing Radiation*, vol. 21, no. 1. 2001. doi: 10.1088/0952-4746/21/1/609.

[106] T.T. H. Loan, V. N. Ba, N. Van Thai Bang, T. H. N. Thy, H. T. Y. Hong, and N. Q. Huy, "Natural radioactivity and radiological health hazard assessment of chemical fertilizers in Viet Nam," *J. Radioanal. Nucl. Chem.*, vol. 316, no. 1, pp. 111–117, 2018, doi: 10.1007/s10967-018-5719-2.

[107] A. El-Taher and S. S. Althoyaib, "Natural radioactivity levels and heavy metals in chemical and organic fertilizers used in Kingdom of Saudi Arabia," *Appl. Radiat. Isot.*, vol. 70, no. 1, pp. 290–295, 2012, doi: 10.1016/j.apradiso.2011.08.010.

[108] M. Samad, M. Ali, D. Paul, and S. Islam, "Assessment of Radioactivity in the Wastes Generated from the Diammonium Phosphate (DAP) Fertilizer Factory, chittagong, Bangladesh," *Jahangirnagar University Environmental Bulletin*, vol. 1. pp. 15–24, 2013. doi: 10.3329/jueb.v1i0.14543.

[109] Icrp,"Annals of the ICRP Published on behalf of the International Commission on Radiological Protection", doi: 10.1177/ANIB_37_2-4.

[110] J. Billa *et al.*,"Evaluation of radioactivity levels in fertilizers commonly

used in the Southern USA," *J. Radioanal. Nucl. Chem.*, vol. 306, no. 1, pp. 183–191, Oct. 2015, doi: 10.1007/S10967-015-4071-Z/METRICS.

[111] L. E. De Geer, "Currie detection limits in gamma-ray spectroscopy," *Appl. Radiat. Isot.*, vol. 61, no. 2–3, pp. 151–160, 2004, doi: 10.1016/j.apradiso.2004.03.037.

[112] F.Alshahri, "Natural and anthropogenic radionuclides in urban soil around non-nuclear industries (Northern Al Jubail), Saudi Arabia: assessment of health risk," *Environ. Sci. Pollut. Res.*, vol. 26, no. 36, pp. 36226–36235, 2019, doi: 10.1007/s11356-019-06647-0.

[113] J. Li *et al.*, "Evaluation of Natural Radioactivity in Marine Sand Deposits from Offshore China," *Open J. Mar. Sci.*, vol. 07, no. 03, pp. 357–378, 2017, doi: 10.4236/ojms.2017.73026.

[114] M.S.D. Sarker, R.Rahman, M.M.M.Siraz, M.U.Khandaker, and S. Yeasmin, "The presence of primordial radionuclides in powdered milk and estimation of the concomitant ingestion dose," *Radiat. Phys. Chem.*, vol. 188, no. May, p. 109597, 2021, doi: 10.1016/j.radphyschem.2021.109597.

[115] K. Holmes, "Solid Materials," *Tribol. Ser.*, vol. 26, no. C, pp. 271–286, 1993, doi: 10.1016/S0167-8922(08)70015-4.

Appendix: Specimen Calculations.

From the table: 01, we can calculate the value of Radium equivalent activity all Fertiliser using equation 4.2

Calculation No 1: For average specific activity of ^{226}Ra, ^{232}Th , ^{40}K in TSP fertiliser

$Ra_{\mathrm{eq}} = C_{\mathrm{Ra}} + 1.43C_{\mathrm{Th}} + 0.077C_{\mathrm{k}}$ ……(4.2)

Here, Specific activity of ^{226}Ra, C_{Ra}=304.6 Bq Kg^{-1}

Specific activity of ^{232}Th, C_{Th}= 304.571Bq Kg^{-1}

Specific activity of ^{40}K,C_K= 0 Bq Kg^{-1}

$$Ra_{\mathrm{eq}} = 304.6 + 1.43 \times 304.57 + 0.077 \times 0$$

$$Ra_{\mathrm{eq}} = 740.13 \text{ Bq Kg}^{-1}$$

Calculation No 2:

Radium equivalent activity (Ra_{eq}).

For average specific activity of ^{226}Ra, ^{232}Th , ^{40}K in MOP Fertiliser of ^{226}Ra

C_{Ra}=0 Bq Kg^{-1},

C_{Th}= 0Bq Kg-1 ,

C_K= 10520 Bq Kg^{-1}

$Ra_{\mathrm{eq}} = C_{\mathrm{Ra}} + 1.43C_{\mathrm{Th}} + 0.077$……..…….(4.2)

$$Ra_{\mathrm{eq}} = 1 \times 0 + 1.43 \times 0 + 0.077 \times 10520 \text{ Bq Kg}^{-1}$$

$$Ra_{\mathrm{eq}} = 0.077 \times 10520 \text{ Bq Kg}^{-1}$$

$$Ra_{\mathrm{eq}} = 810.04 \text{ Bq Kg}^{-1}$$

Calculation no 3: From the table 01 average specific activity of ^{226}Ra, ^{232}Th, ^{40}K in organic Fertiliser,

Again using equation (4.3) we can determine the outdoor dose rate and indoor dose rate

$D_{\mathrm{out}} = 0.462\ C_{\mathrm{Ra}} + 0.604CC_{\mathrm{Th}} + 0.0417\ C_{\mathrm{K}}$….4.3

The average specific activity of ^{226}Ra, ^{232}Th , ^{40}K in organic Fertiliser

C_{Ra}=19.216Bq Kg^{-1}

C_{Th}= 33.58 Bq Kg^{-1}

C_K= 1224 Bq Kg^{-1}

$$D_{\text{out}} = 0.462\ C_{\text{Ra}} + 0.604CC_{\text{Th}} + 0.0417\ C_{\text{K}}$$

$$D_{\text{out}} = 0.462 \times 19.21 + 0.604 \times 33.58 + 0.0417 \times 1224 \text{ nGy h}^{-1}$$

$$D_{\text{out}} = 80.198 \text{ nGy h}^{-1}$$

Calculation no 4: Again using equation (4.4) we can determine the indoor dose rate.

$$D_{\text{in}} = 0.92\ C_{\text{Ra}} + 1.1C_{\text{Th}} + 0.081\ C_{\text{K}} \ldots\ldots 4.4$$

For average specific activity of ^{226}Ra, ^{232}Th , ^{40}K in organic Fertiliser,

C_{Ra}=19.216Bq Kg^{-1}

C_{Th}= 33.58 Bq Kg^{-1}

C_K= 1224 Bq Kg^{-1}

$$D_{\text{in}} = 0.92 \times 19.21 + 1.1 \times 33.58 + 0.081 \times 1224) \text{ nGy h}^{-1}$$

$$D_{\text{in}} = 0.92 \times 19.21 + 1.1 \times 33.58 + 0.081 \times 1224) \text{ nGy h}^{-1}$$

$$D_{\text{in}} = 153.75 \text{ nGy h}^{-1}$$

Calculation no 5:

The annual effective dose equivalent (AEDE) in Organic fertiliser

$$AEDC(Outdoor) = D_{\text{out}} \times 8760 \times 0.2 \times 0.7 \times 10^{-6} \ldots 4.5$$

Here from above calculation it can be write

$$D_{\text{out}} = 80.198 \text{ nGy h}^{-1}$$

$$AEDC(Outdoor) = 80.198 \times 8760 \times 0.2 \times 0.7 \times 10^{-6} \text{ mSv y}^{-1}$$

$$AEDC(Outdoor) = 98354.82 \times 10^{-6} \text{ mSv y}^{-1}$$

$$AEDC(Outdoor) = 0.0983 \text{mSv y}^{-1}$$

Calculation 6:

Again, The annual effective dose equivalent (AEDE) in organic fertiliser

$$\text{AEDC (indoor)} = D_{\text{in}} \times 8760 \times 0.8 \times 0.7 \times 10^{-6} \ldots (4.6)$$

$D_{\text{in}} = 153.75 \text{ nGy h}^{-1}$

Therefore,

$$\text{AEDC (indoor)} = 153.75 \times 8760 \times 0.8 \times 0.7 \times 10^{-6}$$

$$\text{AEDC (indoor)} = 0.754236 \text{ mSv y}^{-1}$$

Calculation 6: The average specific activity of ^{226} Ra, ^{232} Th , ^{40}K in organic Fertiliser

C_{Ra}=19.216 Bq Kg^{-1}

C_{Th}= 33.58 Bq Kg^{-1}

C_K= 1224 Bq Kg^{-1}

External Hazard Index

$$H_{ex} = \frac{C_{Ra}}{370} + \frac{C_{Th}}{259} + \frac{C_K}{4810} \ldots\ldots\ldots\ldots\ldots\ldots (4.7)$$

$$H_{ex} = \frac{19.21}{370} + \frac{33.58}{259} + \frac{1224}{4810}$$

$$H_{ex} = \frac{19.21}{370} + \frac{33.58}{259} + \frac{1224}{4810}$$

$$H_{ex} = 0.052 + 0.12 + 0.25$$

$$H_{ex} = 0422$$

Calculation 7:

The equation of Internal Hazard index(H_{in})

$$H_{in} = \frac{C_{Ra}}{185} + \frac{C_{Th}}{259} + \frac{C_K}{4810} \ldots\ldots\ldots\ldots\ldots\ldots (4.8)$$

$$H_{in} = \frac{19.21}{185} + \frac{33.58}{259} + \frac{1224}{4810}$$

$$H_{in} = .01 + 0.12 + 0.25$$

$$H_{in} = 0.47$$

Calculation :8

γ-radiation hazard index (I_γ):

$$I_\gamma = \frac{C_{Ra}}{300} + \frac{C_{Th}}{200} + \frac{C_K}{3000} \ldots\ldots\ldots\ldots\ldots (4.9)$$

The average specific activity of ^{226} Ra, ^{232} Th , ^{40} K in organic Fertiliser

C_{Ra}=19.216 Bq Kg^{-1}

C_{Th}= 33.58 Bq Kg^{-1}

C_K= 1224 Bq Kg^{-1}

$$I_\gamma = \frac{19.216}{300} + \frac{33.58}{200} + \frac{1224}{3000}$$

$$I_\gamma = 0.064 + 0.1679 + 0.4$$

$$I_\gamma = 0.632$$

Calculation: 9

Excess lifetime cancer risk (ELCR):

$\mathrm{ELCR} = \mathrm{AEDC} \times \mathrm{DL} \times \mathrm{RF}$……...(4.10)

For the Organic fertiliser

$AEDC(Outdoor) = 0.0983\mathrm{mSv\ y^{-1}}$,

DL = 70 years

RF = 0.05 $\mathrm{Sv^{-1}}$

$$\mathrm{ELCR} = 0.0983 \times 70 \times 0.05$$

$$\mathrm{ELCR} = 0.34405$$

International Journal of Environmental Analytical Chemistry

ISSN: (Print) (Online) Journal homepage: https://www.tandfonline.com/loi/geac20

Assessment of naturally occurred radiation hazards in chemical and organic fertilizers used in Chattogram area, Bangladesh

Kanchan Sarkar, Animesh Kumer Chakraborty, Mahiuddin Ahmed & Shahadat Hossain

To cite this article: Kanchan Sarkar, Animesh Kumer Chakraborty, Mahiuddin Ahmed & Shahadat Hossain (18 Oct 2022): Assessment of naturally occurred radiation hazards in chemical and organic fertilizers used in Chattogram area, Bangladesh, International Journal of Environmental Analytical Chemistry, DOI: 10.1080/03067319.2022.2135998

To link to this article: https://doi.org/10.1080/03067319.2022.2135998

Published online: 18 Oct 2022.

INTERNATIONAL JOURNAL OF ENVIRONMENTAL ANALYTICAL CHEMISTRY
https://doi.org/10.1080/03067319.2022.2135998

Assessment of naturally occurred radiation hazards in chemical and organic fertilizers used in Chattogram area, Bangladesh

Kanchan Sarkar[a], Animesh Kumer Chakraborty[a], Mahiuddin Ahmed[b] and Shahadat Hossain[c]

[a]Department of Physics, Chittagong University of Engineering and Technology, Chittagong, Bangladesh; [b]Institute of Nuclear Science and Technology, Bangladesh Atomic Energy Commission Savar, Dhaka, Bangladesh; [c]Bangladesh Atomic Energy Commission, Atomic Energy Centre, Chattogram, Bangladesh

ABSTRACT

The present work deals with identifying and determining the activity levels of naturally occurring radionuclides ^{226}Ra and ^{232}Th series, their decay products and ^{40}K in chemical and organic fertilisers used in the Chattogram area, Bangladesh. A total of 39 samples collected from retail markets were investigated, out of which 28 are chemical fertilisers and the others are organic fertilisers. The average activity concentration of ^{226}Ra and ^{232}Th found in TSP fertiliser are 304.57 ± 36.0 and 19.1 ± 6.8 Bq kg^{-1} respectively and the average activity concentration of ^{40}K in MOP fertiliser is found as 10,311.11 ± 1168 Bq kg^{-1}. In the organic fertiliser samples, the mean concentration of ^{226}Ra, ^{232}Th and ^{40}K are 17.35 ± 3.1[1], 7.20 ± 1.74 and 437.14 ± 42.58 Bq kg^{-1}, respectively. The mean absorbed dose rates were measured after the end of our experiment, and the value was found to be 91.39 nGy h^{-1}. The combined (indoor + outdoor) annual effective dose equivalent was also estimated as 0.322 mSv year^{-1}. The mean radium equivalent activity found to be 190.15 ± 26.74 Bq kg^{-1} is well below the recommended level of 370 Bq kg[1]. The internal hazard index, external hazard index, and radioactivity level index of the investigated fertiliser samples were found as 0.56 ± 0.034, 0.54 ± 0.08 and 0.69 ± 0.10, respectively. From the calculated hazard parameters, the excess lifetime cancer risk (ELCR) was found to be higher than the world average in most of the chemical fertilisers except in DAP and BOR, while the organic fertilisers show lower than the world average. The obtained results reveal that there are no significant radiation hazards due to natural radionuclides of the fertiliser samples in the studied area, but the higher concentration of ^{40}K in MOP suggests strengthening the regulatory work. Overall, this study highly recommends the use of organic fertilisers, as these kinds have hazard parameters lower than the recommended levels.

ARTICLE HISTORY
Received 5 August 2022
Accepted 26 September 2022

KEYWORDS
Radiation hazards; chemical fertiliser; organic fertiliser; radium equivalent activity; hazard index; cancer risk

1. Introduction

In the last decade, Bangladesh has drawn enormous global attention for its remarkable advances in agricultural products, attaining food self-sufficiency and ensuring sustainable

CONTACT Animesh Kumer Chakraborty animeshbd@yahoo.com

food security. To achieve high-yielding varieties of crops for her 168 million population [1], it is needed to use the same cultivable land at least three times a year. Recurrent use of the land severely depletes the essential nutrients for the plants and consequently lessens the production. To cover up this challenge, it is recommended to use fertilisers for dispensing the required nutrients in the soil.

In 2019, around 5.58 million metric tons of fertilisers were used for growing 41.5 million metric tons of food grain and other harvests [2]. Among the two general categories of fertilisers, inorganic and organic, the former kind mixes with soil at a faster rate. On the other hand, organic or bio or natural fertilisers, which are mostly made from animal manure and plant compost, mixes with the soil at a slower rate. This particular type is good at raising the physical and chemical properties of soil, holding intermediate nitrogen, and controlling over-fertilisation. Then again, chemical fertilisers from potassium ores, nitrogenous compounds, gypsum, alluvial and incendiary rock mostly contain potassium, fluorapatite, goethite, quartz mineral, anatase, magnetite, thorium and uranium. Among these elements, potassium (^{40}K), thorium (^{232}Th) and uranium (^{238}U) are radioactive and capable of producing radioactive progenies like radium (^{226}Ra) [3]. Thus, the use of these fertilisers in agricultural activities leads to an increase in radioactivity in soil and the environment. Eventually, these radionuclides will be absorbed by the plants [3] and transferred to the human body through the food chain [4]. Workers in fertiliser production factories and agricultural fields are mostly exposed to gamma radiation externally and the consumers of the final products are expected to have internal exposure by inhalation and ingestion of the radionuclides thrown up from fertilisers.

Besides this, human activities of utilising nuclear materials and radiation sources in technology, industry, medicine, and the military are increasing day by day, which is contributing to elevating the terrestrial background radiation level. But it is unpleasant that exposure to ionisation radiation is also one of the reasons for malignant diseases [5]. So, from the perspective of radiation protection, i.e. keeping the exposure level as low as possible, monitoring the radioactivity in one of the widely used commodities like fertiliser is highly regarded. Researchers all around the world, most noticeably from neighbouring countries, have done studies on radionuclide concentrations in fertilisers and related hazards [6–14]. In this era of extensive transboundary trading, the quality of crops is one of the priorities. To maintain so, monitoring the constituents in fertilisers and related effects is like solving an issue from the root level.

Therefore, it is obligatory to identify and assess the concentration of gamma radiation emitting Naturally Occurring Radioactive Materials (NORM) and artificially produced radioisotopes in numerous fertilisers, which are commercially available in Chattogram, the largest geographical division of Bangladesh. In this study, High Purity Germanium (HPGe) spectroscopy set-up of 40% relative efficiency at Atomic Energy Centre, Chattogram has been used for acquiring data. Afterwards, radiation-induced hazard indices like Radium equivalent activity (Ra_{eq}), external hazard index (H_{ext}), internal hazard index (H_{int}), external (γ-radioactivity) level index (I_γ), annual effective dose equivalent (AEDE) and excess lifetime cancer risk (ELCR) were estimated. The obtained results were compared with other research of a kind from different parts of the world and were justified with safety standards suggested by the United Nations Scientific Committee on the Effects of Atomic Radiation (UNSCEAR). Thus, the output of this research could contribute to making the baseline data of health risks due to radiation from fertiliser,

establishing a justified regulatory framework, and further awareness of using those fertilisers.

2. Materials and methods

2.1. Sample collection and preparation

To identify and quantify the presence of natural and anthropogenic radionuclides, a total of 49 fertiliser samples were collected from the retail market and farmers of Chattogram, Bangladesh. Among the collected samples, 16 samples were organic fertilisers, and the rest were chemical fertilisers. Nonetheless, collected 39 numbers of chemical fertilisers from eight different varieties are as follows: 7 samples of triple superphosphate (TSP), 5 of diammonium phosphate (DAP), 8 of muriate of potash (MOP), 1 of Q-potash, 4 of boron (BOR) fertilisers, 1 of gypsum (GYP), 1 of single superphosphate (SSP) and 11 of organic (ORG) fertilisers.

The selected samples were powdered and sieved through a 1-mm mesh to make them more homogeneous. Then, to remove the unwanted aqueous content, the samples were air-dried for a few days followed by 24 h oven-dried at 110°C [15]. After the complete removal of moisture, the samples cooled down in the desiccator. Each sample was airtight into a plastic container of 5 cm in diameter and 8 cm in height and kept aside for 1 month before the core experimental proceedings [16]. Thus, the secular equilibrium of short-lived members of the ^{226}Rn series was achieved, and radon gas was confined within the volume [7,9]. Then, before taking for radioactivity measurement, all the contained samples were weighed with a high precision laboratory balance machine.

2.2. System set-up and calibration

Gamma-ray spectrometry is generally the most effective technique, among the other existing analysis systems of radionuclides, to analyse the gamma-emitting radionuclides in various types and geometry of samples [17]. A liquid nitrogen-cooled coaxial *p*-type HPGe gamma-ray detector (BSI, GCD 40,190, S/N 2465–17) coupled with associated electronics including a digital spectrum analyser (MCA 527, GBS Elektronik GmbH) was used for the measurement of radionuclide concentration in the sample. As the detector has 40% relative efficiency for energy 1332 keV to NaI(Ti) due to its sensitive area of 63.3 mm × 61.3 mm and energy resolution of 1.74 keV FWHM at the 1332 keV peak of ^{60}Co; this device was the better choice for detecting photons of energy ranging from 40 to 10,000 keV while it was attached with 16k multi-channel analyzer (MCA). Nonetheless, to obtain the best net result from the target samples, the whole detection part was properly shielded from background radiation with the help of a fixed-bottom and movable-cover cylindrical lead ($_{82}$Pb) enclosure of thickness 10 cm jacketed by 5 mm steel outer housing and 1 mm thin inner layer.

Energy calibration and the absolute photo-peak efficiency evaluation were performed using a standard (Code: 8501-EG-SVE, Eckert & Ziegler Analytics) certified multinuclear gamma-ray source (^{241}Am, ^{109}Cd, ^{57}Co, ^{139}Ce, ^{113}Sn, ^{85}Sr, ^{137}Cs, ^{88}Y, ^{60}Co) having homogeneously distributed activity, maintaining the same geometry and density as the beakers containing the samples. Spectra Line GP software was used to analyse the measured

gamma rays emitted from the samples. To minimise the statistical counting error, the samples were counted for 60,000 s. An empty sealed plastic container was counted under the same conditions as of the samples to determine the background counts and was deducted from the counts of each sample to obtain the net counts.

The minimum detectable activities (MDA in Bq kg^{-1}) of the gamma-ray measuring system, that has been used in this study, was calculated as follows (Equation (1)) [18–20].

$$MDA = \frac{C_F \times \sqrt{B}}{\varepsilon I_\gamma t m} \tag{1}$$

where C_F is the statistical coverage factor for 95% confidence level, B is the background counts over the region of interest for each radionuclide, ε is the absolute efficiency of the HPGe detector, I_γ is the gamma emission probability, t is the measuring time (86,400 s) and m is the mass of the sample in kg.

2.3. Measurement of activity concentration

The activity concentration of ^{226}Ra (^{238}U) was measured by the characteristic gamma peaks of its progeny: 351.93 keV from ^{214}Pb; 1120.29 keV and 1764.49 keV from ^{214}Bi [14]. The γ-ray lines of 238.63 keV from ^{212}Pb, 911.20 keV from ^{228}Ac and 583.19 keV from ^{208}Tl were used to estimate the activity of ^{232}Th. The single transition photo-peak of energy 1460.822 keV was used to determine the activity concentrations of ^{40}K [13]. To lessen the ambiguity of multi-photo-peaks progenies of ^{226}Ra and ^{232}Th, a weighted mean approach was practical while evaluating these aforementioned nuclides' activity [15]. The activity concentration of the radionuclides of interest was calculated using Equation (2) [21,22]:

$$A = \frac{N}{\varepsilon_\gamma I_\gamma T_s M_s} \tag{2}$$

where A is the specific activity (Bq kg^{-1}), N is the net count under a photopeak, ε_γ is the efficiency of the detector for the corresponding peak, I_γ is the gamma emission probability, T_s is the sample counting time in s and M_s is the sample mass in kg.

For better precise output, the total uncertainty in the specific activity of every studied sample was calculated by accepting the following uncertainties: detector efficiency (5%), photopeak area analysis (2–7%), gamma-ray emission probability (<0.2%) and sample weight (0.01%). Thus, the overall uncertainties were in the range of 5–9%.

2.4. Calculation of radiological parameter

2.4.1. Radium equivalent activity (Ra_{eq})

Radium equivalent concentration (Ra_{eq}) is a widely used hazard index that implies the comparison of activity concentration of radium, thorium and potassium present in the samples. It is assumed that 370 Bq kg^{-1} of ^{226}Ra, 259 Bq kg^{-1} of ^{232}Th and 4810 Bq kg^{-1} of ^{40}K produced the equivalent γ-ray dose. In this study, Equation (3) is used to calculate Ra_{eq} [14,15].

$$Ra_{eq} = C_{Ra} + 1.43C_{Th} + 0.077C_K \tag{3}$$

where C_{Ra}, C_{Th} and C_K are the specific activities (Bq kg^{-1}) of ^{226}Ra, ^{232}Th and ^{40}K, respectively.

The radium equivalent is related to both the external γ-dose and the internal α-dose from radon and its progeny. The permissible maximum value of Ra_{eq} is 370 Bq kg^{-1} which corresponds to an effective dose of 1.5 mSv y^{-1}.

2.4.2. Air absorbed gamma dose rate: utdoor (D_{out}) and ondoor (D_{in})

Assuming the equal distribution of γ-radiation from ^{226}Ra, ^{232}Th and ^{40}K in the ground and all decay products of ^{226}Ra and ^{232}Th are in radioactive equilibrium with their precursors, the outdoor external dose rate (D_{out}) from these γ-rays in the air at 1 m above the ground was calculated according to Equation (4) [23]:

$$D_{out} = 0.462\ C_{Ra} + 0.604\ C_{Th} + 0.0417\ C_K \tag{4}$$

Likewise, the γ-ray dose (D_{in}) present in the indoor is calculated using Equation (5) [23].

$$D_{in} = 0.92\ C_{Ra} + 1.1\ C_{Th} + 0.081\ C_K \tag{5}$$

where D_{out} and D_{in} are in nGy h^{-1}.

2.4.3. Annual effective dose equivalent (AEDE)

To estimate the AEDE, the conversion factor (0.7 Sv Gy^{-1}) is used in the assessment of radiobiological health hazard levels related to natural radioactivity. It is also assumed that an individual's occupancy factor in indoor (0.8) and outdoor (0.2) for a year (8760 h). The AEDE for outdoor and indoor in mSv y^{-1} was calculated using the following formulas [9]:

$$\text{AEDE(outdoor)} = D_{out} \times 8760 \times 0.2 \times 0.7 \times 10^{-6} \tag{6}$$

$$\text{AEDE(indoor)} = D_{in} \times 8760 \times 0.8 \times 0.7 \times 10^{-6} \tag{7}$$

where D_{out} and D_{in} are the absorbed dose in nGy h^{-1} and the factor 10^{-6} is for unit conversion.

2.4.4. External (H_{ex}) and internal (H_{in}) hazard index

Limiting the usage of materials consisting of NORM isotopes, there are two dimensionless radiological health hazards indicating parameters named external hazard index (H_{ex}) and internal hazard index (H_{in}) are been extensively used. To meet the safety standards for protecting people from external gamma radiation dose and internal exposure from radon along with its progenies to respiratory organs, the H_{ex} and H_{in} values should be less than unity. Equations (8) and (9)define H_{ex} and H_{in} [24].

$$H_{ex} = \frac{C_{Ra}}{370} + \frac{C_{Th}}{259} + \frac{C_K}{4810} \tag{8}$$

$$H_{in} = \frac{C_{Ra}}{185} + \frac{C_{Th}}{259} + \frac{C_K}{4810} \tag{9}$$

where C_{Ra}, C_{Th} and C_K are the specific activities (Bq kg^{-1}) of ^{226}Ra, ^{232}Th and ^{40}K, respectively.

2.4.5. γ-Radiation hazard index (I_γ)

To assess the safety level of radiation, the European Commission [25] proposed an index called the activity concentration index or representative level index. In this study, I_γ was calculated by using the following formula [25]:

$$I_\gamma = \frac{C_{Ra}}{300} + \frac{C_{Th}}{200} + \frac{C_K}{3000} \tag{10}$$

2.4.6. Excess lifetime cancer risk (ELCR)

This gives the additional probability of developing cancer induced by exposure to ionising radiations at a given level over a lifetime. The ELCR has been calculated using the following equation [26]:

$$ELCR = AEDE \times DL \times RF \tag{11}$$

where AEDE, DL and RF are the outdoor annual effective dose equivalent, duration of life (70 years), and risk factor, respectively. The risk factor is fatal cancer risk per sievert, which is assigned to a value of 0.05 Sv^{-1} for the public for stochastic effects, recommended in ICRP Publication 103 [27].

3. Results and discussion

3.1. Activity concentrations

Radiological valuation of the most commonly used chemical and organic fertilisers in Chattogram, Bangladesh was accomplished by a high-purity germanium (HPGe) gamma-ray spectroscopic system at the Atomic Energy Centre, Chattogram. In this study, 39 fertiliser samples comprising nine different varieties were picked to investigate the presence and concentration level of radionuclides. The activity concentrations, as well as the uncertainties of identified radionuclides ^{226}Ra, ^{232}Th and ^{40}K, are presented in Table 1(a–e).

It is clear from Table 1(a) that the specific activities of ^{226}Ra vary from 98 ± 10.8 to 460 ± 55.2 Bq kg^{-1} with an average of 304.6 ± 6.1 Bq kg^{-1} for Triple Superphosphate (TSP) fertiliser, and this observation is in accordance with the study of Alam et al. [28] and Najam et al. 2022 [8]. The detected average concentration of ^{232}Th is 19.1 ± 3.5 Bq kg^{-1} and can be considered normal compared to the previous study [28]. In addition, it is observed that the concentration of ^{238}U and ^{232}Th series radionuclides in our studied TSP fertilisers are considerably lower than the typical concentrations presented in UNSCEAR 2008 report [29], while the ^{40}K in TSP remains undetected.

In Table 1(b), it is seen that the measured concentrations of ^{226}Ra and ^{232}Th in diammonium phosphate (DAP) fertilisers range from 1.4 ± 0.7 to 6.9 ± 1.3 Bq kg^{-1} with an average of 4.8 ± 1.1 Bqkg^{-1} and 7 ± 1.6 to 33 ± 5.6 Bq kg^{-1} with an average of 20 ± 3.6 Bq kg^{-1}, respectively. It can be depicted from the result that in our study we get relatively lower concentrations of ^{226}Ra and ^{232}Th compared to the studies of Loan et al. [12], El-Taher et al. [10], Najam et al. [8] and Samad et al. [30]. Although three out of five DAP and one out of seven TSP samples have ^{232}Th below the minimum detectable activity (2.8 Bq kg^{-1}), the ^{40}K for all studied TSP and DAP samples were found below the detectable limit (40 Bq kg^{-1}) [27,28].

Table 1. Activity concentrations of ^{226} Ra, ^{232}Th and ^{40}K in fertiliser samples in Bq kg^{-1}.

	Specific activity				Specific activity		
Sample code	^{226} Ra	^{232}Th	^{40}K	Sample code	^{226} Ra	^{232}Th	^{40}K
(a) TSP fertiliser					(b) DAP fertilisers		
TSP-1	320 ± 35.2	8.6 ± 2.6	<40	DAP-1	1.4 ± 0.7	<2.8	<40
TSP-2	460 ± 55.2	26 ± 4.9	<40	DAP-2	3.8 ± 1.1	33 ± 5.6	<40
TSP-3	400 ± 48	16 ± 3.4	<40	DAP-3	5 ± 1.1	<2.8	<40
TSP-4	104 ± 10.4	18 ± 3.3	<40	DAP-4	6.9 ± 1.3	7 ± 1.6	<40
TSP-5	98 ± 10.8	20 ± 3.6	<40	DAP-5	6.8 ± 1.3	<2.8	<40
TSP-6	400 ± 40	26 ±12	<40	DAP Avg.	4.8 ± 1.1	20 ± 3.6	-
TSP-7	350 ± 52.5	<2.8	<40		(d) Boron fertiliser		
TSP Avg.	304.6 ± 6.1	19.1 ± 3.5	-	BOR-1	8±3.2	<2.8	<40
(c) MOP fertiliser				BOR-2	<1.2	7 ± 1.7	<40
MOP-1	<1.2	<2.8	10600 ± 1484	BOR-3	5.7 ± 2.9	<2.8	<40
MOP-2	8 ± 2.3	<2.8	10300 ± 1442	BOR-4	11.4 ± 1.9	10 ± 2.2	<40
MOP-3	<1.2	<2.8	9800 ± 1372	BOR Avg.	8.4 ± 2.7	8.6 ± 1.9	-
MOP-4	2 ± 0.8	<2.8	10700 ± 1070		(e) Organic fertiliser		
MOP-5	<1.2	<2.8	11000 ± 1100	ORG-1	<1.2	7 ± 1.8	<40
MOP-6	<1.2	<2.8	11100 ± 1110	ORG-2	55 ± 9.9	68 ± 8.8	320 ± 48
MOP-7	<1.2	<2.8	10700 ± 1070	ORG-3	<1.2	3.4 ± 1.4	700 ± 105
MOP-8	<1.2	<2.8	10500 ± 735	ORG-4	138 ±17.9	<2.8	1250 ± 187.5
MOP-9	<1.2	<2.8	8100 ± 1134	ORG-5	29 ± 7.3	<2.8	3440 ± 275.2
Q-Potash	<1.2	<2.8	12400 ± 1240	ORG-6	12 ± 3.6	31	<40
MOP Avg.	5 ± 1.52	-	10520 ± 1175.7	ORG-7	4.3 ± 2.2	<2.8	<40
(f) Gypsum and SSP fertilisers				ORG-8	4.6 ± 1.3	9.1 ± 2.2	410 ± 65.6
GYP	242 ± 29.1	<2.8	<40	ORG-9	9 ± 3.6	<2.8	<40
SSP	84 ± 15.1	60 ± 13.2	710 ± 78.1	ORG-10	4.8 ± 1.1	9.4 ± 1.7	<40
				ORG-11	8 ± 4	<2.8	<40
				ORG Avg.	33.6 ± 5.8	19.2 ± 4.4	1224 ± 136.3

Outcomes from the gamma-ray spectroscopy analysis of Muriate of Potash (MOP) samples are presented in Table 1(c). The obtained results expose the dominant presence of ^{40}K with an average specific activity of 10,520 ± 1175.7 Bq kg^{-1}, while the minimum and maximum values are 8100 ± 1134 and 12,400 ± 1240 Bq kg^{-1}, respectively. This massive presence of ^{40}K in MOP fertiliser is due to the higher concentrations (60%) of potassium [9].

The presence of primordial radionuclides, ^{226}Ra and ^{232}Th shown in Table 1(d), is found at lower concentrations in Boron (BOR) fertilisers with an average of 8.4 ± 2.7 and 8.6 ± 1.9 Bq kg^{-1}, respectively, while ^{40}K remains undetected. Table 1(f) represents the detected radionuclides in gypsum (GYP) and single superphosphate (SSP) fertilisers. These two particular types of samples have a moderate level of radionuclide concentrations.

Analysed data from 11 different organic fertilisers, which are mostly from animal manure and plant compost, are presented in Table 1(e). The average radioactivity per unit mass of the samples due to ^{226}Ra, ^{232}Th and ^{40}K are found: 33.6 ± 5.8, 19.2 ± 4.4 and 1224 ± 136.3 Bq kg^{-1} respectively. Although the organic fertilisers are made from biocombustible natural sources, the average level of ^{40}K is found to be higher than the population-weighted average concentration in soil (420 Bq kg^{-1}) presented in UNSCEAR 2000 report [31].

Figure 1 represents not only the pictorial view of the average specific activity of NORM found in our studied samples but also a comparison with the worldwide average specific activity of NORM in soil reported in the UNSCEAR 2000 report [31]. It is clear that most of the samples have lower contents of hazardous radionuclides rather than the UNSCEAR

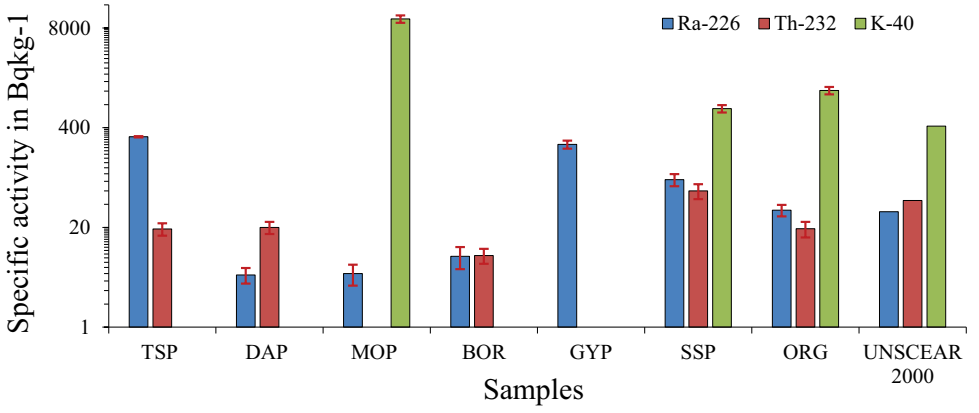

Figure 1. Average specific activity in studied samples compared to the worldwide average activity in soil reported by UNSCEAR 2000 [31].

2000 value except for the MOP fertilisers, where the ^{40}K are present at an elevated level. Moreover, measured concentrations still coincide with the permissible international radioactivity levels, given by IAEA, 1000 Bq kg^{-1} for ^{238}U and ^{232}Th series radionuclides and 10,000 Bq kg^{-1} for ^{40}K [11]. In contrast, the sample of Q-potash has been found to have a higher content of ^{40}K (12400 ± 1240 Bq kg^{-1}) than the exemption limit, which indicates that further studies are essential to find more reliable information and hence to take regulatory measures thereafter, if necessary.

3.2. Radium equivalent activity

As discussed earlier, radium equivalent activity is the widely used hazard index which implies the comparison of activity concentration of radium, thorium, and potassium present in the samples. The value of this index is calculated by using Equation (3) and the results are shown in Figure 2 as well as in Table 2. The results demonstrate that the average Ra_{eq} concentrations of MOP fertilisers are almost double than the recommended limits of 370 Bq kg^{-1} [32–34], while for other kinds of fertilisers, Ra_{eq} is found in the green zone of the safe level. The higher presence of ^{40}K in MOP is the first and foremost reason for exceeding the suggested limits of Ra_{eq}. Comparatively, lower average-Ra_{eq} of organic fertilisers (83.07 ± 12.69 Bq kg^{-1}) indicates that using these particular kinds of fertilisers is a rational choice. Nonetheless, our results suggest that MOP fertilisers should be used under radiation protection regulations.

3.3. Hazard indices

Radiological threats in the studied samples were estimated in numerous hazard parameters. External hazard index (H_{ex}), internal hazard index (H_{in}) and γ-radiation hazard index (I_γ) are three well-known parameters addressed by the Organization for Economic Co-operation and Development (OECD) and European Commission [18,33]. The calculated H_{ex}, H_{in} and I_γ presented in Table 2 clearly indicate that MOP fertilisers exceeded the recommended level (≤1) in all of these indices [35,36] while the TSP and GYP surpassed

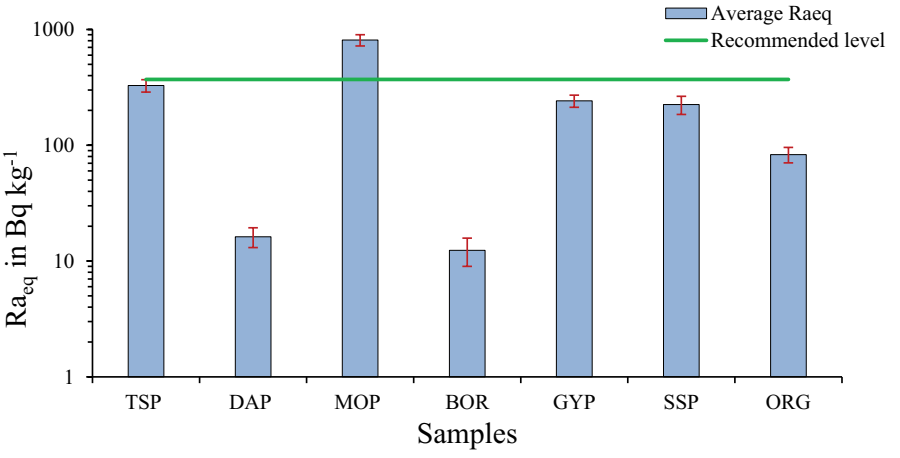

Figure 2. Average radium equivalent activity (Ra_{eq}) in different fertiliser samples.

Table 2. The average radium equivalent activity (Ra_{eq}), external hazard index (H_{ex}), internal hazard index (H_{in}) and γ-radiation hazard index (I_γ) of different kinds of fertilisers.

Fertiliser type	Ra equivalent activity, Bq kg^{-1}	External hazard index, H_{ex}	Internal hazard index, H_{in}	γ-Radiation hazard index, I_γ
TSP	327.98 ± 40.32	0.89 ± 0.11	1.71 ± 0.21	1.10 ± 0.14
DAP	16.22 ± 3.15	0.04 ± 0.01	0.06 ± 0.01	0.06 ± 0.01
MOP	811.04 ± 90.83	2.19 ± 0.25	2.19 ± 0.25	3.51 ± 0.39
BOR	12.39 ± 3.40	0.03 ± 0.01	0.05 ± 0.01	0.04 ± 0.01
GYP	242.00 ± 29.04	0.65 ± 0.08	1.31 ± 0.16	0.81 ± 0.10
SSP	224.47 ± 40.01	0.61 ± 0.11	0.83 ± 0.15	0.82 ± 0.14
ORG	83.08 ± 12.69	0.22 ± 0.03	0.29 ± 0.05	0.32 ± 0.05
Mean value	245.31 ± 31.35	0.66 ± 0.08	0.92 ± 0.12	0.95 ± 0.12

the non-violent level of H_{in} due its higher content of Ra-226. In the case of I_γ, TSP and MOP along with MOP fertilisers have overstepped the safety margin (≤1) [25]. The outcomes of these hazard parameters studies point towards that, the production and uses of the recommended-level-exceeded fertilisers should be controlled by the radiation protection principles.

3.4. Exposures, dose rates and cancer risk

Fertilisers with elevated contents of radionuclides are sources of possible exposure to the public due to their extensive use in agriculture. So, it is essential to estimate the exposure rate and associated equivalent dose. In this study, the air absorbed gamma dose rate for outdoor (D_{out}) and indoor (D_{in}) was calculated by using Equations (4) and (5), as shown in Table 3. The average D_{out} for different variety of fertilisers was found to vary from 5.48 ± 1.52 to 439.15 ± 49.17 nGy h^{-1}, where most of the chemical fertilisers, except DAP and BOR, show higher values than the reported world average value of 59 nGy h^{-1}. The value of D_{in} for different types of fertilisers are ranging from 10.48 ± 2.92 to 853.04 ± 95.51 nGy h^{-1}, where the fertilisers type TSP, MOP, GYP and SSP exceeded the world average value (84 nGy h^{-1}) in a degree of 2–10 times. Annual effective dose equivalent for outdoor

Table 3. Air absorbed dose rate and annual effective dose equivalent at indoor and outdoor, and excess lifetime cancer risk at outdoor.

Sample	Air absorbed dose rate(D), nGy h^{-1}		Annual effective dose equivalent (AEDE), mSv y^{-1}		ELCR $\times 10^{-3}$
	D_{out}	D_{in}	$AEDE_{outdoor}$	$AEDE_{indoor}$	
TSP-1	153.03 ± 17.82	303.86 ± 35.22	0.19 ± 0.02	1.49 ± 0.17	0.66
TSP-2	228.22 ± 28.48	451.8 ± 56.22	0.28 ± 0.03	2.22 ± 0.27	0.98
TSP-3	194.46 ± 24.21	385.6 ± 47.86	0.24 ± 0.03	1.89 ± 0.23	0.83
TSP-4	58.92 ± 6.76	115.48 ± 13.13	0.07 ± 0.01	0.57 ± 0.06	0.25
TSP-5	57.36 ± 7.155	112.16 ± 13.88	0.07 ± 0.01	0.55 ± 0.07	0.25
TSP-6	200.51 ± 20.52	396.6 ± 40.52	0.25 ± 0.03	1.95 ± 0.19	0.86
TSP-7	161.7 ± 24.26	322 ± 48.3	0.20 ± 0.03	1.58 ± 0.24	0.69
TSP Avg.	150.6 ± 18.46	298.21 ± 36.45	0.18 ± 0.02	1.46 ± 0.18	0.65
DAP-1	0.65 ± 0.32	1.29 ± 0.64	0.001 ± 0.0003	0.01 ± 0.003	0.003
DAP-2	21.69 ± 3.88	39.79 ± 7.15	0.03 ± 0.01	0.20 ± 0.04	0.09
DAP-3	2.31 ± 0.49	4.60 ± 0.97	0.003 ± 0.0006	0.02 ± 0.01	0.01
DAP-4	7.42 ± 1.58	14.05 ± 2.98	0.01 ± 0.002	0.07 ± 0.01	0.03
DAP-5	3.14 ± 0.60	6.26 ± 1.19	0.004 ± 0.001	0.03 ± 0.01	0.01
DAP Avg.	7.04 ± 1.37	13.20 ± 2.59	0.01 ± 0.002	0.07 ± 0.01	0.03
MOP-1	442.02 ± 61.88	858.60 ± 120.20	0.54 ± 0.08	4.21 ± 0.59	1.90
MOP-2	433.21 ± 61.17	841.66 ± 118.86	0.53 ± 0.08	4.13 ± 0.58	1.86
MOP-3	408.66 ± 57.21	793.80 ± 111.13	0.50 ± 0.07	3.89 ± 0.55	1.75
MOP-4	447.114 ± 44.99	868.54 ± 87.41	0.55 ± 0.06	4.26 ± 0.43	1.92
MOP-5	458.70 ± 45.87	891.00 ± 89.10	0.56 ± 0.06	4.37 ± 0.44	1.97
MOP-6	462.87 ± 46.29	899.10 ± 89.91	0.57 ± 0.06	4.41 ± 0.44	1.99
MOP-7	446.19 ± 44.62	866.70 ± 86.67	0.55 ± 0.05	4.25 ± 0.43	1.92
MOP-8	437.85 ± 30.65	850.50 ± 59.54	0.54 ± 0.04	4.17 ± 0.29	1.88
MOP-9	337.77 ± 47.29	656.10 ± 91.85	0.41 ± 0.06	3.22 ± 0.45	1.45
Q-Potash	517.08 ± 51.71	1004.40 ± 100.44	0.63 ± 0.06	4.93 ± 0.49	2.22
MOP Avg.	439.15 ± 49.17	853.04 ± 95.51	0.54 ± 0.06	4.18 ± 0.47	1.88
BOR-1	3.70 ± 1.48	7.36 ± 2.94	0.005 ± 0.001	0.04 ± 0.02	0.02
BOR-2	4.05 ± 1.05	7.37 ± 1.92	0.005 ± 0.001	0.04 ± 0.01	0.02
BOR-3	2.63 ± 1.32	5.24 ± 2.62	0.003 ± 0.002	0.03 ± 0.01	0.01
BOR-4	11.55 ± 2.21	21.93 ± 4.18	0.014 ± 0.003	0.11 ± 0.02	0.05
BOR Avg.	5.48 ± 1.52	10.48 ± 2.92	0.007 ± 0.002	0.05 ± 0.01	0.02
GYP	111.80 ± 13.42	222.64 ± 26.72	0.14 ± 0.02	1.09 ± 0.13	0.48
SSP	104.66 ± 18.22	200.79 ± 34.76	0.13 ± 0.02	0.98 ± 0.17	0.45
ORG-1	4.47 ± 1.07	8.14 ± 1.95	0.01 ± 0.001	0.04 ± 0.01	0.02
ORG-2	77.98 ± 12.07	148.98 ± 22.91	0.10 ± 0.02	0.73 ± 0.11	0.33
ORG-3	31.24 ± 5.20	60.44 ± 10.00	0.04 ± 0.01	0.30 ± 0.05	0.13
ORG-4	115.88 ± 16.11	228.21 ± 31.69	0.14 ± 0.02	1.12 ± 0.16	0.50
ORG-5	156.85 ± 14.83	305.32 ± 28.96	0.20 ± 0.02	1.50 ± 0.14	0.67
ORG-6	24.27 ± 7.28	45.14 ± 13.54	0.03 ± 0.01	0.22 ± 0.07	0.10
ORG-7	1.97 ± 0.99	3.96 ± 1.98	0.002 ± 0.001	0.02 ± 0.01	0.01
ORG-8	24.72 ± 4.65	47.45 ± 8.90	0.03 ± 0.01	0.23 ± 0.04	0.11
ORG-9	4.16 ± 1.66	8.28 ± 3.31	0.01 ± 0.002	0.04 ± 0.02	0.02
ORG-10	7.90 ± 1.51	14.76 ± 2.83	0.01 ± 0.001	0.07 ± 0.01	0.03
ORG-11	3.700 ± 1.85	7.36 ± 3.68	0.004 ± 0.002	0.04 ± 0.02	0.02
ORG Avg.	41.20 ± 6.11	79.82 ± 11.80	0.05 ± 0.01	0.40 ± 0.06	0.18

($AEDE_{outdoor}$) and indoor ($AEDE_{indoor}$) was calculated using Equations (6) and (7), respectively. Results are presented in Table 3. Except for the ORG, DAP and BOR fertilisers, all others have surpassed the limit (0.07 mSv y^{-1}) reported in UNSCEAR 2000 [31]. Figure 3, the illustrative comparison of D_{out} and $AEDE_{outdoor}$ with respective world average values, clearly shows that most of the chemical fertilisers have up to 10 times higher values than the world average. The measured data for $AEDE_{indoor}$ presented in Table 3 shows that TSP, MOP, GYP and SSP fertilisers have higher outcomes of indoor dose and $AEDE_{indoor}$ alone exceeded the ICRP-103 criterion limit (1mSv y^{-1}) for total annual effective dose [27]. Therefore, this study strongly suggests that the work can be repeated by some other

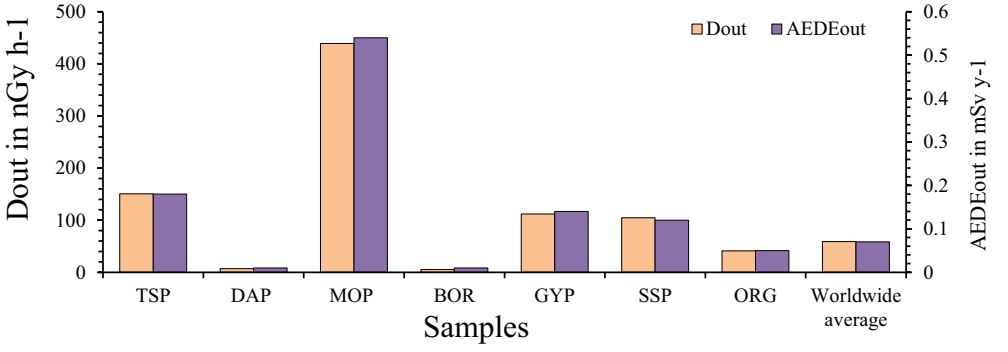

Figure 3. Average absorbed dose rate (D_{out}) and annual effective dose equivalent ($AEDE_{outdoor}$) with compared to the worldwide average value reported in UNSCEAR 2000 [31].

groups for the optimising results so that the production and inadvertent use of these fertilisers can be controlled by the regulations for the protection of the public and the environment.

Based on the values of outdoor annual effective dose, ELCR (outdoor) has been calculated by using Equation (10) and presented in Table 3. The ELCR for all the samples is ranging from 0.003×10^{-3} to 2.22×10^{-3} with an average of 0.68×10^{-3}, which is more than double of the world average of 0.3×10^{-3}.

4. Conclusions

Fertilisers are one of the key elements to boosting agriculture production. Farmers from all over the world use a variety of fertilisers, mostly two major groups: organic and chemical fertilisers. Likewise, for the maximum utilisation of cultivable land to grow food for one of the most densely populated countries, Bangladesh stands among the top 15 consumers of chemical fertilisers. As most chemical fertilisers are made from phosphorus and potassium which are naturally radioactive, the fertilisers are likely to have a certain level of radioactivity. To assess the activity concentrations of ^{226} Ra, ^{232}Th and ^{40}K in the fertiliser of seven different varieties from Chattogram, Bangladesh, 39 individual samples were investigated using HPGe gamma-ray spectrometry. The extracted data show that potash fertilisers (MOP) contain a little more ^{40}K concentrations than the regulatory exemption limit. The presence of ^{226} Ra in phosphate fertilisers is still under the regulatory exemption limit [37], but 3 to 10 times higher than the average concentration in the soil reported by UNSCEAR 2000 [31]. One category of phosphate fertiliser (SSP) shows an elevated concentration of ^{232}Th compared to the UNSCEAR 2000 report [31]. Organic fertilisers show an almost normal level of radioactivity concentrations except for higher concentrations of ^{40}K in two samples. Nonetheless, the radium equivalent activity for organic fertilisers is still below the safety margin. As per the findings in this present work, it can be summarised that organic fertilisers are looking comparatively better than those composed of chemicals in respect of radiological hazards although both types are found to be within the safety limit. Finally, this study will hopefully play an important role as a reference for the studies on the cumulative effect of fertilisers on soil and crops along

with strengthening baseline information on environmental radiation monitoring as well. Further study is suggested to be conducted periodically so that regulatory control could be implemented as needed. A study of the transfer factor of radionuclides from fertiliser to the soil to grain may add an additional layer to the safety information of extensive use of chemical fertilisers.

Acknowledgment

Authors are grateful to the authority of the Atomic Energy Centre, Chattogram, Bangladesh, for providing laboratory facilities for this study.

Disclosure statement

No potential conflict of interest was reported by the author(s).

ORCID

Animesh Kumer Chakraborty http://orcid.org/0000-0003-1430-6230
Mahiuddin Ahmed http://orcid.org/0000-0002-6357-9246

References

[1] Ministry of Finance, Socio-Economic Indicators of Bangladesh 33, 2021.
[2] The Centre for Research and Information (CRI), *Bangladesh Towards Achieving Food Security 2009-2019* (Dhaka, 2019).
[3] B.N. Thien, V.N. Ba, N.T.T. Vy and T.T.H. Loan, Chemosphere **259**, 127432 (2020). doi:10.1016/j.chemosphere.2020.127432.
[4] H.M. Khan, Z.S. Chaudhry, M. Ismail and K. Khan, Water Air Soil Pollut. **213**, 353 (2010). doi:10.1007/s11270-010-0390-4.
[5] T. Kubale, R. Daniels, J. Yiin, G. Kinness, J. Couch, M. Schubauer Berigan, S. Silver, S. Nowlin and P. Chen, Radiat. Res. **164** (6), 810 (2004). doi:10.1667/RR3473.1.
[6] N.F. Kadhim, Y.A. Baqir and L.A. Najam, J. Radiat. Nucl. Appl. **5**, 127 (2020).
[7] M.S. Hamideen, S. Manigandan, A. Chandrasekaran, A. Tamilarasi and V. Sathish, Int. J. Environ. Anal. Chem. 1–12 (2021). doi:10.1080/03067319.2021.2014467.
[8] L.A. Najam, R.H. Mahmmod and O.M.J. Albanna, Iran. J. Sci. Technol. Transac. A. **46** (3), 979–987 (2022). doi:10.1007/s40995-22-01306-5.
[9] J. Billa, F. Han, S. Didla, M. Ankrah, H. Yu, J. Dimpah, O. Brempong and S. Adzanu, J. Radioanal. Nucl. Chem. **306**, 183 (2015). doi:10.1007/s10967-015-4071-z.
[10] A. El-Taher and M.A.K. Abdelhalim, J. Life Sci. **10** (3), 701 (2013).
[11] N.G. Servitzoglou, S. Stoulos, D. Katsantonis, M. Papageorgiou and A. Siountas, Radiat. Prot. Dosim. **181** (3), 190 (2018). doi:10.1093/rpd/ncy009.
[12] T.T.H. Loan, V.N. Ba, N. van Thai Bang, T.H.N. Thy, H.T.Y. Hong and N.Q. Huy, J. Radioanal. Nucl. Chem. **316**, 111 (2018). doi:10.1007/s10967-018-5719-2.
[13] N.M. Hassan, B.U. Chang and S. Tokonami, J. Chem. **2017**, 1 (2017). doi:10.1155/2017/9182768.
[14] M.A.M. Uosif, A.M.A. Mostafa, R. Elsaman and E. Moustafa, J. Radiat. Res. Appl. Sci. **7**, 430 (2014). doi:10.1016/j.jrras.2014.07.006.
[15] T. Barua, A.K.M. Saiful Islam Bhuian, S. Hossain, N. Deb, M. Ahmed, S. Hossain, M.A. Rashid and M.U. Khandaker, J. Radioanal. Nucl. Chem. **322**, 173 (2019). doi:10.1007/s10967-019-06579-6.

[16] A.A. Md Sirajul Islam, M.M. Hossain Miah, M. Ahmed, S. Hossain and M.U. Khandaker, Int. J. Environ. Anal. Chem. **1**, 1 (2021). doi:10.1080/03067319.2021.1912339.
[17] G.F. Knoll, *Radiation Detection and Measurement*, 4th ed. (2010).
[18] F. Alshahri, Environ. Sci. Pol. Res. **26**, 36226 (2019). doi:10.1007/s11356-019-06647-0.
[19] L.A. Currie, Anal. Chem. **40**, 586 (1968). doi:10.1021/ac60259a007.
[20] L.A. Currie, *Lower Limit of Detection: Definition and Elaboration of a Proposed Position for Radiological Effluent and Environmental Measurements* (National Bureau of Standards, Washington, DC, 1984).
[21] S. Yasmin, B.S. Barua, M. Uddin Khandaker, M. Kamal, M. Abdur Rashid, S.F. Abdul Sani, H. Ahmed, B. Nikouravan and D.A. Bradley, Results Phys. **8**, 1268 (2018). doi:10.1016/j.rinp.2018.02.013.
[22] D.A.E. Darwish, K.T.M. Abul-Nasr and A.M. El-Khayatt, J. Radiat. Res. App. Sci. **8**, 17 (2015). doi:10.1016/j.jrras.2014.10.003.
[23] S.M. El-Bahi, A. Sroor, G.Y. Mohamed and N.S. El-Gendy, Appl. Radiat. Isot. **123**, 121 (2017). doi:10.1016/j.apradiso.2017.02.031.
[24] N.M. Hassan, J. Taibah Univ. Sci. **10**, 296 (2016). doi:10.1016/j.jtusci.2015.08.009.
[25] E. Commission and D.-G. for Environment, *Radiological Protection Principles Concerning the Natural Radioactivity of Building Materials* (Office for the Official Publications of the European Communities, Luxembourg, 2000).
[26] D. Roy, M.M.M. Siraz, M.J. Dewan, S. Pervin, A.F.M.M. Rahman, M.U. Khandaker and S. Yeasmin, J. Radioanal. Nucl. Chem. **331**, 1299 (2022). doi:10.1007/s10967-022-08196-2.
[27] ICRP, Ann. ICRP **37**, 2–4 (2007).
[28] M.N. Alam, M.I. Chowdhury, M. Kamal, S. Ghose, H. Banu and D. Chakraborty, Appl. Radiat. Isot. **48** (8), 1165 (1997). doi:10.1016/S0969-8043(97)00019-5.
[29] United Nations Scientific Committee on the Effects of Atomic Radiation, *Sources and Effects of Ionizing Radiation, UNSCEAR 2008 Report*, 2010. p. 221.
[30] M. Samad, M. Ali, D. Paul and S. Islam, Jahangirnagar Univ. Environ. Bull. **1**, 15 (2013). doi:10.3329/jueb.v1i0.14543.
[31] United Nations Scientific Committee on the Effects of Atomic Radiation, *Sources and Effects of Ionizing Radiation, UNSCEAR 2000 Report*, 2000. p. 83.
[32] M.D.A. Mojumder, M. Ahmed, M. Kamal, M.B. Hossen and A.R. Md, J. Environ. Prot. (Irvine, Calif) **11** (10), 767 (2020). doi:10.4236/jep.2020.1110047.
[33] L.E. de Geer, Appl. Radiat. Isot. **61** (2–3), 151 (2004). doi:10.1016/j.apradiso.2004.03.037.
[34] O. el Samad and R. Baydoun, J. Radiat. Nucl. Appl. **3**, 9 (2018). doi:10.18576/jrna/030102.
[35] NEA-OECD, *Exposure to Radiation from Natural Radioactivity in Building Materials; Report by NEA Group of Experts*. (Paris, 1979).
[36] H.H. Azeez, H.H. Mansour and S.T. Ahmad, Pol. J. Environ. Stud. **29**, 1059 (2020). doi:10.15244/pjoes/106032.
[37] International Atomic Energy Agency, *Clearance Levels for Radionuclides in Solid Materials: Application of Exemption Principles Interim Report for Comment*. IAEA-TECDOC-855 (Viena: IAEA, 1996).